8-2015

GATING MECHANISMS OF THE CANONICAL TRP CHANNEL ISOFORM TRPC4

Dhananjay P. Thakur

GATING MECHANISMS OF THE CANONICAL TRP CHANNEL ISOFORM TRPC4

By
Dhananjay Thakur M.Sc., M.S.

APPROVED:

_____
Michael X. Zhu, Ph.D.
Advisory Professor

_____
Carmen W. Dessauer, Ph.D.

_____
Richard B. Clark, Ph.D.

_____
Roger G. O'Neil, Ph.D.

_____
Neal M. Waxham, Ph.D.

APPROVED:

_____
Dean, The University of Texas
Graduate School of Biomedical Sciences at Houston

GATING MECHANISMS OF THE CANONICAL TRP CHANNEL ISOFORM TRPC4

A

DISSERTATION

Presented to the Faculty of
The University of Texas
Health Science Center at Houston
and
The University of Texas
MD Anderson Cancer Center
Graduate School of Biomedical Sciences
in Partial Fulfillment

of the Requirements

for the Degree of

DOCTOR OF PHILOSOPHY

by

Dhananjay Thakur M.S., M.Sc.
Houston, Texas

August, 2015

Dedication

This dissertation is dedicated to my family:

Juilie Thakur, Arundhati Thakur and Pramod Thakur

Their endless love and support have made everything possible

Acknowledgements

This wonderfully convoluted trajectory that my journey in science has followed so far has been perceptibly and imperceptibly guided by several people. Friends, family, mentors and colleagues - and the distinctions blurred very often - have made me who I am. To Dr. Michael X. Zhu, I owe the deepest gratitude, for guiding me with great patience through the strangest and roughest roads that this project took. Dr. Zhu taught me to make that critical distinction between testable and non-testable hypotheses, and the importance of clearly defining both negative and positive controls for all tests, which very often, turned out not to be a trivial exercise. These lessons have shaped the way I think about every scientific problem now. Regularly, the tendency towards reductionism clashed with the demands for a comprehensive hypothesis. Without Dr. Zhu's guidance, I would not have been able to achieve that dynamic balance between these two states that is necessary for the resolution of complex biological problems. I would also like to especially thank the members of my advisory and candidacy examination committees, Dr. Carmen Dessauer, Dr. Richard Clark, Dr. Roger O'Neil, Dr. Neal M. Waxham, Dr. Hongzhen Hu, Dr. Michael Beirlein, Dr. Alemayehu Gorfe and Dr. Raymond Grill. Their guidance – in both technical aspects and the scientific process – has been invaluable. Their early lessons in maintaining an eye for detail while not losing the forest for the trees, their generous help with insights stemming from their extensive knowledge, as well as with materiel – protocols, reagents and instruments have been invaluable for my work and development as a scientist. Dr. Jinbin Tian and Dr. Jaepyo Jeon were closely involved in several steps in this work. I am deeply thankful for their guidance and collaboration

and I am looking forward to many more equally enjoyable and fruitful interactions. The American Heart Association made the last two years of research possible through their generous funding. I am very grateful to the reviewers of my grant applications who (anonymously) taught me how to chisel out a good grant application. I also thank the University Of Texas Graduate School Of Biomedical Sciences, and especially - Dr. Priscilla Saunders, who established and supported the Investing in Student Futures Award, which gave strong and timely encouragement. Students, staff and faculty in the Department of Integrative Biology were extremely generous with their reagents, advice and friendship. Without the deepest friendships that evolved over the last several years, life/science would have been impossible. For those invaluable hours filled with laughter, food, bickering and the mutual indulgence in each other's existential crises, I would like to thank David, Mykola, Renu, Kelsey, Caitlin, Karolina, Jennifer, Tanya, Yukti, Yingmin, Alexis, Nabila, Faiza, Aparna, Radhika, Rasika, Ching-On, Kevin, Sujay, Sourabh, Deepti, Franco, Susanna, Dries, and Joe. The blame for my transition from physics to biology lands squarely on the shoulders of Ambrose Bierce, who with one flick of a pen (*"Brain, n. An apparatus with which we think we think." The Devil's Dictionary, 1911*) planted a seed in my head – that any comprehension of physics was meaningless without its application in biology – which set me off on this journey that has taken me to the TRP channel world. I would also like to thank my mentors in Physics, Dr. Raka Dabhade and Dr. Pandit Vidyasagar at the University of Pune, and Mr. Preesty Thomas at Tata Motors Ltd. Their guidance and encouragement helped me through every important step and transition in my early career. Lastly, I would like to

thank my family again for their unrelenting love and support. Their patience and understanding was critical for this work.

GATING MECHANISMS OF THE CANONICAL TRP CHANNEL ISOFORM TRPC4

Dhananjay Thakur, M.Sc., M.S.

Advisory Professor: Michael X. Zhu, Ph.D.

Non-selective cation channels formed by Transient Receptor Potential Canonical (TRPC) proteins play important roles in regulatory and pathophysiological processes. These channels are known to be activated downstream from phospholipase C (PLC) signaling. However, the mechanism by which the PLC pathway activates TRPC4/C5 remains unclear. Uniquely, TRPC4 is maximally activated only when two separate G protein pathways, $G_{q/11}$ and $G_{i/o}$, are co-stimulated, making it a coincidence detector of $G_{q/11}$- and $G_{i/o}$ -coupled receptor activation. Using HEK293 cells co-expressing mouse TRPC4β and selected G protein-coupled receptors, I observed that coincident stimulation of $G_{i/o}$ proteins and PLCδ1 (and not $G_{q/11}$-PLCβ) is necessary and sufficient for TRPC4 activation. In cells co-expressing TRPC4 and $G_{i/o}$ -coupled μ opioid receptor, μ agonist DAMGO elicited currents in a biphasic manner, with an initial slow phase preceding a second, rapidly developing phase. While the currents were dependent on intracellular Ca^{2+} and phosphatidylinositol 4,5-bisphosphate (PIP_2), both Ca^{2+} and PIP_2 also exhibited inhibitory effects. Depleting PIP_2 abolished the biphasic kinetics and facilitated channel activation by weak $G_{i/o}$ stimulation. TRPC4 activation was inhibited by knocking down PLCδ1 and almost entirely eliminated by a dominant-negative PLCδ1 mutant or a constitutively active RhoA mutant. These results demonstrate an integrative mechanism of TRPC4 for detection of coincident $G_{i/o}$,

Ca^{2+}, and PLC signaling, wherein TRPC4 and PLCδ1 are functionally coupled. This mechanism is not shared with the closely related TRPC5, implicating unique roles of TRPC4 in signal integration. Intracellular acidification further facilitated channel activation in a bimodal manner, with moderate acidification accelerating the $G_{i/o}$-TRPC4 response, while strong acidification was inhibitory. This regulation by H^+ is functionally and mechanistically distinct from that by Ca^{2+}, which involves not only Ca^{2+}-dependent PLCδ1 activation but also a direct modulation by Ca^{2+}-calmodulin. Thus, our findings indicate that TRPC4 is maximally activated when (A) $G_{i/o}$ and PLCδ1 are stimulated and (B) intracellular concentrations of PIP_2, Ca^{2+} and H^+ fall within specific ranges. These findings indicate that TRPC4 serves as a unique coincidence sensor of intracellular environmental changes that accompany not only $G_{i/o}$ stimulation and PLC signaling but also, likely, other pathophysiological conditions, such as metabolic changes and hypoxic stress.

Table Of Contents

List of Illustrations

Abbreviations

2-ABP, 2-aminoethoxydiphenyl borate

AA, amino acid

Ank, ankyrin

ATPD, above-threshold-plateau-depolarization

BAPTA, 1,2-bis(o-aminophenoxy)ethane-N,N,N',N'-tetraacetic acid

BCECF, 2',7'-bis-(2-carboxyethyl)-5-(and-6)-carboxyfluorescein

BTD, below threshold depolarization

$[Ca^{2+}]$, concentration of free Ca^{2+}

$[Ca^{2+}]_i$, concentration of intracellular free Ca^{2+}

CaM, calmodulin

CCh, carbachol

cDNA, complementary DNA

CIRB, calmodulin- and IP3R-binding

cryo-EM, cryogenic-electron microscopy

DAG, diacylglycerol

DMEM, Dulbecco's Modified Eagle's Medium

dn, dominant negative

DrVSP, zebrafish voltage-sensitive phosphatase

ECS, extracellular solution

EC, endothelial cell

EGF, epidermal growth factor

EGFP, enhanced green fluorescent protein

EGFR, epidermal growth factor receptor

EGTA, ethylene glycol tetraacetic acid

ER, endoplasmic reticulum

ERG, electroretinogram

FBS, fetal bovine serum

FSGS, Focal segmental glomerulosclerosis

GI, gastrointestinal

GPCR, G-Protein Coupled Receptor

GST, Glutathione S Transferase

HEK293, human embryonic kidney 293 cells

HEPES, 4-(2-hydroxyethyl)-1-piperazineethanesulfonic acid

HIF-α, hypoxia-inducible factor-1 alpha

IM, ionomycin

IP_3, inositol 1, 4, 5-trisphosphate

IP_3R, inositol 1, 4, 5-trisphosphate receptor

I-V, current-voltage relationship

KO, Knock-out

Kv, voltage-gated potassium

LS, lateral septal

LTD, long-term depression

LTP, long-term potentiation

M1R, muscarinic receptor subtype 1

M2R, muscarinic receptor subtype 2

M3R, muscarinic receptor subtype 3

M4R, muscarinic receptor subtype 4

M5R, muscarinic receptor subtype 5

mGluRs, metabotropic glutamate receptors

NFAT, nuclear factor of activated T-cells

NHERF, sodium hydrogen exchanger regulatory factor

NO, nitric oxide

OAG, 1-oleoly-2-acetyl-sn-glycerol

PASMCs, pulmonary arterial smooth muscle cells

PBS, phosphate buffered saline

PCR, polymerase chain reaction

PDZ domain, postsynaptic density/discs-large/zonula occludens domain

PI3K, phosphoinositide 3-kinases

PIP_2, phosphatidylinositol (4,5)-bisphosphate

PKC, protein kinase C

PKG, protein kinase G

PLA2, phospholipase A2

PLC, phosphalipase C

PLD, phospholipase D

P-loop, pore loop

PEI, polyethylenimine

PTX, pertussis toxin

PUFAs, polyunsaturated fatty acids

RFU, relative fluorescence unit

ROCE, receptor-operated calcium entry

RTK, receptor tyrosine kinases

SDS-PAGE, sodium dodecyl sulfate polyacrylamide gel electrophoresis

sEPSC, slow excitatory postsynaptic current

siRNA, small interfering RNA

SOCE, store-operated calcium entry

STIM, stromal interacting molecule

TRP, transient Receptor Potential

TRPA, transient receptor potential ANKTM1

TRPC, transient receptor potential canonical

TRPM, transient receptor potential melastatin

TRPML, transient receptor potential mucolyptin

TRPN, transient receptor potential NOMP

TRPP, transient receptor potential polycystin

TRPV, transient receptor potential vanilloid

μOR, μ opioid receptor

Chapter 1

Introduction

Transient receptor potential channels (TRPs) function as sensors and transducers of a wide variety of environmental and endogenous signals. Within the TRP channel superfamily, members of the Canonical class of TRPs (TRPC) are activated downstream of G-Protein Coupled Receptors (GPCRs) and receptor tyrosine kinases (RTK). GPCRs and RTK receptors transduce biochemical signals (in the form of neurotransmitters, hormones, growth factors and their exogenous analogs), into multiple regulatory or pathophysiological processes. A primary downstream event in receptor-TRPC pathways is the change in $[Ca^{2+}]_i$ (intracellular Ca^{2+} concentrations). Temporal and spatial control of $[Ca^{2+}]_i$ regulates a variety of phenomena including: cell excitability, contraction, secretion, migration, adhesion, gene expression and cell death.

There are several overlaps in the expression profiles of the various TRPC isoforms and several direct and functional interactions within the TRPC sub-family. Although their effects on a variety of cellular events have been observed, their precise contribution(s) are only partly understood, mostly because very little is known about the activation and regulation mechanisms of the various isoforms within this sub-family. Although the $G_{q/11}$ phospholipase C-β (PLCβ) and phospholipase C-γ (PLCγ) pathways have been identified as the primary upstream events for the activation of most TRPCs, TRPC4 and TRPC5 are uniquely sensitive to $G_{i/o}$ coupled receptor activation (Otsuguro, Tang et al. 2008, Jeon, Hong et al. 2012). In this case, while the $G_{q/11}$-PLC pathway is well characterized, the physiological significance and molecular mechanisms of $G_{i/o}$ mediated TRPC4 and TRPC5 activation are unknown. TRPC5 can be activated maximally

downstream of $G_{q/11}$ alone. However, $G_{i/o}$ activation is obligatory to obtain maximal TRPC4 currents. In this study, while there appeared to be a PLC component necessary for TRPC4 activation, it was distinct to the $G_{q/11}$-PLC pathway, suggesting a novel mechanism unique to TRPC4. Elucidation of this pathway would shed light on the physiological significance of TRPC4 function with respect to $G_{i/o}$, $G_{q/11}$ and RTK mediated signaling. Therefore, the major aim of this dissertation was to identify the mechanism(s) underlying the activation and regulation of the channels formed by the TRPC4 isoform.

1.1 Historical background

Early research (1910 ~ 1960) on fruit flies (*Drosophila melanogaster*) focused on genetic manipulations to study heredity. Subsequently, the accumulation of a vast body of knowledge and expertise in *Drosophila* genetics prompted an interest in using fruit flies to examine physiological processes. In search for mutations that would result in neurological impairment in *Drosophila*, Cosens and Manning discovered a mutation that resulted in a retinal defect making flies behave as if they were blind (Cosens and Manning 1969). It was then noted that this mutation resulted in a fast decay of an electroretinogram (ERG) signal during strong light stimulation - compared to the sustained plateau ERG seen in the wild type fly. Therefore, the name Transient Receptor Potential (TRP) was coined (Minke, Wu et al. 1975).

However, it was not until 15 years later that Montell and Rubin cloned the gene responsible for this mutation and predicted a protein structure that could constitute a channel-forming transmembrane protein (Montell and Rubin 1989). Two years following this discovery, Hardie and Minke were able to record light-induced currents from both wild type and *trp* mutant flies and demonstrated that the mutant suffered from the loss of a sustained Ca^{2+} dependent current

downstream of rhodopsin and inositol 1,4,5-trisphosphate (IP_3) receptor activation (Hardie and Minke 1991). Subsequently, two independent groups cloned the first mammalian TRP homolog, TRP1 (or TRPC1) (Wes, Chevesich et al. 1995, Zhu, Chu et al. 1995). Thereafter, six more mammalian homologs based on sequence homology were cloned in full-length (Philipp, Cavalié et al. 1996, Zhu, Jiang et al. 1996, Okada, Shimizu et al. 1998, Philipp, Hambrecht et al. 1998, Okada, Inoue et al. 1999).

Outside of the canonical class, but showing significant sequence similarities, a wide variety of channel-forming proteins were discovered, and later, uniformly designated as TRP superfamily members (Montell, Birnbaumer et al. 2002). Interest in TRP proteins developed rapidly and one of the most widely noted discoveries was that of the high temperature sensor vanilloid receptor 1 (VR1) or transient receptor potential vanilloid (TRPV1) which was also activated by capsaicin, the active ingredient of chili peppers (Caterina, Schumacher et al. 1997). Three other genes, closely homologous to TRPV1, designated TRPV2-4, were subsequently cloned and showed different warm-temperature thresholds. At the opposite end of the temperature spectrum, two independent groups discovered a cool temperature-activated TRP channel, transient receptor potential melastatin 8 (TRPM8) (McKemy, Neuhausser et al. 2002, Peier, Moqrich et al. 2002). TRPM8 is activated at temperatures approximately below 26 °C. Then the transient receptor potential ANKTM1 (TRPA1) channel was discovered and shown to be highly sensitive to cold temperatures (Story, Peier et al. 2003) and the compound allyl isothiocyanate (Bandell, Story et al. 2004, Jordt, Bautista et al. 2004). TRPA1 is activated at a lower temperature threshold (~14 °C) than TRPM8 (Sawada, Hosokawa et al. 2007, Karashima, Talavera et al. 2009). These characteristics impart distinct roles for TRPM8 and TRPA1 as cool and cold sensors, respectively. In addition, there is a difference in modalities of thermosensation between species

even though there is strong conservation of sequence for these isoforms. For instance, the *Drosophila* and snake TRPA1 channels are warm temperature sensors (Rosenzweig, Brennan et al. 2005, Hamada, Rosenzweig et al. 2008, Gracheva, Ingolia et al. 2010).

In general, based on sequence alignment and function, the mammalian TRP superfamily was divided into six sub-families: canonical TRPs (TRPC) are those that show highest homology to the original *Drosophila* TRP protein; melastatin TRPs (TRPM), named after the founding member Melastatin (TRPM1); vanilloid TRPs (TRPV) named after the founding member vanilloid receptor 1 (VR1 or TRPV1); Ankyrin TRP (TRPA1) representing the single mammalian ANK-TRP; polycystin TRPs (TRPP) named after polycystic kidney disease gene PKD2 and mucolipin TRPs (TRPML) which are homologs of the gene responsible for mucolipidosis type IV (Montell, Birnbaumer et al. 2002). Some TRPs, such as the transient receptor potential NOMP (TRPN) are only found in invertebrates. So far, by species, the number of TRP channel genes identified are: 28 in rodents, 27 in human, 17 in *C. elegans*, and 13 in *Drosophila* (Montell 2011). The evolutionary relationships of mammalian TRPC proteins along with the *Drosophila* TRP are shown in **figure 1**.

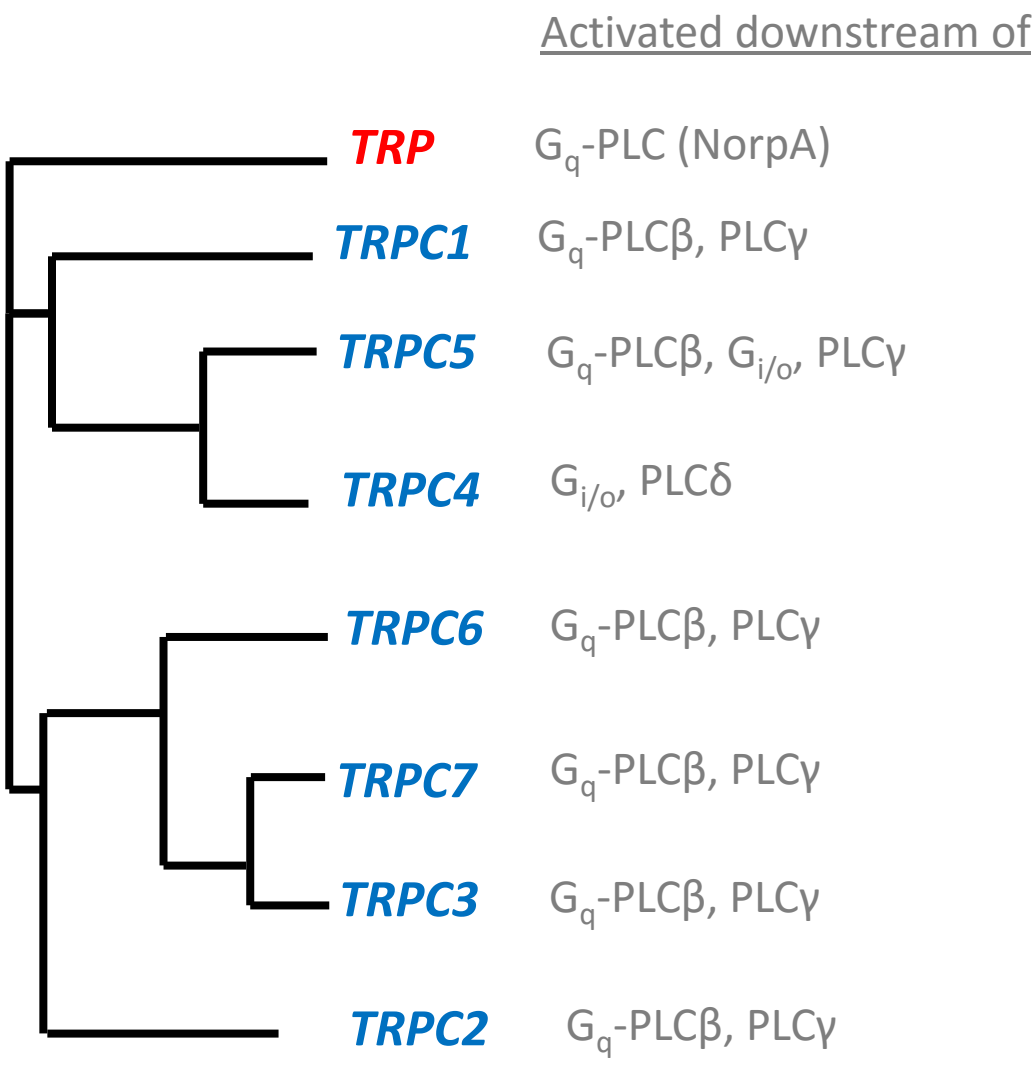

Figure 1. Evolutionary relationship of TRPC homologs

Phylogenetic tree of *Drosophila* TRP (red) and mammalian (mouse) TRPCs (blue) constructed using ClustalW-Phylogeny. Known mechanisms upstream of TRP and TRPC activation are shown to the right in grey

TRPC channel subunits can assemble into homotetramers as well as heterotetramers (**Fig 2**). It has been suggested that the sequence similarities between TRPC subclasses (between TRPCs 1, 4 and 5 *vs*. TRPCs 3, 6 and 7) might underlie their preference for heteromerization (Schaefer 2005). However, as yet, a rule that governs heteromerizing combinations has not been established. Empirically determined heteromerizing partners that have been identified so far are: TRPC1 with TRPC3, 4, 5, 7; TRPC3 with TRPC4; TRPC3 with TRPC6, 7; TRPC4 with TRPC5; TRPC6 with TRPC3, 7; TRPC7 with TRPC3,6 (Poteser, Graziani et al. 2006, Ambudkar and Ong 2007).

The isoforms TRPC1, 3, 4, 5, 6, 7 are ubiquitous in human tissues with varying heteromerizing-combinations and expression levels. As a consequence of this, they show diverse functions throughout the body (Abramowitz and Birnbaumer 2009). The exception - TRPC2, is a pseudogene in humans (Wes, Chevesich et al. 1995), apes and old world monkeys (Zhang and Webb 2003). However, in mice and rats it plays a principal role in pheromone sensing (Freichel, Vennekens et al. 2004).

With the exception of TRPC4 and TRPC5, all mammalian isoforms are maximally activated downstream of the G_q-PLCβ or PLCγ pathways (**Fig. 1**). TRPC5 can be maximally activated downstream of $G_{i/o}$ protein activation in addition to G_q-PLCβ or PLCγ activation. However, maximal activation of TRPC4 is highly selective to $G_{i/o}$ activation (Otsuguro, Tang et al. 2008, Jeon, Hong et al. 2012).

1.2 Basic structure of TRPCs

Each TRPC subunit consists of six transmembrane segments (S1-S6) with both N and C termini located in the cytoplasm (**Fig. 2a**). The P-loop is found between the segments S5 and S6, similar to the P-loop of voltage-gated potassium (K_v) channels and determines ionic selectivity. Composite channels are formed when four subunits assemble to form a tetramer (**Fig. 2b**). Similar to K_v channels, two sets of interactions are involved for assembly – one between N termini and the other between C termini and N termini of different subunits (Lepage, Lussier et al. 2006). TRPC3, 6, 7 share ~75% homology and TRPC4, 5 share 65% homology. All TRPC isoforms contain the conserved amino acid sequence EWKFAR (the TRP domain), which is also common, with less conservation, to the TRP superfamily at the C-termini. They have upto 4 ankyrin-like repeats at their N termini which are thought to be important for heteromerization and lipid and protein interactions (Gaudet 2008). TRPCs have a competitive Ca^{2+}/CaM (calmodulin) and IP_3 receptor (IP_3R) binding (CIRB) site at their C termini (Zhang, Tang et al 2001). Along with CaM and IP_3R, all TRPC isoforms participate in a diverse range of protein-protein interactions with STIM, Orai, SESTD1, Homer, Junctate, sodium hydrogen exchanger regulatory factor (NHERF) and several other proteins (Kiselyov, Kim et al. 2005, Ong and Ambudkar 2011). As this work primarily deals with TRPC4 (and to a lesser extent TRPC5), the domains of TRPC4 and TRPC5 subunits are labeled in detail in **Fig. 3** below.

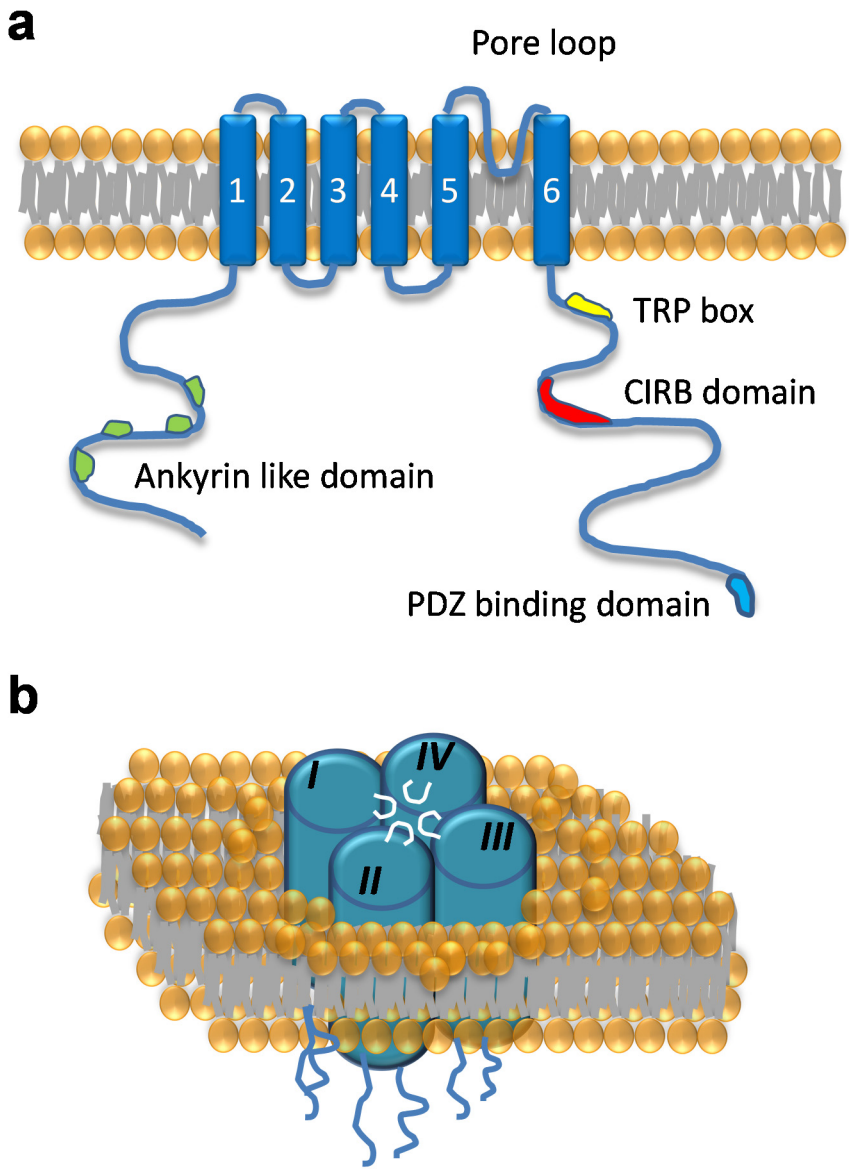

Figure 2. Topology of TRPC channels

a. Rendering of a single TRPC subunit (not to scale) consisting of cytoplasmic N and C termini and 6 transmembrane segments. Various protein and lipid interacting domains on N and C termini are indicated. **b**. A TRPC-containing channel is formed by assembly of four subunits into homomeric or heteromeric complexes with each subunit contributing a pore loop (P-loop) that imparts the selectivity filter to the channel complex.

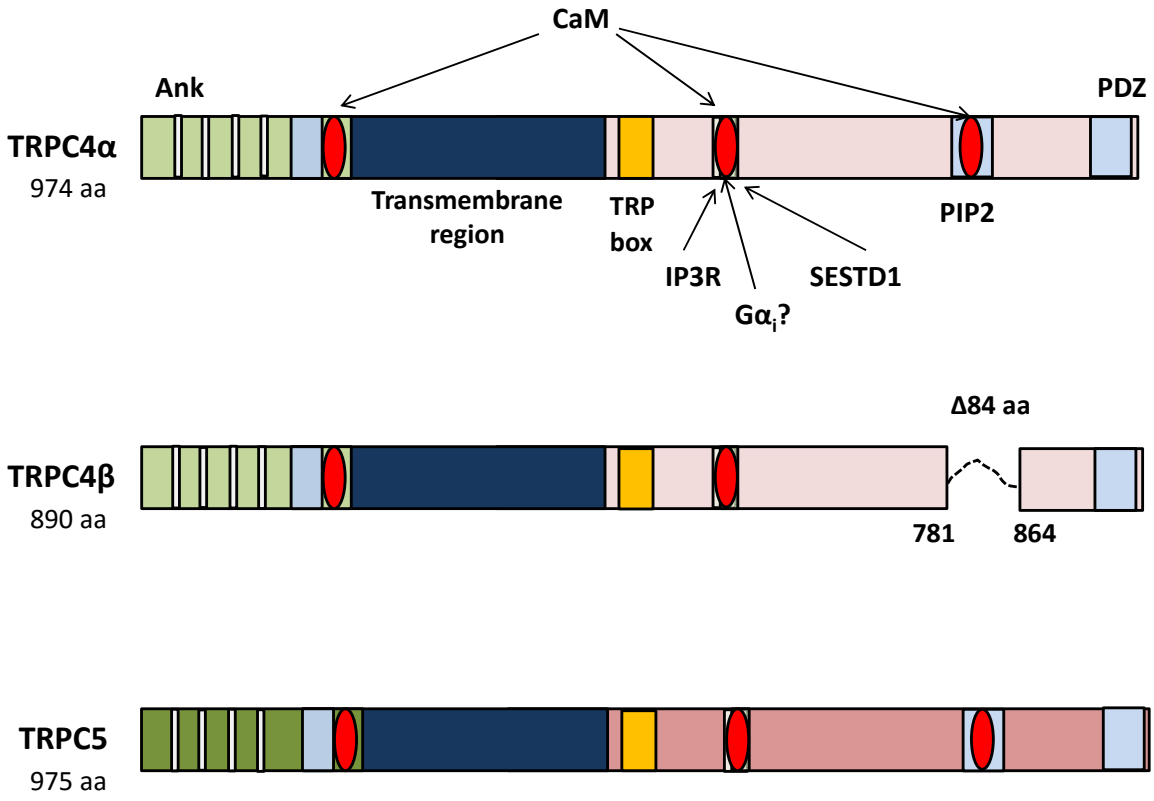

Figure 3. Important domains in TRPC4 and TRPC5

An 84 amino acid region encoding a phosphatidylinositol (4,5)-bisphosphate (PIP_2) and CaM binding site is truncated in TRPC4β, as compared to the TRPC4α isoform. TRPC5 is closely homologous, yet shares only a 65% sequence similarity with TRPC4α with maximum diversity seen in the C termini of the two proteins with 44% identity measured using NCBI Protein BLAST. Ank: ankyrin-like domain, SESTD1: SEC14 and spectrin domains 1

1.3 Endogenous regulatory pathways

Stimulation of $G_{q/11}$ coupled receptors and RTKs activates downstream effectors phospholipases PLCβ and PLCγ, respectively, which hydrolyze the membrane phospholipid PIP_2. The products of phosphatidylinositol (4,5)-bisphosphate (PIP_2) hydrolysis are diacylglycerols (DAG) and IP_3. Though the precise mechanism is not fully understood, DAG directly activates TRPC3, 6, 7 but has no effect on the activity of TRPC4 and 5. The other product of PIP_2 hydrolysis, IP_3 activates IP_3 receptors expressed on the membranes of intracellular Ca^{2+} stores

such as the endoplasmic reticulum - releasing Ca^{2+} into the cytosol which can sensitize TRPC4, 5 activity and desensitize TRPC3, 6, 7.

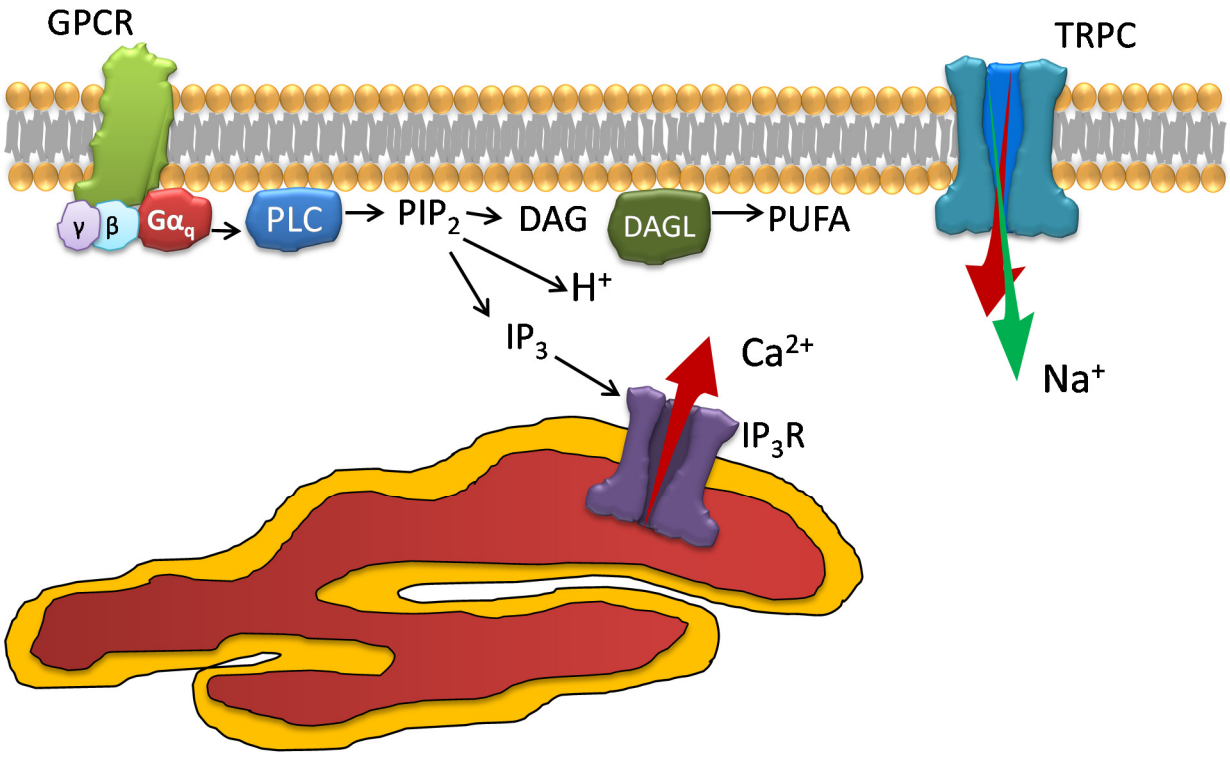

Figure 4. Activation mechanism of TRPC channels

The G_q-PLC pathway that induces TRPC activation contains several elements downstream of PIP_2 hydrolysis that differentially modulate TRPC isoforms. Several DAG species and polyunsaturated fatty acids (PUFAs) have been shown to be essential for *Drosophila* TRP activation (Chyb, Raghu et al. 1999). Protons generated during hydrolysis of PIP_2 modulate the *Drosophila* TRP activation (Huang, Liu et al. 2010). However, their role in the modulation of mammalian TRPCs is not well understood.

Ca^{2+}, Ca^{2+} binding proteins, IP_3 receptors and phosphokinases modulate all TRPC isoforms. As mentioned before, uniquely, $G_{i/o}$ coupled receptors have been shown to have an excitatory effect on TRPC4 and TRPC5 (Otsuguro, Tang et al. 2008, Jeon, Hong et al. 2012). In addition to being key players in Receptor Operated Calcium Entry (ROCE) (De Petrocellis and Di Marzo 2009), direct sensitivity to Ca^{2+} or to Ca^{2+} sensing proteins such as CaM and stromal

interacting molecules (STIMs) also allows TRPCs to participate in Store Operated Calcium Entry (SOCE) (Li, Sukumar et al. 2008, Blair, Kaczmarek et al. 2009, Gross, Guzman et al. 2009)

Influx of Ca^{2+} and GPCR activation can also lead to vesicular trafficking to the plasma membrane. TRPCs sequestered in vesicular membranes are therefore trafficked to the plasma membrane downstream of Ca^{2+} influx/GPCR activation after which they show increased basal and/or stimulated activity. Therefore, there are several distinct modes of TRPC recruitment: by G protein activation, PLC activation, trafficking to the plasma membrane and intracellular increase in Ca^{2+}.

1.4 Ionic selectivity and effects on membrane excitability

Though all TRPCs are non-selective for cations, their preference for conduction of Ca^{2+} over Na^{+}, Mg^{2+}, K^{+} and other cations varies individually and is not predicted by their sequence or subclassification mentioned above. There is considerable variation in the ionic specificities measured in different laboratories. For example, Gees et al. collected the assortment of permeability measurements which show that: while relative permeability for Ca^{2+} over Na^{+} can be upto 10:1 (for $P_{Ca2+}/P_{Na+(or\ Cs+)}$: TRPC5 >TRPC6 >TRPC7 >TRPC2 >TRPC3 >TRPC4 >TRPC1), a few studies indicate more permeability for Na^{+} than Ca^{2+} for some but not all TRPC isoforms (Gees, Colsoul et al 2010)(Eder, Poteser et al. 2005). For all isoforms, the total cationic influx ($I_{Na+} + I_{Ca2+}$) can sufficiently depolarize the membrane to activate voltage gated calcium channels which trigger contraction in smooth muscle cells and activation of voltage gated sodium channels in neurons (Gross, Guzman et al. 2009, Phelan, Shwe et al. 2013). Additionally, some TRPCs directly couple to membrane ion transporters such as the Na^{+}-Ca^{2+} exchanger (NCX) (Eder, Probst et al. 2007). NCX operation depends on the membrane potential and concentration

gradients for Na^+ and Ca^{2+}. In the 'forward mode', when cytosolic Ca^{2+} levels rise, it transports Ca^{2+} out of the cell to restore resting Ca^{2+} levels inside the cell and transports Na^+ inwardly in exchange of Ca^{2+} efflux. The Na^+ influx through TRPC channels raises intracellular [Na^+], which drives the "reverse mode" of NCX. This reverses the action of the exchanger for Na^+ efflux and Ca^{2+} influx, amplifying the Ca^{2+} load in the cell (Eder, Poteser et al. 2005, Eder, Probst et al. 2007). Moreover, NCX can function in both 'forward' and 'reverse' modes in different locations of the cell depending on local membrane ionic environments. Therefore, in combination with TRPC activity, NCX activity adds another significant dimension in the spatiotemporal modulation of $[Ca^{2+}]_i$ and membrane potential. TRPCs also associate with large conductance Ca^{2+}-activated potassium (BK) channels which are activated by Ca^{2+} influx through TRPCs (Kwan, Shen et al. 2009). Activation of BK hyperpolarizes the membrane. Therefore, though the spatiotemporally localized effect of TRPC activation is a depolarizing cationic influx, globally - TRPC activation may cause either depolarization or hyperpolarization, depending on association with other proteins either directly or in signal-complexes. The ionic selectivity of heteromeric TRPCs has not been thoroughly investigated and is of particular interest in order to determine whether natively expressed TRPCs function solely as $[Ca^{2+}]_i$ modulators or also as key mediators of membrane excitability.

1.5 Sensitivity to lipids and endogenous/exogenous ligands

The effects of the membrane phospholipid PIP_2 on TRPCs are varied and complex. PIP_2 inhibits TRPC3, 6 and 7 (Albert, Saleh et al. 2008, Itsuki, Imai et al. 2014) whereas PLC hydrolysis of PIP_2 is essential for TRPC4 and TRPC5 activation as the application of exogenous PIP_2 inhibits TRPC4 and TRPC5 activities (Otsuguro, Tang et al. 2008, Kim, Kim et al. 2008,

Trebak, Lemonnier et al. 2009, Kim, Jeon et al. 2013). However, depletion of PIP_2 using phosphatases other than PLC inhibited TRPC5, implying that a critical initial level of PIP_2 has to be maintained at the plasma membrane for the activation of these channels (Trebak, Lemonnier et al. 2009). Whether the PIP_2 dependence of the current stems from a PIP_2 dependent membrane localization is not known. In studies conducted in human platelets, TRPC1, 4, 5 were shown to localize in detergent resistant cholesterol rich lipid rafts and that disruption of this localization resulted in a reduction of channel response to agonist application (Brownlow and Sage 2005). TRPC3, 6 are found in two populations – lipid raft bound and 'freely floating' in the plasma membrane unaffected by cholesterol depletion. However, these effects vary by cell type and may depend on several other factors such as scaffolding proteins and protein-binding partners such as caveolin-1 (Levitan, Fang et al. 2010).

Lysophospholipids such as lysophosphatidylcholine (LPC) can activate TRPCs (Flemming, Dedman et al. 2006). Group-6 phospholipase A2 (PLA2) enzymes, which generate LPC, are upstream of channel activation (Al-Shawaf, Tumova et al. 2011). Oxidized phospholipids, 1-palmitoyl-2- glutaroyl-phosphatidylcholine and 1-palmitoyl-2-oxovaleroyl-phosphatidylcholine, activated TRPC5 in a $G_{i/o}$ dependent manner (Al-Shawaf, Naylor et al. 2010). Eicosanoid compound, 20-hydroxy-eicosatetra-enoic acid (20-HETE), an important arachidonic acid metabolite, activated mouse TRPC6 (Basora, Boulay et al. 2003). Flufenamic acid can reversibly enhance TRPC6 currents at micromolar concentrations, whereas it inhibits TRPC3 and TRPC7 (Jung, Strotmann et al. 2002).

Redox states, through unknown mechanisms, can stimulate homomeric TRPC3 and heteromeric TRPC3/4 channels in native systems (Poteser, Graziani et al. 2006). Nitric oxide activates TRPC5 by S-nitrosylation of Cys553 and Cys 558 residues approached from the

cytoplasmic side and the formation of a disulfide bond that stabilizes the open state of the channel (Yoshida, Inoue et al. 2006). Paradoxically, extracellular thioredoxins or dithiothreitol can break the disulphide bridge, involving the same Cys553 residue thought to be in the extracellular loop adjacent to the ion selectivity filter of TRPC5 and potently activate the channel, implying that TRPC5 senses both oxidizing and reducing agents (Xu, Sukumar et al. 2008, Takahashi and Mori 2011).

The lanthanides La^{3+} or Gd^{3+} differentially modulate TRPC sub-families TRPC4, 5 (potentiation) and TRPC1, 3, 6, 7 (inhibition) and are therefore commonly used in laboratories to distinguish between the subfamilies. TRPC1, 3, 6, 7 are inhibited by La^{3+} or Gd^{3+} in the submicromolar to several hundred micromolar range whereas TRPC4, 5 are potentiated by these cations in the same concentration range. Although the precise mechanism of this differential modulation for TRPC channels is not known, for TRPC5, two glutamate residues situated close to the mouth of pore have been suggested to be responsible for the La^{3+} sensitivity (Jung, Muhle et al. 2003). These sites are also implicated in sensitivity of TRPC5 to protons, where low extracellular pH has a similar effect as lanthanides – inhibition of TRPC6 and potentiation of TRPC4, 5 (Semtner, Schaefer et al. 2007). Compounds containing mercury have been shown to activate TRPC4, 5 but not other TRPC isoforms. In this case, extracellular cysteine residues have been identified near the TRPC5 P-loop to be mercury sensors (Xu, Zeng et al. 2012). TRPC5 has also been shown to be sensitive to anesthetics such as halothane, chloroform and propofol though the exact mechanisms have not been identified (Bahnasi, Wright et al. 2008). Extensive characterization of TRPC5 as a detector of exogenous ionic, redox and lipid sensitive molecules has led to the channel being proposed as a toxicity sensor. Whether by homology TRPC4 or other

TRPCs also share this characteristic is not known and remains an interesting avenue for exploration.

As is the case for other TRP superfamilies, TRPCs are not gated at physiological potentials but show voltage dependent gating when depolarized to high, positive, non-physiological potentials. Stimulation of TRPCs using ligands left-shifts the voltage dependence to allow activation at physiological potentials. Though voltage dependence has not been thoroughly characterized for all TRPCs, TRPC5 has been shown to have both voltage dependent and voltage independent states (Obukhov and Nowycky 2008). Ligands, such as La^{3+}, promote reversible transitions to the voltage independent state. Membrane stretch originating from flow stress or pressure has been suggested to activate mechanically induced calcium entry into cells and TRPC1, 5, 6 have been suggested to be the channels underlying this event. While ligand independent stretch can stimulate TRPC6 via activation of G_q (Sharif-Naeini, Folgering et al. 2010). G_q independent TRPC6 mechanosensitivity has also been demonstrated (Spassova, Hewavitharana et al. 2006). It has been suggested that temperature changes can also regulate TRPC activity, though only homomeric TRPC5 has been shown to be highly sensitive to temperature changes in the range of 37-25 ºC (Zimmermann, Lennerz et al. 2011).

Dissecting TRPC-activated pathways and their physiological significance and identification of specific targets for therapy are often complicated by the fact that they contribute to both SOCE and ROCE in concert with STIM, homomeric TRPC1 and Orai proteins. An additional complicating factor is that they can heteromerize to significantly alter the properties of the assembled channels, such as in the case of TRPC1 heteromerizing with TRPC4 or TRPC5, where the conductance of the channel is reduced by 10-fold. At the single channel levels there is little agreement over the measured conductance, with different values for the same channel being

reported by different groups. It has been suggested that heteromerization and different pore structures may account for this variation and add to the diversity of TRPC modalities.

1.6 Drugs targeting TRPCs

Thermo-sensitive TRPs have attracted a majority of the early efforts in drug discovery as they offer viable and specific targets for pain treatment (several thermo-TRP antagonists are in clinical trials). In comparison, the screening and identification of drugs for TRPCs is in its nascent stages. The lack of specific agonists/antagonists for TRPCs has also hindered wider exploration of their physiological roles. Many experimentally used blockers, such as flufenamic acid and 2-aminoethoxydiphenyl borate (2-APB), have to be used at concentrations that exhibit non-specific effects and are thus unreliable for distinguishing between TRPC isoforms and for establishing the physiological role of TRPCs. However, recent discoveries of agonists and antagonists for TRPC isoforms, such as ML-204 which is a specific antagonist of TRPC4 and TRPC5 (Miller, Shi et al. 2011), englerin-A which has been identified as a specific TRPC4 and TRPC5 activator (Akbulut, Gaunt et al. 2015), SAR7334 which inhibits TRPC6, TRPC3 and TRPC7 (but not TRPC4 and TRPC5) (Maier, Follmann et al. 2015) and pyrazoles (Pyr6 and Py10) which can distinguish between TRPC3 and Orai mediated ROCE (Schleifer, Doleschal et al. 2012), provide important experimental- and possibly, therapeutic- tools.

While cryogenic-electron microscopy (cryo-EM) structures have been constructed for TRPV1 (Cao, Liao et al. 2013, Liao, Cao et al. 2013) and TRPA1 (Paulsen, Armache et al. 2015), neither X-ray crystallographic nor cryo-EM techniques have been applied to TRPC isoforms. In conjunction with physiological and biochemical assays, drug screens and structure elucidation would provide a more comprehensive picture of TRPC regulatory mechanisms and pharmacology.

1.7 Physiological functions of TRPC isoforms

1.7.1 TRPCs in the nervous system

Relatively high expression levels of TRPCs and heterogeneity of expression in the nervous system has stimulated several research groups to focus on the function of TRPCs in different brain regions (Strübing, Krapivinsky et al. 2001, 2003, Fowler, Sidiropoulou et al. 2007). Significant contribution of TRPCs have been noted in neuronal development, synaptic function (Abramowitz and Birnbaumer 2009, Bollimuntha, Selvaraj et al. 2011), and neuromodulation in mature neurons - where TRPC channels mediate membrane depolarization downstream of GPCR and neurotrophin receptor stimulation (Plant and Schaefer, 2005, Bollimuntha, Selvaraj et al. 2011, Li, Xu et al. 1999, Amaral and Pozzo-Miller 2007). TRPC knock-out (KO; also denoted by '-/-') mice and rats (in which individual or groups of TRPCs encoding genes have been inactivated) have been useful laboratory tools for examining physiological roles of TRPCs. Reminiscent of the sustained cationic influx associated with the *Drosophila* TRP, mammalian TRPC-mediated $[Ca^{2+}]_i$ elevation and membrane depolarization are slow and long lasting compared to NMDA, AMPA or voltage gated channel behavior. These differences in kinetics have been noted to be potentially important for the modulation of learning and memory associated long-term potentiation (LTP), long-term depression (LTD), and synaptic plasticity.

In the nervous system, TRPC isoforms have been observed to have diverse functions. TRPC1 is widely expressed in different brain regions and influences the function of other TRPC isoforms. In astrocytes isolated from the mouse visual cortex, TRPC1 contributes to $[Ca^{2+}]_i$ increase downstream of GPCR stimulation, leading to glutamate release (Malarkey, Ni et al. 2008). In cultured *Xenopus* spinal neurons, TRPC1 is necessary for the turning of growth cones (Shim, Goh et al. 2005, Wang and Poo 2005).

Although TRPC2 is a pseudogene in humans, apes and old-world monkeys, it has high expression levels in other mammals. In mice, it is expressed in the vomeronasal organ, dorsal root ganglion (DRG) and brain. However, in rats, its expression is thought to be restricted to the vomeronasal organ (Löf, Viitanen et al. 2011). TRPC2 is essential for olfactory signal transduction. $TRPC2^{-/-}$ mice showed significant effects in social and sexual behavior with reduced aggression in both males and females and a lack of sexual discrimination during mating (Stowers, Holy et al. 2002, Leypold, Yu et al. 2002).

Lateral septal (LS) neurons express high levels of TRPC4-containing channels along with group I metabotropic glutamate receptors (mGluRs). TRPC4-containing channels integrate mGluR stimulation with intracellular Ca^{2+} signals to generate two inter-convertible depolarization responses – 1) a below threshold depolarization (BTD) characterized by an immediate increase in firing rate and 2) an above-threshold-plateau-depolarization (ATPD) characterized by an initial burst followed by a pause of firing (Tian, Thakur et al. 2013). BTD and ATPD are entirely absent in $TRPC4^{-/-}$ mice. Therefore, TRPC4, downstream of metabotropic receptor activation, directly affects excitability of LS neurons. The inter-conversion of BTD and ATPD depends on the strength of activation of TRPC4, which in turn, might depend on the strength of the receptor and G protein stimulation in addition to $[Ca^{2+}]_i$ rise.

Showcasing a severe effect, stimulation of mGluRs in mouse brain slices resulted in elicited epileptiform discharges in CA1/CA3 neurons (Wang, Bianchi et al. 2007, Phelan, Shwe et al., 2013). The CA1 discharge is absent in either $TRPC1^{-/-}$ or $TRPC1^{-/-}/TRPC4^{-/-}$ (double KO) mice but is unaffected in $TRPC5^{-/-}$ mice (Phelan, Shwe et al., 2013). In $TRPC5^{-/-}$, (but not $TRPC1^{-/-}$ or $TRPC1^{-/-}/TRPC4^{-/-}$) LTP in Schaffer collateral synapses (in the hippocampal CA1) is ablated,

strongly indicating divergent and distinct roles for TRPC1/C4 and TRPC5 channels in the hippocampus (Phelan, Shwe et al., 2013).

TRPC1/4- and 5-containing channels have also been identified as mediators in excitotoxicity. The hippocampi and dorsolateral septa of $TRPC1^{-/-}/TRPC4^{-/-}$ mice and hippocampi of $TRPC5^{-/-}$ mice show reduced seizure-induced neuronal death (Phelan, Mock et al., 2012), implying that TRPC1, 4, 5 positively influence membrane polarity in these cells.

TRPC channels in rat Purkinje cells mediate mGluR1 dependent induction of cerebellar LTD (Chae, Ahn et al. 2012). TRPC3-containing channels are highly expressed in mouse cerebellar Purkinje cells where they regulate slow excitatory postsynaptic current (sEPSC) (Hartmann, Dragicevic et al. 2008). Interestingly, in addition to $G_{q/11}$-PLCβ signaling, activation of TRPC3-containing channels in Purkinje cells was seen to require stimulation of phospholipase D (PLD) (Glitsch 2010) and was insensitive to inhibition by protein kinase C (PKC), protein kinase G (PKG) (Nelson and Glitsch 2012), and Ca^{2+} - the known negative regulators of TRPC3. This was shown to be due to the expression of an alternative splice variant of TRPC3 that lacks the TRPC3 CIRB site (Kim, Wong et al. 2012). Strikingly, a gain-of-function TRPC3 mutation in mice leads to an impaired walking phenotype called the moonwalker syndrome (Becker, Oliver et al. 2009). These mice exhibit cerebellar ataxia and Purkinje cell loss, demonstrating that TRPC3-containing channels in cerebellar Purkinje neurons underlie the mechanism of mGluR1 evoked sEPSC and that this pathway is essential for cerebellar LTD and motor coordination.

Expression of TRPC6 peaks at P7–P14 in the rat hippocampus. Through the CaM Kinase IV (CaMKIV) – cyclic AMP response element-binding protein (CREB) pathway, TRPC6 promotes dendritic spine and excitatory synapse formation (Tai, Feng et al. 2008, Zhou, Du et al. 2008). In hippocampal pyramidal neurons, brain-derived neurotrophic factor (BDNF) activates

TRPC6 via the TrkB-PLCγ pathway. In developing neurons, mammalian target of rapamycin (mTOR) activation causes translocation of GluA1, a subunit of the calcium conducting AMPA receptor transiently expressed during early postnatal formation of glutamatergic synapses. Ca^{2+} influx through TRPC6 stimulates CaMKK followed by Akt phosphorylation which leads to mTOR activation in these cells. Thus, TRPC6 activity is linked to increasing synaptic strength. TRPC5 has also been shown to be upstream of mTOR in a similar manner (Fortin, Srivastava et al. 2012). However, TRPC5 and TRPC6 have been shown to have converse effects on dendritic growth. BDNF and neurotrophin-4 activation of TRPC6 through TrKB-PLCγ promotes dendritic growth downstream of CaMKIV, whereas neurotrophin-3 stimulation of TRPC5 through TrkC-PLCγ inhibits dendritic growth downstream of CaMKIIα (He, Jia et al. 2012). Similarly, TRPC4 signaling downstream of $G_{i/o}$ stimulation in neurons, which is currently under investigation, may have cross-talk with both TRPC5 and TRPC6 functions.

1.7.2 TRPCs in the cardiovascular system

Calcium signaling is central to normal heart function and signaling abnormalities that underlie cardiac arrhythmias, hypertrophy and heart failure. In normal heart function, Ca^{2+} channels are responsible for the initiation and modulation of cardiomyocyte contractility, regulation of vascular tone via regulation of vascular smooth muscle cell (VSMC) contractility and permeability of endothelial cells (ECs). As transducers of both ROCE and SOCE, TRPCs play significant roles in these processes.

ECs lining the blood vessel wall control permeability between blood and tissues, regulate VSMC contractility, participate in immune responses and regulate angiogenesis. $[Ca^{2+}]_i$ signaling is central to all of these processes. Ca^{2+} influx through TRPCs has been implicated in endothelial

barrier function – increased Ca^{2+} influx increases endothelial permeability (Cioffi, Lowe et al. 2009, Cioffi, Barry et al. 2010, Ahmmed and Malik 2005). Specifically, for TRPC1, upon stimulation with thrombin, the small GTPase RhoA can drive IP_3R interaction with TRPC1 at the plasma membrane of ECs, leading to an increase in SOCE, with resultant increase in endothelial permeability (Mehta, Ahmmed et al. 2003). In $TRPC4^{-/-}$ mice, defects in microvascular permeability, SOCE in ECs and endothelium-dependent vasorelaxation have been observed but a direct effect on VSMC function has not been seen (Tiruppathi, Freichel et al. 2002, Ahmmed and Malik 2005). Additionally, in the $TRPC4^{-/-}$ mice, ROCE in aortic ECs and the vasorelaxation of aortic rings induced by acetylcholine is reduced (Freichel, Suh et al 2001).

In VSMCs, TRPC6 contributes to ROCE in response to α1-adrenergic receptor and vasopressin receptor activation and has also been identified as a stretch sensor in myogenic tone regulation (Guibert, Ducret et al. 2008, Sharif-Naeini, Folgering et al. 2010). In bovine aortic ECs, TRPC6-mediated Ca^{2+} influx is obligatory for the inhibitory actions of LPC on cell migration. The mechanism of LPC-induced inhibition of cell migration is an excellent illustration of TRPC determined spatiotemporal Ca^{2+} signaling and crosstalk between different TRPC isoforms. LPC activates TRPC6 to transiently increase Ca^{2+} influx which triggers plasma membrane localization of TRPC5. TRPC5 activity then gives a prolonged Ca^{2+} influx that inhibits EC migration (Chaudhuri, Colles et al. 2008).

Several interesting observations have been made with dominant negative (dn) forms of TRPCs. dnTRPC3, dnTRPC4 or dnTRPC6 mice were found to be partially protected from loss of cardiac function following long-term pressure-overload. Additionally, dnTRPC4 inhibited the activity of native TRPC3, 6, 7 subfamily in the heart, demonstrating that the two subfamilies (TRPC1, 4, 5 and TRPC 3, 6, 7) can function in coordination (Wu, Eder et al. 2010).

TRPC expression in the sino-atrial node pacemaker cells underlies SOCE which regulates the pacemaker firing rate. Though specific isoforms were not identified, as Gd^{3+} inhibits this activity TRPC1, 3, 6, 7 seem to be the likely candidates (Ju, Chu et al. 2007).

The most common pathway that has emerged from studies identifying TRPCs in cardiomyocyte function is the TRPC-calcineurin-nuclear factor of activated T-cells (NFAT) axis, which regulates gene transcription (Eder and Molkentin 2011, Kuwahara, Wang et al. 2006). Calcineurin is a calcium-dependent serine-threonine phosphatase which activates NFAT, which in turn binds to the promoter region of TRPC1, 3, 6, leading to a further increase in Ca^{2+} influx. Therefore, there is a positive-feedback mechanism involving these three TRPC isoforms (Rowell, Koitabashi et al. 2010). The positive feedback cycle can be triggered with an assortment of stimuli. In hypoxic conditions, for example, hypoxia-inducible factor-1 alpha (HIF-1α) which is a transcriptional regulator of hypoxic response, through an unknown mechanism upregulates TRPC3 and TRPC6, leading to an increase in Ca^{2+}-calcineurin signaling, setting off hypertrophy (Chu, Wan et al. 2012). Additionally, in other contractile cells such as myofibroblasts, which can differentiate into smooth muscle cells or fibroblasts, the TRPC6-calcineurin-NFAT pathway is necessary for myofibroblast driven wound healing and tissue remodeling (Davis, Burr et al. 2012).

TRPC3 activity regulates cardiac fibroblast proliferation and differentiation. Atrial fibrillation triggers increased expression of TRPC3 and causes TRPC3-dependent enhancement of fibroblast proliferation and differentiation (Harada, Luo et al. 2012). In cardiomyocytes, it is known that insulin increases DAG concentration in the lipid bilayer (Okumura, Matsui et al. 1996). Consequently, in addition to increased levels of TRPC3 expression, increased TRPC3 activity with application of insulin is also seen (Fauconnier, Lanner et al. 2007). TRPC3 activity

triggered NFAT translocation to the nucleus and gene expression, however, require PKC dependent phosphorylation of TRPC3 (Poteser, Schleifer et al. 2011).

Whether expression of multiple TRPC isoforms in the same cells indicates only redundancy or can also lead to functionally significant crosstalk remains an open question. Several studies, however, indicate that both modalities are viable in VSMCs: Endothelin-A receptor-operated TRPC1, 5, 6 are mediated by class I phosphoinositide 3-kinases γ (PI3Kγ) and TRPC3, 7 by class II/III PI3K isoforms. Importantly, receptor-activated and constitutively active PI3Kγ-mediated pathways inhibit TRPC3, 7 activation (Shi, Ju et al. 2012b). Heteromerization of TRPC1 with TRPC5 confers some of the sensitivity of TRPC1 to TRPC5 in mouse VSMCs. These TRPC1/5 heteromeric channels are activated by PKC, PI-4,5-P2, PI-3,4,5-P3 (Shi, Ju et al. 2012a). In VSMCs from human veins, oxidized phospholipids can activate TRPC1/5 in a $G_{i/o}$ dependent manner and enhance cell migration without observable Ca^{2+} release in the cells (Al-Shawaf, Naylor et al. 2010). In mesenteric artery smooth muscle cells, angiotensin activation of TRPC1/5 inhibits TRPC6 activity in a Ca^{2+} and PKC phosphorylation dependent manner (Shi, Ju et al. 2010).

1.7.3 TRPCs in the pulmonary system

In pulmonary function Ca^{2+} signaling controls VSMCs and ECs to regulate the rate of blood-oxygen exchange as well as responses to inflammation arising from exposure to allergens. Several TRPC isoforms influence these functions.

In pulmonary ECs, more is known about the role of TRPC4 than other isoforms. Studies so far have focused on the role of TRPC4 in the modulation of endothelial permeability. Lung ECs from $TRPC4^{-/-}$ mice show impairment in actin stress fiber formation and reduced cell

retraction in response to thrombin stimulation. The increase in lung microvascular permeability in response to thrombin receptor activation is absent in TRPC4$^{-/-}$ mice (Tiruppathi, Freichel et al. 2002). Plus, TRPC1 and TRPC4 can interact with STIM1 to form functional SOCE channels necessary for mediating the disruption of the endothelial barrier (Sundivakkam, Freichel et al. 2012). Also, TRPC3 and TRPC4 can heteromerize to form a redox sensitive channel (Poteser, Graziani et al. 2006), imparting a redox sensitive modulatory capacity for endothelial barrier function.

It has been suggested that a complex of Orai1, STIM1 and TRPC1 is responsible for SOCE in PASMCs (Ng, McCormack et al. 2009, Ng, Airey et al. 2010). Expression of TRPC1 and TRPC4 is enhanced in pulmonary arteries of hypertensive rats and is associated with the development of hypertension (Liu, Zhang et al. 2012). As in the case with cardiovascular smooth muscle cells, the role of TRPC4 is PASMCs is not well understood. However, one study showed that low levels of extracellular ATP and CREB protein can upregulate TRPC4 in PASMCs to promote cell proliferation (Zhang, Remillard et al. 2004).

TRPC1 can form store-operated channels in pulmonary endothelial cells and induce cell shape remodeling via Ca^{2+}-induced changes in the actin cytoskeleton (Moore et al. 2013, Kwiatek, Minshall et al. 2006). TRPC1 is not active in normal airway smooth muscle cells function. It can however mediate signaling in asthmatic conditions (Xiao, Zheng et al. 2010). TRPC1 signaling in lymphocytes increases inflammation, leading to lung hyper-responsiveness in response to allergens (Yildirim, Carey et al. 2012). TRPC3 regulates resting membrane potential, intracellular calcium and consequently asthma-evoked membrane depolarization and airway hyper-responsiveness. High TRPC3 expression in tumor cells has been considered as an

independent predictor of better prognosis for patients with lung adenocarcinoma (Saito, Minamiya et al. 2011).

In conditions of hypoxia, constriction of arteries in response to low oxygen levels leads to redistribution of blood to better ventilated areas to optimize oxygenation. TRPC6 plays a significant role in the Ca^{2+} influx regulated arterial constriction (Fuchs, Dietrich et al. 2010, Fuchs, Rupp et al. 2011). Oxygen sensing enzymes such as P450 convert arachidonic acid to epoxides and increase TRPC1 and TRPC6 expression (Liu, Wang et al. 2011). Caveolin-1 interacts with TRPC1 and IP_3R and enables TRPC1-IP_3R association in caveolae upon agonist stimulation to regulate SOCE in ECs (Sundivakkam, Kwiatek et al. 2009). A gain-of-function TRPC6 mutation primes PASMCs to an exaggerated response to transcription factor NFκB which activates cellular responses to stress. This increases the risk to the development of pulmonary arterial hypertension (Hamid and Newman 2009). Development of pulmonary hypertension has also been identified downstream of TRPC6 upregulation which contributes to increased PASMC proliferation (Yu, Keller et al. 2009). TRPC6 has a prominent role in the development of chronic obstructive pulmonary disease where it modulates inflammatory signals in various cell types including mast cells, eosinophils and lymphocytes (Banner, Igney et al. 2011). Particularly, loss of TRPC6 reduces airway response to allergen exposure (Sel, Rost et al. 2008. TRPC6 and cystic fibrosis transmembrane conductance regulator are functionally coupled in airway epithelial cells and abnormal Ca^{2+} signaling in cystic fibrosis arises with loss of this coupling (Antigny, Norez et al. 2011). In lung ECs, TRPC6 contributes as an essential factor behind the development of edema (Samapati, Yang et al. 2012, Weissmann, Sydykov et al. 2012). PTEN associates with TRPC6 to target it to the plasma membrane and the PTEN-TRPC6 complex leads to increase in endothelial permeability and promotes angiogenesis (Kini, Chavez et al. 2010).

1.7.4 TRPCs in kidneys

Amongst several ion channel families that are involved in filtration, secretion and resorption processes in the kidney, TRPCs have been identified to have significant roles as modulators of Ca^{2+} signaling in normal renal function as well as disease states. Autosomal dominant poly-cystic kidney disease (ADPKD) is an inheritable disorder primarily associated with mutations in two genes PKD1 and PKD2, which ultimately lead to formation of clusters of cysts in the kidneys. This condition leads to abnormalities in cell growth, fluid secretion, and extracellular matrix along with further complications. The TRPC3, 6, 7 subfamily is again prominent: association of TRPC3 and TRPC7 with mutant PKD-2 in kidneys enhances ROCE, which leads to abnormal cell growth (Miyagi, Kiyonaka et al. 2009). Sparse evidence also links TRPC3 to basal and pathophysiological renal conditions: In the renal nephron ATP release in response to mechanical stress specifically activates TRPC3 in the apical membrane of principal cells of the collecting duct (Goel and Schilling 2010). TRPC3 is elevated in kidney ECs obtained from renal cell carcinoma patients with a history of hypertension, but not in those with normal blood pressure (Thilo, Loddenkemper et al. 2009).

TRPC1/4 have also been shown to express in mouse glomerular mesengial cells though their physiological roles have not been identified (Wang, Pluznick et al. 2004). As for cardiovascular or pulmonary systems, the role for TRPC6 is prominent in renal physiology as well. Podocytes create foot projections at glomeruli to form a structure called the slit diaphragm where filtration of blood occurs. Abnormal function in podocytes leads to glomerular kidney disease. TRPC6 is expressed in podocytes and its modulation promotes stability of the slit diaphragm or adhesion of podocytes to the glomerular basement membrane, marking it as a key

player in slit diaphragm function (Kim, Anderson et al. 2012). Increased levels of angiotensin II (a peptide hormone that causes vasoconstriction) plus increase in blood pressure or shear stress can lead to upregulation of TRPC6 expression and engage angiotensin II receptor type 1 to activate TRPC6 channels, leading to closing of the slit diaphragm (Nijenhuis, Sloan et al. 2011). TRPC6 in glomerular mesengial cells is down-regulated with increased glucose levels in conditions such as diabetes and the resultant decrease in ROCE through TRPC6 contributes to impaired contractility in mesengial cells (Graham, Gorin et al. 2011). Conversely, insulin increases the surface expression of TRPC6 channels in podocytes in a nitric oxide-dependent manner as a response to maintain the stability of the glomerular filtration. However, in contradiction to this model, $TRPC6^{-/-}$ mice show no corresponding loss of function and it is believed that similar to the case of cardiovascular TRPC6, increase of TRPC3 expression compensates for the loss of TRPC6 (Dietrich, Chubanov et al. 2010).

The TRPC6-calcinerurin-NFAT pathway seen in the cardiovascular system is also prominent in renal cell types. Focal segmental glomerulosclerosis (FSGS) is a disorder inflicting scarring and inflammation on a subset of glomeruli. Gain-of-function TRPC6 mutations P112Q, R895C, and E897K result in increased NFAT-mediated transcription, increased actin polymerization, giving rise to a rigid cytoskeleton, lowered cell motility and increased cell death leading to FSGS (Dietrich, Chubanov et al. 2010, Wang, Jarad et al. 2010). However, TRPC6 has not been shown to be exclusively responsible for kidney disorders and failure. Simultaneous mutations in TRPC6 and in other targets are implicated in kidney failure arising from FSGS (Dietrich, Chubanov et al. 2010).

TRPC isoforms can also differentially regulate cell fate: Active TRPC5 can induce Rac1 activation promoting cell migration in podocytes while TRPC6 activity triggers RhoA which

inhibits cell migration. The TRPC5-Rac1 and TRPC6-RhoA signaling complexes are spatially and functionally segregated and provide signaling crosstalk that ultimately modulates cell migration (Tian, Jacobo et al. 2010).

1.8 Summary and experimental considerations

Native channels composed of TRPC4 subunits have been observed to be likely heteromeric, associating with TRPC1 subunits more frequently than with TRPC5 or other TRP isoforms. TRPC1 subunits, when heteromerized with other TRPC isoforms, act as negative regulators reducing the conductance of TRPCx by ten-fold. TRPC4/TRPC1 currents are therefore significantly small and, as their reversal potential is around 0 mV, are often not clearly distinguishable from background currents of other endogenous conductances such as chloride channels and ion transporters. Therefore, to identify biophysical mechanisms of TRPC4 activation, a heterologous expression system was used where TRPC4 overexpression produced predominantly homomeric channels (based on the large observed conductance - in spite of endogenous TRPC1 levels). Additionally, in the case of homomeric channels formed by TRPC4 and TRPC5, the characteristic signature of maximally activated currents through these channels is a current-voltage (I-V) curve which is double rectifying – with a characteristic 'dip' in the outward rectification between 40 mV to 60 mV of holding potential. Observing this distinct signature of maximally activated TRPC4 and TRPC5 channels helps to eliminate contaminating currents from other non-specific conductances.

In physiological conditions (in the caveolae of ECs or in neuronal dendritic boutons) it is more likely that these channels are activated locally and sub-maximally. It is in these conditions that the coincident signaling of $G_{i/o}$ and $G_{q/11}$ would be of significance. At low levels of $G_{i/o}$ signaling, the channels would remain silent and might only be activated when $G_{i/o}$ is supplemented

with $G_{q/11}$ stimulation. However, delineating the contributions of each pathway would be difficult due to the reasons of contaminating currents described above. Therefore, for a large part of this study, strongly activated TRPC4 or TRPC5 currents were used for the characterization of their activation mechanism(s).

While there are 11 known splice variants of TRPC4: TRPC4α, TRPC4β, TRPC4γ, TRPC4δ, TRPC4ε, TRPC4ζ, TRPC4η, TRPC4θ, TRPC4ι, TRPC4κ (Plant and Schaefer 2003), the isoforms TRPC4α and TRPC4β are most commonly found in rodents and humans (Mery, Magnino et al. 2001, Schaefer, Plant et al. 2002). Therefore, I focused on the characterization of murine TRPC4α and TRPC4β isoforms. Of these, TRPC4β, lacking the 84 amino acid PIP_2 and CaM binding site at the C terminus shows less PIP_2- (and likely CaM-) dependent inhibition and is therefore optimal for investigating the possible role of direct G protein interactions with the channel. Therefore, a significant number of assays were conducted using the murine TRPC4β isoform.

Throughout this study, the whole-cell patch clamp technique has been used predominantly. This is because TRPC channels are regulated downstream of receptor signaling and therefore there was a possibility that several cytoplasmic components were involved in the channel activation mechanism. In more parsimonious experimental conditions, such as excised patch clamp - the contributions of these components could, in principle, be observed directly. Excised patches (inside-out mode, described in **Methods, Ch. 2**) were performed in the expectation that G protein subunits might directly activate TRPC4 (similar to direct G protein activation of GIRK channels). Also, if any other cytoplasmic components were necessary, they could be added to the intracellular side subsequently. However, while single channel recordings could be performed to isolate TRPC5 (**Fig. 5**) or TRPC4 activity, addition of purified subunits of

G proteins directly to the inside-out patches did not result in an increase in activity (**Fig. 6**), suggesting that there could be additional, previously uncharacterized cytoplasmic components/conditions that are necessary for TRPC4 activation. Therefore, the whole-cell patch clamp configuration was selected for a principal number of assays.

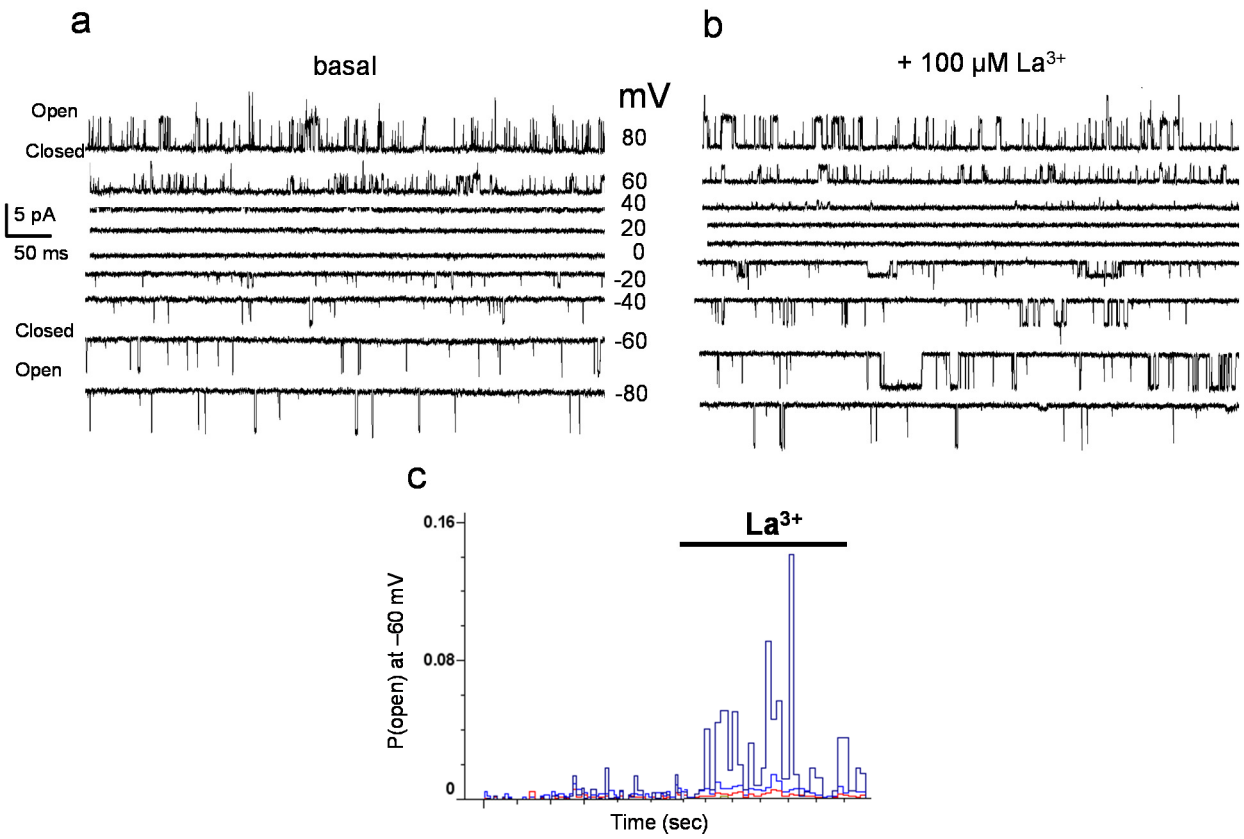

Figure 5. Excised patch clamp showing TRPC5 currents

a. In HEK293 cells stably expressing TRPC5, inside-out recordings were made using symmetric solutions, i.e., the same solution was used on both sides of the patch. The solution consisted of (in mM) 140 CsCl, 1 $MgCl_2$, 10 HEPES and 500 nM free Ca^{2+} buffered with 10 mM EGTA at pH 7.4. **b.** 100 µM La^{3+} dissolved in the same solution was added to the extracellular side by gentle pipetting in the vicinity of the patch pipette tip. **c.** P(open) was measured using Clampfit (Molecular Devices) and plotted for traces recorded at – 60 mV holding potential.

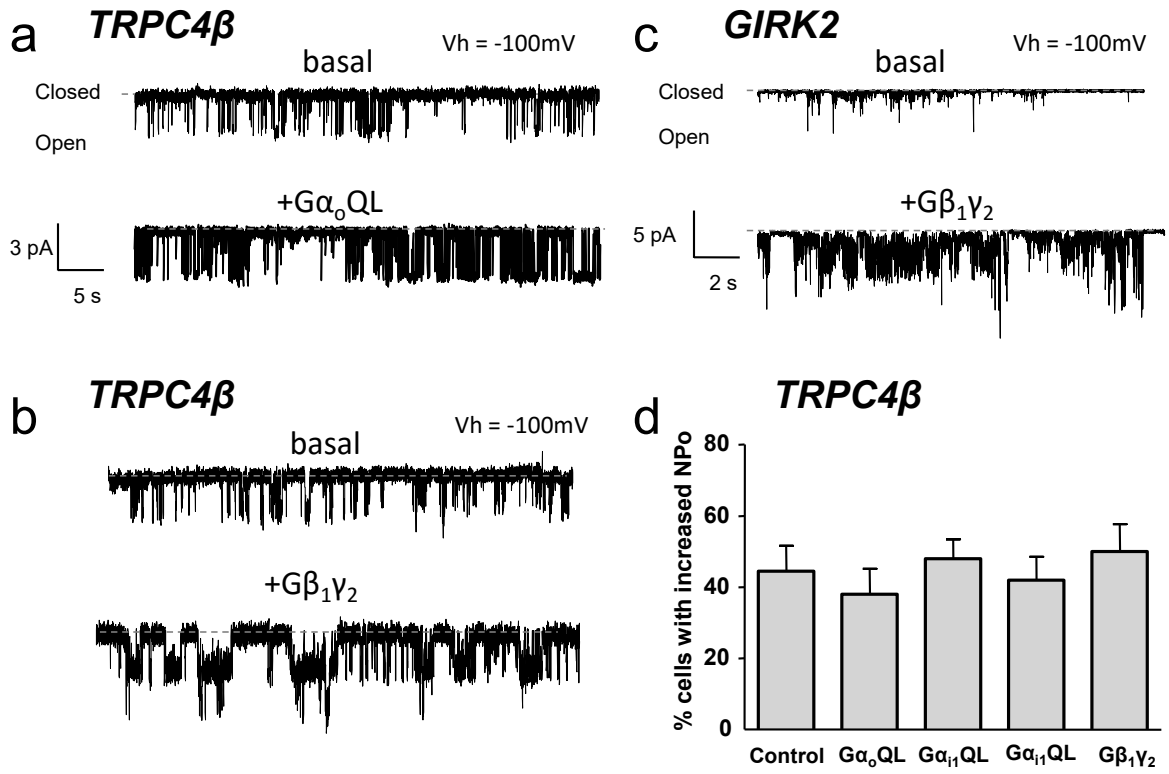

Figure 6. Inside-out patch clamp for TRPC4 currents

a.,**b.**, In HEK293 cells stably expressing μ opioid receptor (μOR) and TRPC4β, inside-out recordings were made using symmetric solutions as in **Fig. 5**. After recording basal currents at the holding potential (Vh) of -100 mV, for upto 2 mins, 10 nM (final concentration) of purified G protein subunits [kindly provided by Dr. L. Birnbaumer (NIH, NIESH) and Dr. C. Dessauer (UT)] were added to the bath solution by gentle pipetting in the vicinity of the patch pipette tip. When the storage buffers used to solubilize G proteins were added similar changes in activity were observed (not shown). **c.** To verify viability of purified $G\beta_1\gamma_2$ protein subunits, HEK293 cells were transfected with human GIRK2 cloned in a pIRES-EGFP vector. Similar 'positive' controls for $G\alpha_{i/o}$ were unavailable. Solutions used to record GIRK2 currents consisted of: 140 mM KCl, 5 mM NaCl, 1 mM EGTA, 1 mM $MgCl_2$, 10 mM HEPES (pH 7.2) (bath solution – luminal side), 5 mM KCl, 140 mM NaCl, 2 mM $CaCl_2$, 1 mM $MgCl_2$ and 10 mM HEPES (pH 7.4) (pipette solution – extracellular side). Similar to **b**., protein containing solution was added to the excised patch after 2 mins of recording basal activity. **d**. Open probability (NP_o) for patches from cells expressing TRPC4β was measured using Clampfit (Molecular Devices) (n = 25 - 40). In the control condition an equal volume of recording solution without proteins or protein storage buffer was applied.

Chapter 2

Methods

2.1 Reagents, *complementary DNA* (cDNA) and mutations

(D-Ala2, N-MePhe4, Gly-ol)-enkephalin (DAMGO) was from Bachem Chemicals Co; carbamylcholine (carbachol), heparin, ionomycin (IM), phorbol 12-myristate 13-acetate (PMA), R59 022, RHC 80267, U73122, U73343 were purchased from Sigma-Aldrich; Fura-2 AM was from TEFLabs. D-myo-inositol 1,4,5-trisphosphate (IP_3, Na^+ salt) and 1-oleoyl-2-acetyl-sn-glycerol (OAG) were from Cayman Chemical Co. Pertussis toxin (PTX) was from List Biological Laboratories, Inc. cDNA constructs for mouse TRPC4β, TRPC4α, TRPC5, PLCδ1, μ opioid receptor (μOR), and muscarinic receptors were in pIRES-neo, pIRES-hygro or PCMVSport6 vectors. cDNA for downward DAG sensor (Tewson, Westenberg et al. 2012) was obtained from Montana Molecular. cDNA construct for DrVSP was kindly provided by Dr. Y. Okamura (Okazaki Institute for Integrative Bioscience), Lyn-FRB and CFP-FKBP-Inp54p by Dr. T. Meyer (Stanford University), PLCδ1-WT, PLCδ1-ΔXY, PLCβ2 WT by Dr. J. Sondek (University of North Carolina), RhoA WT and mutants (L63 and N19) as well as C3 exoenzyme by Dr. J. Frost (University of Texas Health Science Center at Houston). PLCδ1 mutant E341R/D343R was created using the QuikChange mutagenesis method (Stratagene) and primers 5'-GGCCCGTCCCAGCAGCGAAGCCTCAGGCATCGGCAGCC-3', and 5'-GGCTGCCGATGCCTGAGGCTTCGCTGCTGGGACGGGCC-3'. Small interfering RNA (siRNA) oligomers were designed based on previously characterized sequences (Thompson and Shuttleworth 2011) (Díaz Añel 2007) (for PLCδ1 sense: 5'-CAACAAGAAUAAGAAUUCA-3', antisense: 5'-UGAAUUCUUAUUCUUGUUG-3', PLCδ3 sense: 5'-

GCAGCUCAUUCAGACCUAU-3', antisense: 5'- AUAGGUCUGAAUGAGCUGC-3', PLCβ1 sense: 5'-AACAAUUCUCCUUUCGUUUGA-3', antisense: 5'UCAAACGAAAGGAGAAU-UGUU-3', PLCβ3 sense:5'- CCUGUGGCCUCAAAUUCAA-3', antisense: 5' UUGAAUU-UGAGGCCACAGG-3') and synthesized by Sigma-Aldrich. Polyplus INTERFERin reagent (Polyplus Transfection) was used to transfect siRNA (50 nM) into cells; the transfection was repeated 48 hours later and cells used for western blotting and patch clamping assays after an additional 24 hours. Polyethylenimine (PEI) transfection reagent was kindly provided by Dr. G. Du (University of Texas Health Science Center at Houston).

2.2 Cell lines and cell culture

Human embryonic kidney 293 cells (HEK293) were grown in Dulbecco's Modified Eagle's Medium (DMEM; high glucose) supplemented with 10% heat-inactivated fetal bovine serum (FBS), 100 units/ml penicillin and 100 μg/ml streptomycin at 37°C, 5% CO_2. Stable cell lines that expressed μOR only, μOR plus TRPC4β, μOR plus TRPC4α, μOR plus TRPC5, and muscarinic receptor subtype (M2R) plus TRPC4β were created and maintained by using antibiotic selection pressure [hygromcin for μOR and M2R encoded in the pIRES-hygro vector, neomycin for TRPC4 and TRPC5 constructs encoded in the pIRES-neo vector (Miller, Shi et al. 2011)]. For experiments where transient expression was used, cells were transfected using Lipofectamine 2000 (Invitrogen) or PEI (Feng, Huang et al. 2014). For Lipofectamine 2000-based transfections in a 1 mL volume of cell culture, 0.5 μg of cDNA was mixed with 50 μL of DMEM (without FBS). Separately, 4 μL of Lipofectamine 2000 was mixed with 50 μL of DMEM (without FBS) and both mixtures were left at room temperature for 10 minutes, following which the two solutions were mixed by vortexing and then left at room temperature for a further 10 minutes. This mixture

was then added to a freshly trypsinized batch of cells at ~ 90% confluence in a poly-L-ornthine coated dish. Media were changed after 4 hours and the cells were used for experiments after 16-20 hours. For PEI-based transfections (for a 1 mL volume), cells were seeded on poly-L-orntihine coated dishes 24 hours prior to transfection. cDNA (0.5 µg) was mixed with 50 µL of sterile NaCl (0.15 M) and 4 µL of PEI reagent. The mixture was vortexed and left at room temperature for 10 mins, followed by addition to the cells containing dish. Cells were used for experiments after 16-20 hours.

2.3 Patch clamp electrophysiology

Cells were seeded on 12-mm coverslips coated with poly-L-orntihine between 4-16 hours before whole-cell recordings. Transiently transfected cells were identified by the green fluorescence from the expressed enhanced green fluorescent protein (EGFP) encoded in the plasmid for the protein of interest or the co-transfected pEGFP-N1 vector. Recording pipettes were pulled from micropipette glass (Sutter Instruments) to 3-5 MΩ when filled with a pipette solution containing (in mM): 140 CsCl, 1 $MgCl_2$, variable ethylene glycol tetraacetic acid (EGTA) or 1,2-bis(o-aminophenoxy)ethane-N,N,N',N'-tetraacetic acid (BAPTA), variable $CaCl_2$, and 10 4-(2-hydroxyethyl)-1-piperazineethanesulfonic acid (HEPES), buffered to pH 7.2 with CsOH and placed in the bath or extracellular solution (ECS) containing (in mM): 140 NaCl, 5 KCl, 2 $CaCl_2$, 1 $MgCl_2$, 10 glucose, and 10 HEPES, buffered to pH 7.4 with NaOH. Specific EGTA, BAPTA, and free Ca^{2+} concentrations in the pipette solutions are explained in figure legends. Ca^{2+}-free external solutions had 0.2 mM EGTA added and $CaCl_2$ omitted. Note, the use of NaCl in the bath solution was very important for results reported here. Several previous studies used Cs^+-based bath solutions, which strongly enhance TRPC4 currents and tend to mask the strict requirements

of channel activation on $G_{i/o}$ and PLC pathways (Zholos, Zholos et al. 2004, Jeon, Hong et al. 2012, Kim, Jeon et al. 2013).

Isolated cells were voltage-clamped in the whole-cell or outside-out mode using an Axon 200B amplifier and 1440A Digitizer (Molecular Devices). Currents were acquired at 2 kHz. For whole-cell recordings, a membrane test pulse was applied every 10 s to test for membrane resealing. Cells that resealed were eliminated from analysis. As Ca^{2+} is a key modulator in these studies, to ensure that external Ca^{2+} did not contaminate recordings, all patch-pipettes were fire-polished and cells which retained membrane seal resistance > 1 GΩ were used. Cells were continuously perfused with the bath solution through a gravity-driven multi-outlet device with the desired outlet placed ~50 μm away from the cell being recorded. Drugs were diluted to the final concentration in the bath solutions and applied to the cell at the rate of ~ 0.2 mL/min except where added through the patch pipette after dilution in the pipette solution. Intracellular dialysis was used for U73122 and U73343 to avoid the potential electrophilic effect of U73122 on reactive cysteines at the outer mouth of the P-loop (Otsuguro, Tang et al. 2008, Xu, Sukumar et al. 2008).

Outside-out patches were performed using patch pipettes demonstrating 5-7 MΩ resistance in solution. Cells were patched in the whole-cell configuration after which, with the help of the coarse-movement setting on the micromanipulator, the patch pipettes were quickly but gently pulled away diagonally above and across the cell so that the final position of the pipette tip (along with the pulled membrane) rested a few millimeters on the side of the cell which was opposite to the side from which the cell was initially approached by the pipette. This procedure was followed as it was noted that pulling the patch away from the cell back towards the side from which the cell was initially approached by the pipette often resulted in a significantly larger section of the membrane tearing away along with other internal components of the cells - resulting

in a suboptimal patch (with leaky currents and was prone to collapse during the experiment). Pulling the patch across the cell, instead, gave stable patches. After pulling, the patch was allowed to stabilize for upto 60 seconds. The patch resistance was > 1 GΩ.

Inside-out patches were performed using patch pipettes demonstrating 7-8 MΩ resistance in solution. In this case, as opposed to the procedure used for outside-out patches, it was noted that pulling the patch pipette vertically upwards from the cell resulted in a higher success of patches that showed >1 GΩ in resistance. Solutions to the luminal side were then either added via pipetting or via a gravity driven perfusion system.

Patch clamp recording data were analyzed using Clampfit (Molecular devices). For visualization, whole-cell and outside-out records were filtered at 25 Hz with a high-pass 8-pole Bessel filter. Inside-out records were filtered at 200 Hz.

The sodium acetate (NaAc) gradient method was applied and calibrated using 10 μM nigericin in KCl solutions and the proton sensitive dye BCECF (2',7'-Bis-(2-Carboxyethyl)-5-(and-6)-Carboxyfluorescein, Life Technologies) in its free acid form (calibration method is described in further detail in the figure legend of **Fig. 40**). Briefly, patch-pipette solution contained (in mM): 140 CsCl, 5 NaAc, 1 $MgCl_2$, 0.05 EGTA, and 10 HEPES, pH 7.2. Bath solutions contained (in mM): 140 NaCl, 5 KCl, 2 $CaCl_2$, 1 $MgCl_2$, 10 glucose, and 10 HEPES with equal molar replacement of NaCl by 7.9 NaAc (for pH_i = 7.2), 12.6 NaAc (for pH_i = 7.0), 39.48 NaAc (for pH_i = 6.5), 70 NaAc (for pH_i = 6.25), 100 NaAc (for pH_i = 6.1), 125.4 NaAc (for pH_i = 6.0). Induced pH was calculated based on the formula:

$$pHi = pHo - \log\left(\frac{[NaAc]extracellular}{[NaAc]intracellular}\right)$$

Solutions were allowed to dialyze into cells for 5 minutes to allow for complete replacement of endogenous intracellular buffers before start of recordings. External buffers corresponding to different pH_i values to be induced were then applied for 30 seconds before receptor activation.

2.4 Calcium and DAG imaging

HEK293 cells heterologously expressing TRPC channels were seeded on 15-mm coverslips coated with poly-L-orntihine between 4-16 hours before loading with 2 μM Fura2-AM + 0.01% F-127 at 37°C in the cell culture media for 40 minutes, after which the media were replaced with ECS (described in 2.3). Alternating excitation wavelengths at 340 nm and 380 nm were provided using the Sutter lambda-10B Smartshutter system controlled by Incytim2 software (Intracellular Imaging). Cells were visualized at a magnification of 20X or 40X on a Nikon TE200 microscope. Fluorescence images from emission at 520 nm were taken using a Basler Scout camera at the rate of 20 frames per minute. Drugs were applied via perfusion at the same rate as for patch clamp experiments. For DAG measurements, a GFP-based 'Downward DAG sensor' (Montana Molecular) containing cDNA was transfected into cells and after 16-20 hours imaged with 490 nm excitation and 535 nm emission using Incytim1 software (Intracellular Imaging).

2.5 Immunoblot

Cells were washed with ice-cold phosphate-buffered saline (PBS) followed by harvesting in a RIPA lysis buffer containing: 10 mM Tris-HCl, 140 mM NaCl, 1 mM EDTA, 1% Triton X-100, 0.1 % SDS, 0.1% sodium deoxycholate and protease inhibitors (Roche) (pH 7.4). Proteins were separated by sodium dodecyl sulfate polyacrylamide gel electrophoresis (SDS-PAGE) and transferred to polyvinylidene difluoride (PVDF) membrane (Thermo Scientific). The membrane

was blocked with a blocking buffer: 5% milk and 0.1% Tween-20 in PBS (pH 7.4) for 12-16 hrs with primary antibodies with the following dilution: rabbit anti-TRPC4 (1:500, 781EB affinity purified (Meissner, Obmann et al 2011)), anti-PLCδ1 (1:1000, Thermo Scientific), anti-PLCδ3 (1:1000, Santa Cruz), anti-PLCβ1 (1:1000, Santa Cruz), anti-PLCβ3 (1:1000, Santa Cruz), mouse anti-actin (1:5000, MP Biomedicals). After several washes with washing buffer (0.1% Tween-20 in PBS), the membrane was exposed to horseradish peroxidase-conjugated secondary antibodies (1:10,000, Roche) for 30 minutes. After extensive washes with the washing buffer, the immunoblots were visualized by exposure to an enhanced chemiluminescent susbtrate (Thermo Scientific).

2.6 Glutathione S transferase (GST) pull down assays

Mouse TRPC4α amino acids 615-974 and 765-974 were cloned in-frame into the pGEX-4T-1 vector for expression of GST-TRPC4 fusion proteins. Protein expression in *E. coli* BL21 was induced at O.D. 0.6 – 0.8 with 0.2 mM isopropyl-d-thiogalactoside for 4 h at 37 °C. The cells were subsequently collected by centrifugation and resuspended in a buffer composed of: 10 mM Tris–HCl, pH 8.0, 150 mM NaCl, 1 mM EDTA and cOmplete protease inhibitor cocktail (Roche) on ice. Following addition of 200 µg/mL of lysozyme and incubation on ice for a further 15 minutes, DTT (final 5 mM) and Sarkosyl (final 1%) were added and this was followed by incubation on ice for a further 15 minutes. The samples were sonicated until clear and supernatant was collected after centrifugation at 14000 rpm for 15 min at 4 °C. For every 360 µL of supernatant, 40 µL 20% Triton X-100 was added along with 50% gluthathione sepharose bead slurry (Life Technologies). Proteins were allowed to interact during rotation at room temperature for 30 minutes and subsequently collected by centrifugation at 5000 rpm for 5 mins. The beads

were washed 4 times with a buffer containing 0.5 % NP-40, 1 mM EDTA, 20 mM Tris, pH 8.0, and 150 mM NaCl. Proteins were extracted by addition of Laemmli buffer containing β-mercaptoethanol.

2.7 Surface biotinylation

HEK293 cells stably expressing μOR and TRPC4β were cultured on poly-L-ornithine coated dishes 12 hours prior to transfection with desired cDNA using PEI. At 24 hours after transfection, the cells were washed 2 times with ice-cold PBS, followed by incubation with 0.5 mg/mL Sulfo-NHS-S-S-Biotin (Pierce) for 30 min on ice. Unreacted biotinylation reagent was washed quickly and gently with PBS containing 100 mM glycine. Cells were harvested in a lysis buffer containing: 50 mM HEPES, 150 mM NaCl, 2 mM EDTA, 2 mM $MgCl_2$, 1% Triton X-100, and protease inhibitors (Roche) (pH 7.4). The homogenates were passed repeatedly through 23 gauge syringe needles to break DNA complexes and centrifuged at 20,000 g for 10 min at 4 °C. Protein concentrations in the supernatant were measured using a BCA assay (Pierce) and 400 μg of protein was incubated with 40 μL of 50% NeutraAvidin agarose (Pierce) in a total volume of 300 μL with PBS for 1 hr at room temperature with rotation. After NeutraAvidin agarose was washed 6 times with PBS + 0.5% Triton X-100, bound proteins were eluted with SDS sample buffer by heating in the presence of 1% β-mercaptoethanol at 55 °C for 5 min. Total protein and isolated biotinylated proteins were run on SDS-PAGE gels and immunoblotted for TRPC4 and actin.

2.8 Statistical analysis

Data are expressed as means ± S.E.M, and statistical analysis was performed using Student's paired or unpaired t-test, or ANOVA in Graphpad Prism. Differences were considered

significant when p values were < 0.05 by paired or unpaired t test or by One-way ANOVA with Newman-Keuls post-hoc test where indicated.

2.9 Graphics and data visualization

Illustrations were created in Microsoft PowerPoint. Data were processed and visualized in Clampfit (Molecular Devices), Origin (Origin Labs), Prism (Graphpad) and Microsoft Excel.

Chapter 3

$G_{i/o}$ and PLCδ1 are necessary for TRPC4 activation

3.1 Introduction

Of the large mammalian TRP superfamily, the Canonical TRP members (TRPC1-7) are closest in homology to the prototypical *Drosophila* TRP. Like the fly TRP, TRPC channels are activated downstream of receptors that signal through PLC (Venkatachalam and Montell 2007). In both heterologous and native systems, the $G_{q/11}$-PLCβ pathway has most commonly been used to activate TRPC channels. Recent studies, however, also suggest a role for $G_{i/o}$ proteins in the activation of TRPC4/C5 (Jeon, Lee et al. 2008, Otsuguro, Tang et al. 2008, Kim, Kwak et al. 2014).

TRPC4 has been implicated in the regulation of microvascular permeability (Tiruppathi, Freichel et al. 2002), dendritic neurotransmitter release (Munsch, Freichel et al. 2003), intestinal cholinergic neurogenic contraction and motility (Tsvilovskyy, Zholos et al. 2009), neurite extension (Weick, Austin Johnson et al. 2009), epileptiform burst firing and seizure-induced neurodegeneration (Phelan, Mock et al. 2012, Phelan, Shwe et al. 2013). The channel mediates Na^+ and Ca^{2+} influx, causing membrane depolarization and $[Ca^{2+}]_i$ elevation, which in turn alter cell function (Tian, Thakur et al. 2013). Though advances have been made in demonstrating TRPC4 channel activation under $G_{i/o}$ and/or PLC stimulation, as well as its dependence on $[Ca^{2+}]_i$, a precise description of signaling events underlying the mechanism of TRPC4 activation remains elusive.

In this study, I distinguished between $G_{q/11}$ and $G_{i/o}$ pathways by using $G_{q/11}$-coupled muscarinic and $G_{i/o}$ -coupled μ opioid receptors (μOR), for their contributions to TRPC4 activation. I uncovered a strict dependence on $G_{i/o}$ proteins and the PLC pathway. I focused on constituents of PLC signaling that cooperate with $G_{i/o}$ to activate TRPC4 and discovered a necessity for PLCδ1, a PLC isoform co-regulated by Ca^{2+} and PIP_2. My findings suggest that TRPC4 channels are tightly regulated by coincident signaling from $G_{i/o}$ and PLCδ1 stimulation with the latter contributing significantly to the Ca^{2+} dependence and PIP_2 regulation of channel opening.

3.2 Results

3.2.1 TRPC4 activation requires coincident $G_{i/o}$ stimulation and PLC activity

TRPC channels are commonly believed to be activated downstream from PLC stimulated by $G_{q/11}$-coupled receptors or RTK (Venkatachalam and Montell 2007). When overexpressed in HEK293 cells, both $G_{q/11}$- and $G_{i/o}$-coupled muscarinic receptors have been used to trigger TRPC4 currents (Kim, Kwak et al. 2014). However, in spite of the presence of endogenous $G_{q/11}$-coupled muscarinic receptors (**Fig. 7**), muscarinic agonist, carbachol (CCh, 10-100 μM) elicited no or very small currents in cells that stably co-expressed μOR (Miller, Shi et al. 2011) with either TRPC4β or TRPC4α (**Fig. 8a, 11a, 13**).

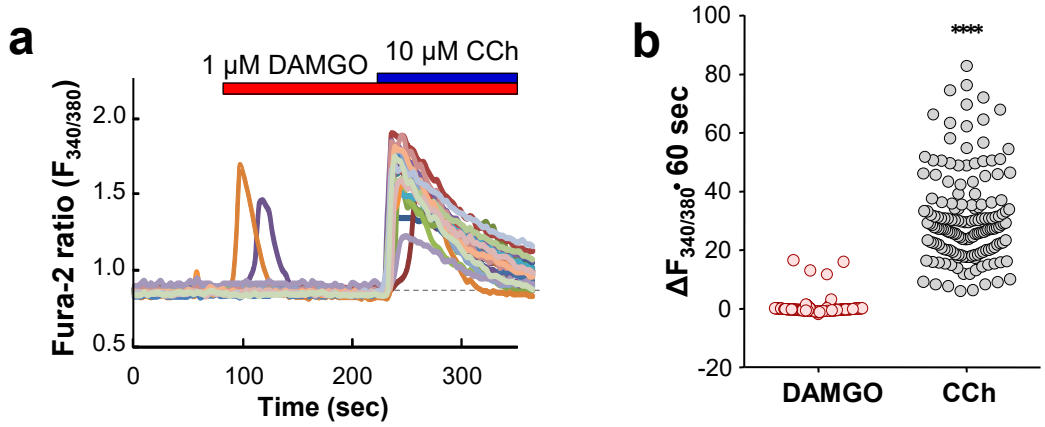

Figure 7. Ca^{2+} responses elicited by exogenously expressed μOR and endogenous muscarinic receptors in HEK293 cells

Stable μOR-expressing cells were seeded on glass coverslips and loaded with Fura-2. Cells were imaged for fluorescence ratio changes when excited alternately at 340 and 380 nm and challenged with DAMGO followed by DAMGO + CCh as indicated over representative traces in **a**. Only few cells responded to DAMGO, but all cells responded to CCh with fluorescence ratio ($F_{340/380}$) increases. Integrated ratio changes over a period of 60 sec (area under the curve) for individual cells are shown in **b.** n = 4 coverslips with a total of 177 cells. **** $p < 0.0001$ by paired *t* test. These data also show that the HEK293 cells endogenously express $G_{q/11}$-coupled muscarinic receptors that respond to CCh to elicit robust $[Ca^{2+}]_i$ increase.

Subsequent addition of μ agonist, DAMGO (1 μM), caused robust currents, with current-voltage (I-V) relationships typical for TRPC4/C5, such as a negative slope between 10 to 40 mV and outward rectification at more positive potentials (Obukhov and Nowycky 2004, Plant and Schaefer 2005, Kim, Kwak et al. 2014). The near linear I-V relation at negative potentials indicates very strong channel activation (Obukhov and Nowycky 2004, Plant and Schaefer 2005). Consistent with μOR being $G_{i/o}$-coupled, the currents were abolished by treatment with PTX (**Fig. 8a, Fig. 13**).

Interestingly, although CCh did not evoke TRPC4 currents via endogenous receptors, overexpressing $G_{q/11}$-coupled M1, M3, or M5 muscarinic receptor (MnR) with TRPC4 allowed CCh to induce such currents, which, much to our surprise, was also blocked by PTX (**Fig.8b-e, Fig. 9**). Therefore, all overexpressed MnRs seem to activate TRPC4 via $G_{i/o}$ proteins. By contrast, I found that TRPC5 activation was only partially blocked by PTX when stimulated via either endogenous or overexpressed M3R (**Fig. 12, 13**). Therefore, TRPC4 is more tightly regulated than TRPC5 and it exhibits an absolute dependence on $G_{i/o}$ proteins for strong channel activation, although very weak activation might be achieved by stimulating only $G_{q/11}$.

My data thus show that obligatory action of $G_{i/o}$ on TRPC4 was independent of receptor subtypes. However, different receptors showed varied peak TRPC4 currents. Whether these differences in peak currents occur because of variations in receptor expression levels, localization or in G protein coupling is not known.

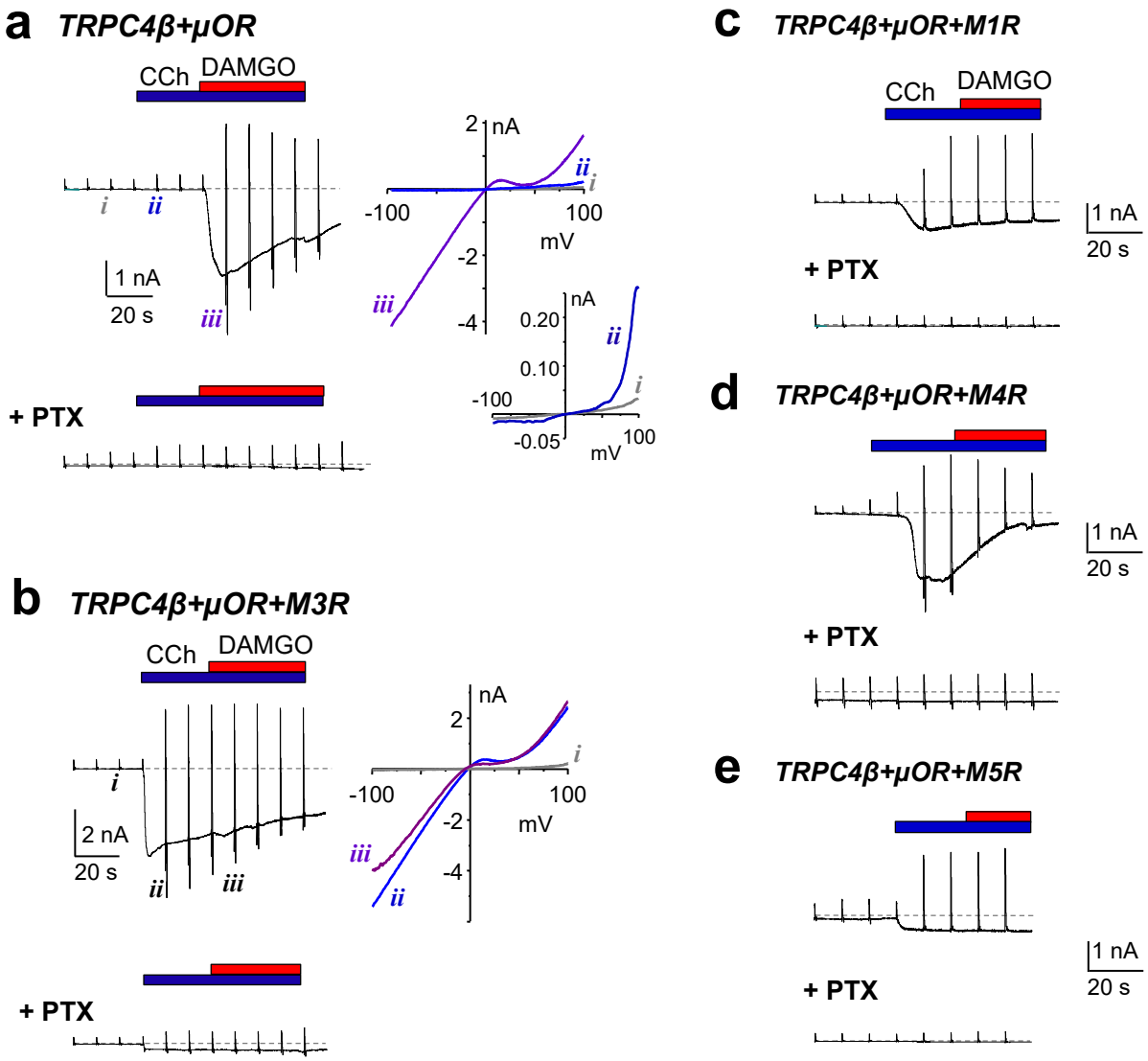

Figure 8. TRPC4β activation is dependent on $G_{i/o}$ signaling

a-c. Whole-cell currents in HEK293 cells that stably co-expressed μOR and TRPC4β (**a**) untreated (*upper panels*) or treated with PTX (0.1 μg/ml, 16 hrs, *lower panels*). In **b-e**, cells also transiently expressed M3R/ M1R/ M4R or M5R. Pipette solution contained 0.05 mM EGTA with no added Ca^{2+} for all cells. CCh (100 μM) and DAMGO (1 μM) were added as indicated. Current-voltage (I-V) relationships obtained from the voltage ramps at the indicated time points are shown to the right of the time course. Note that in the absence of M3R, and in spite of saturating concentration of CCh, CCh induced very small TRPC4β currents (**a**, and expanded I-V curves in inset); PTX inhibited activation of TRPC4β regardless of overexpression of MnR. Summary data are included in **Fig. 13**.

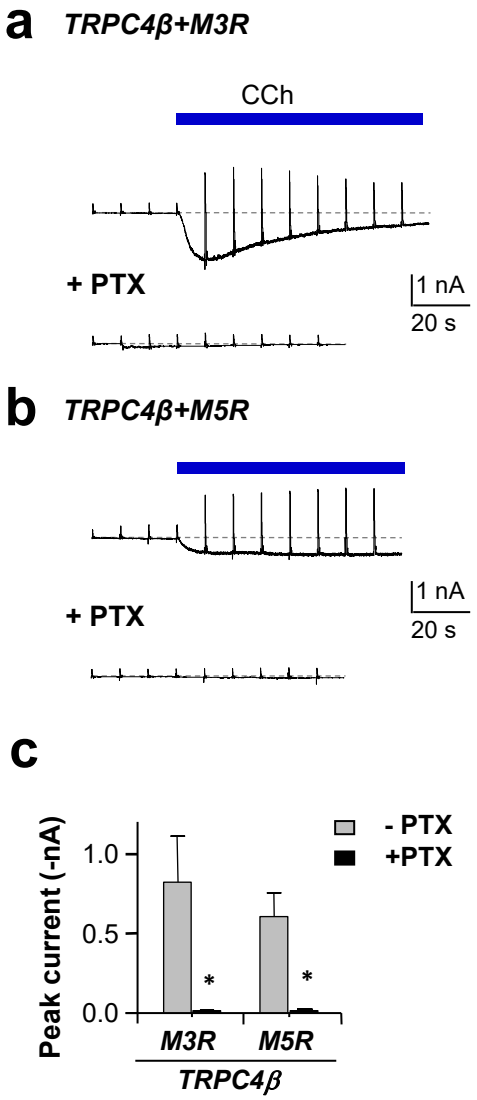

Figure 9. Overexpressed $G_{q/11}$-coupled muscarinic receptors activate TRPC4β in a $G_{i/o}$-dependent manner in the absence of μOR

Whole-cell currents evoked by CCh (100 μM) in wild type HEK293 cells that transiently expressed TRPC4β + M3R (**a**) or TRPC4β + M5R (**b**). Cells were either untreated (*upper panels*) or treated with PTX as above (**Fig. 8**). Summary (means ± SEM) for CCh-evoked peak currents at -60 mV is shown in **c**. n = 5 for each, * $p < 0.05$ *vs* -PTX by unpaired *t* test. Note the inhibition of CCh-evoked currents by PTX even in the absence of μOR overexpression, ruling out the possibility that an enhanced basal $G_{i/o}$ turnover due to the expressed μOR might be responsible for the $G_{i/o}$ dependence. Pipette solution contained 0.05 mM EGTA with no added Ca^{2+} in all cases.

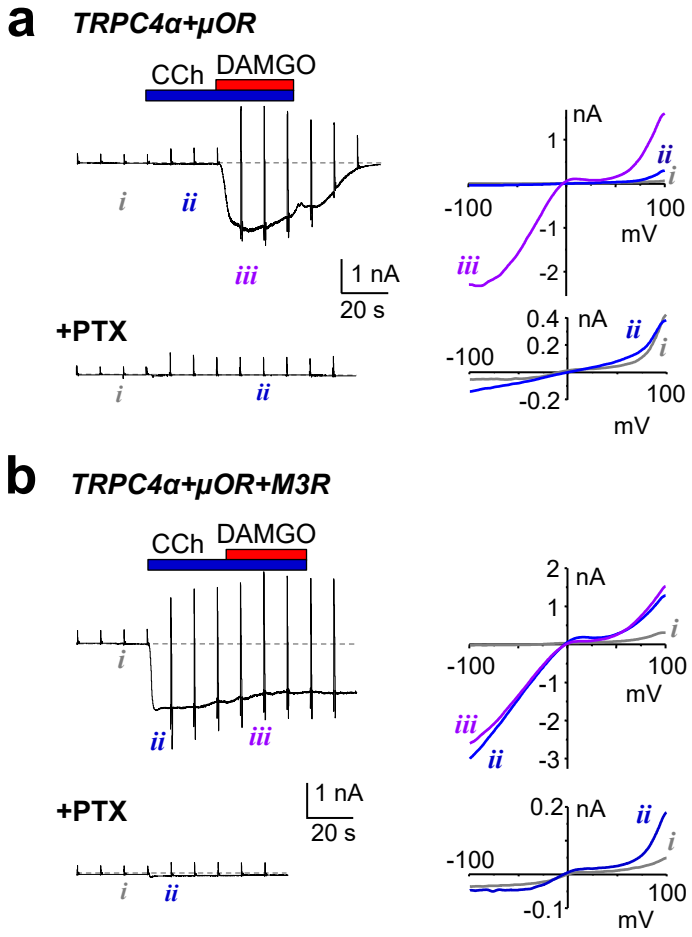

Figure 10. TRPC4α activation is dependent on $G_{i/o}$ signaling

a & **b.** Whole-cell currents in HEK293 cells that stably co-expressed μOR and TRPC4α untreated (*upper panels*) or treated with PTX (0.1 μg/ml, 16 hrs, *lower panels*). In **b**, cells also transiently expressed M3R. Pipette solution contained 0.05 mM EGTA with no added Ca^{2+} for all cells. CCh (100 μM) and DAMGO (1 μM) were added as indicated. I-V relationships obtained from the voltage ramps at the indicated time points are shown to the right of the time course. Summary data are included in **Fig. 13**.

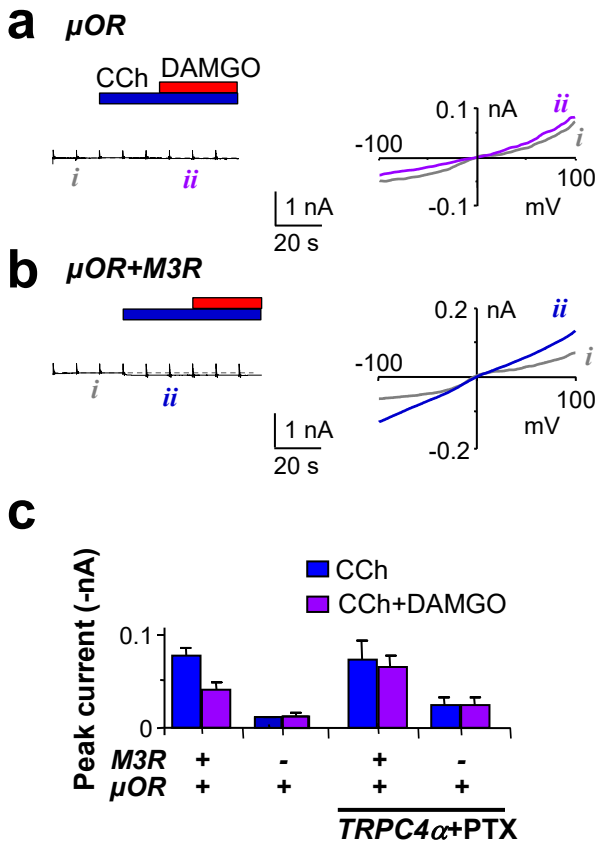

Figure 11. Endogenous currents in response to CCh and DAMGO in the absence of TRPC overexpression

Stable cells expressing only μOR were untransfected (**a**) or transiently transfected with the cDNA for M3R (**b**). In the absence of TRPC4, minimal whole-cell currents were induced by CCh (100 μM) and DAMGO (1 μM). Summary (means ± SEM) of peak current at -60 mV for **a** and **b** are shown in **c** with the same data for PTX-treated TRPC4α from **Fig.10** included for comparison. n = 5 - 7.

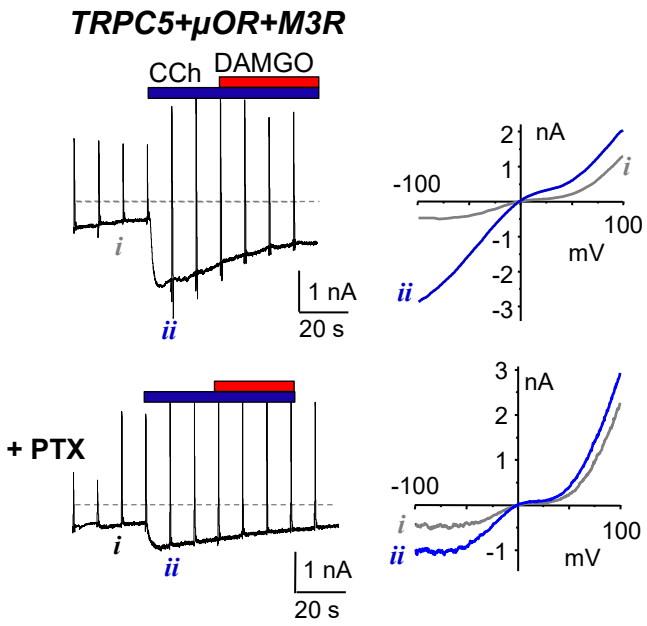

Figure 12. TRPC5 activation is partially dependent on $G_{i/o}$ signaling

Whole-cell currents in HEK293 cells that stably co-expressed μOR and TRPC5 with transiently expressed M3R, untreated (*upper panels*) or treated with PTX (0.1 μg/ml, 16 hrs, *lower panels*). Pipette solution contained 0.05 mM EGTA with no added Ca^{2+}. CCh (100 μM) and DAMGO (1 μM) were added as indicated. I-V relationships obtained from the voltage ramps at the indicated time points are shown to the right of the time course. Summary data are included in **Fig. 13.**

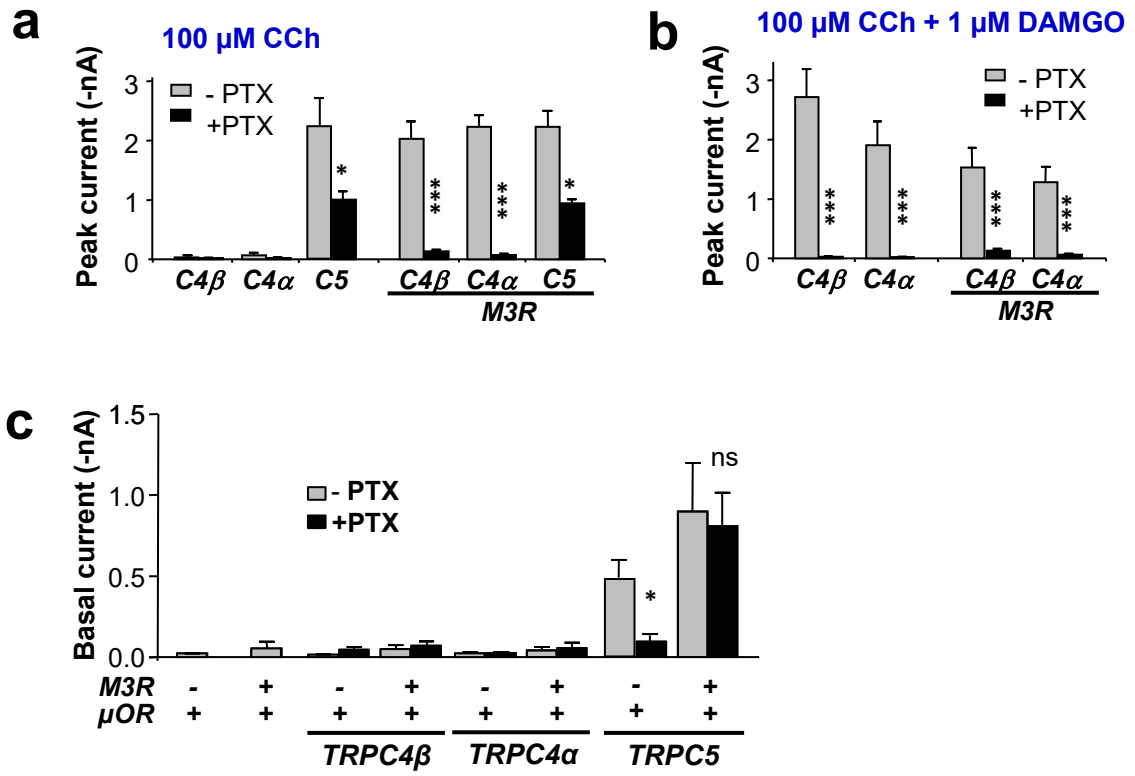

Figure 13. Comparison of basal and agonist-evoked peak currents in HEK293 cells that co-expressed µOR with TRPC4β, C4α and C5 in the absence and presence of overexpressed M3R

Summary of peak currents at -60 mV (means ± SEM) represented in **Figs. 8, 10, 12** evoked by CCh before (**a**) and after (**b**) subsequent addition of DAMGO for cells that co-expressed µOR with TRPC4β, TRPC4α, or TRPC5. Cells that co-expressed M3R are indicated. Note that PTX nearly completely inhibited TRPC4 but was only partially inhibitory to TRPC5. (n = 7 - 10, * $p \leq 0.05$, *** $p \leq 0.001$ *vs* -PTX by *t* test). **c.** Summary (means ± SEM) of basal currents (0 - 30 sec before agonist application) at -60 mV for the same cells included in **a**, as well as for those that expressed µOR ± M3R without a TRPC as in **Figure 11**. Note that TRPC5, but not TRPC4, exhibited marked basal currents. PTX significantly suppressed basal current in cells that co-expressed TRPC5 and µOR (* $p < 0.05$ *vs* -PTX by unpaired *t* test), but not in those that also overexpressed the $G_{q/11}$-coupled M3R in addition to TRPC5 and µOR (ns, not significant). Therefore, although the basal turnover of $G_{i/o}$ proteins in µOR-expressing cells could contribute to constitutive activation of TRPC5, it was extraneous when the turnover of $G_{q/11}$ proteins was also enhanced by M3R overexpression.

Summary I: $G_{i/o}$ signaling is necessary for maximal activation of TRPC4 but only partially contributes to the activation of TRPC5.

I then asked if $G_{i/o}$ stimulation alone is sufficient to activate TRPC4. With $[Ca^{2+}]_i$ weakly buffered by 0.2 mM EGTA, DAMGO (1 μM) elicited currents in a large proportion (~71%, designated as *group 1 or Grp I*) of TRPC4β/μOR-expressing cells (**Fig. 14a, 15b**). This proportion was increased to ~100% if 0.05 mM EGTA was used to buffer internal Ca^{2+} (**Fig. 14d,e**). Subsequent addition of CCh (10 μM) did not further enhance the currents (**Fig. 14a, d**).

It is unlikely that DAMGO caused TRPC4 activation via stimulating PLCβ. Although $G_{i/o}$ proteins activate certain PLCβ subtypes via Gβγ (Camps, Carozzi et al. 1992, Katz, Wu et al. 1992), this does not appear to be a prominent pathway in HEK293 cells, as DAMGO induced Ca^{2+} transients only in ~2% of cells stably expressing μOR (**Fig. 7**). However, PLC activity appeared to be required for DAMGO-evoked TRPC4β current, as it was inhibited by intracellular dialysis of a PLC inhibitor, U73122, but not its inactive analog, U73343 (**Fig. 16**).

Also supporting the role of PLC in $G_{i/o}$ -mediated TRPC4 activation, CCh enhanced the probability of DAMGO to induce TRPC4β activation. Thus, all cells previously exposed to CCh responded to DAMGO with robust currents (**Fig. 15b**); a small proportion of DAMGO-irresponsive cells (*Grp II*) responded to subsequent CCh application with sizeable currents (**Fig. 14b, 15b**); all cells responded to co-application of DAMGO and CCh with large currents (**Fig. 14c, 15b**). Therefore, $G_{q/11}$-PLC activation greatly enhanced the ability of $G_{i/o}$-coupled receptors to activate TRPC4.

Noticeably, although the maximal (peak) current amplitudes evoked by DAMGO alone and DAMGO + CCh were similar (**Fig. 15b**), the rate of current development was significantly slower by DAMGO alone than DAMGO + CCh (**Fig. 15c**). DAMGO-evoked currents exhibited biphasic kinetics – an initial slow phase followed by a fast-rising phase (**Fig. 14**), similar to that reported previously for TRPC5 (Obukhov and Nowycky 2004). Co-application of CCh eliminated the slow

phase (**Fig. 14b, 15c**). Quantification of time to 90% peak current (T_{90}) revealed a significant decrease by >20 s with DAMGO + CCh. This was also seen in cells that co-expressed $G_{i/o}$-coupled M_2R and TRPC4β which allowed simultaneous $G_{q/11}$ and $G_{i/o}$ stimulation by CCh, leading to fast current development (**Fig. 15a,c**), with similar peak amplitudes as TRPC4β/μOR cells (**Fig. 15a,b**).

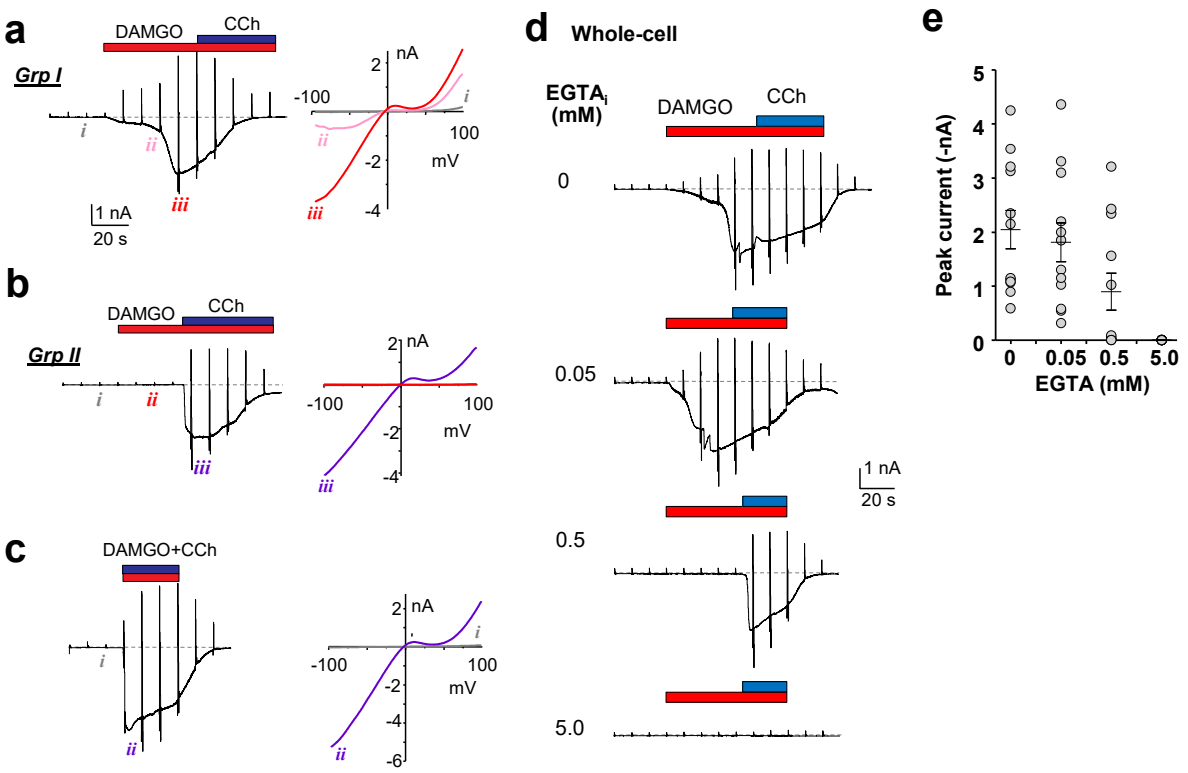

Figure 14. Intracellular Ca^{2+} buffering strength strongly impacts $G_{i/o}$-mediated TRPC4 activation

a-c. Representative whole-cell current traces of HEK293 cells co-expressing TRPC4β and μOR. Pipette solution contained 0.2 mM EGTA and no Ca^{2+}. CCh (10 μM) and/or DAMGO (1 μM) was added as indicated. I-V relationships obtained from the voltage ramps at the indicated time points are shown to the right of the current traces. For DAMGO stimulation alone, cells were divided into Group I (*Grp I*, **a**) and Group II (*Grp II*, **b**) for DAMGO-responsive and irresponsive, respectively. Simultaneous application of DAMGO and CCh evoked currents in all cells (**c**). Summary data are shown in **Figure 15**. **d-e**, Effect of intracellular Ca^{2+} buffering capacity on DAMGO-evoked whole-cell currents. Pipette solutions contained 0, 0.05, 0.5, or 5 mM EGTA with no added Ca^{2+}. All tested cells (100%) responded to DAMGO at 0 and 0.05 mM EGTA. The DAMGO-evoked current activation was blocked in 7 out of 12 cells with 0.5 mM EGTA, but subsequent addition of CCh elicited the current. At 5 mM EGTA, no TRPC4 current was detected in response to DAMGO or DAMGO plus CCh. Representative traces (**d**) and summary data (**e**) for individual cells (circles) and means ± SEM (lines) for DAMGO-evoked peak currents at -60 mV are shown (n=12).

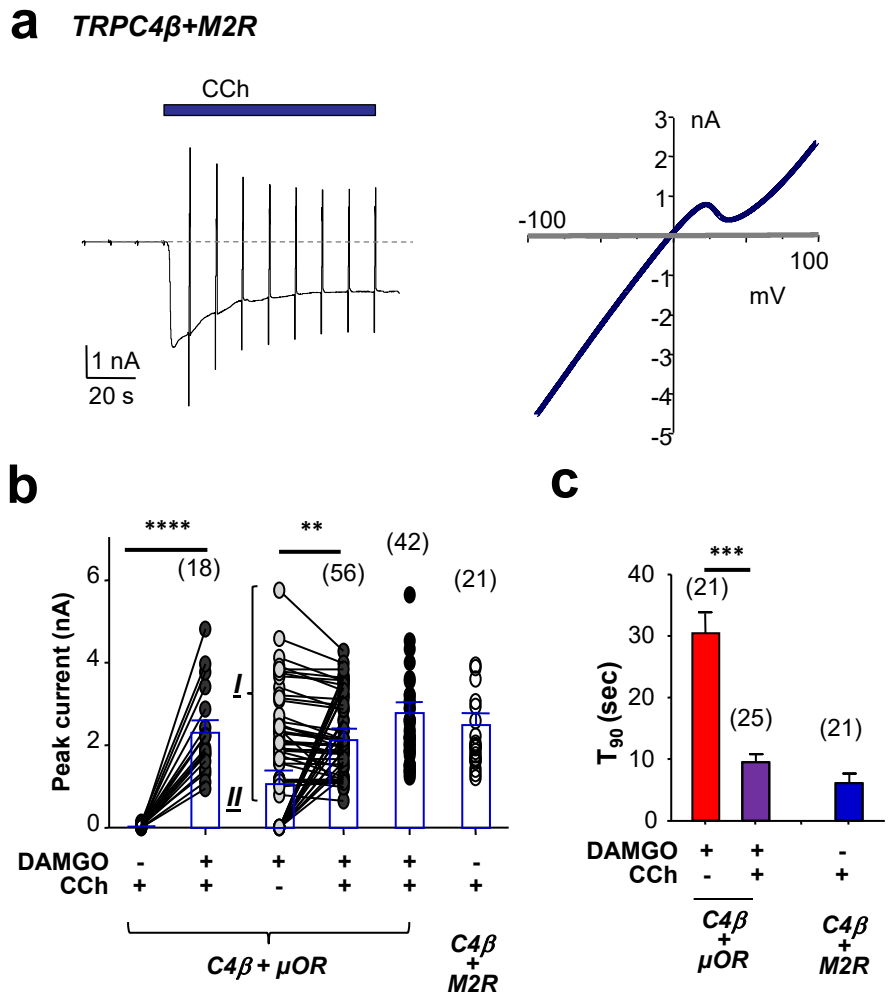

Figure 15. Co-stimulation of $G_{q/11}$ and $G_{i/o}$ pathways strongly enhances the probability and rate of TRPC4 activation

a. Representative whole-cell current trace of HEK293 cells co-expressing TRPC4β and M2R showed a rapid rise to peak current similar to currents induced in TRPC4β and μOR co-expressing cells in **Fig. 14a-c**. Pipette solution contained 0.2 mM EGTA and no added Ca^{2+}. **b.** Peak currents at -60 mV induced by DAMGO and/or CCh as indicated for individual cells from **Figure 14a-c** and **15a**. Blue boxes and bars show means ± SEM. Note the clear segregation between *Grp I* and *Grp II* cells in response to DAMGO alone was abolished by CCh. **c.** Summary of time the current reached 90% peak (T_{90}) for cells stimulated with DAMGO and/or CCh. ** $p < 0.01$, *** $p < 0.001$, **** $p < 0.0001$ by *t* test. Cell numbers are shown in parentheses.

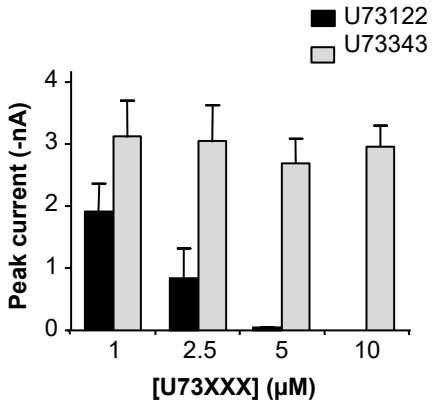

Figure 16. Concentration-dependent inhibition of DAMGO-induced TRPC4β currents by U73122

Pipette solutions contained 0.05 mM EGTA and no added Ca^{2+} but were supplemented with different concentrations of U73122 or U73343. DAMGO (1 μM) was applied extracellularly 5 min after establishment of whole-cell mode to allow sufficient drug dialysis. Shown are means ± SEM (n = 5 each) for DAMGO-evoked peak currents at -60 mV.

Summary II: In addition to $G_{i/o}$ stimulation, TRPC4 activation requires coincident intracellular Ca^{2+} elevation and PLC stimulation, which enhances both the probability and kinetics of current development.

3.2.2 Reducing PIP_2 level suppresses sustained TRPC4 activity but facilitates $G_{i/o}$-mediated channel activation

While physical interaction between $G_{i/o}\alpha$ subunits and TRPC4 C-terminus has been suggested to underlie the mechanism of action of $G_{i/o}$ (Jeon, Hong et al. 2012), the mechanism by which PLC affects TRPC4 gating remains mysterious. PLC activation causes breakdown of PIP_2, generation of DAG and IP_3, which activates IP_3R on the endoplasmic reticulum (ER) membrane, leading to elevation of $[Ca^{2+}]_i$ (Berridge, Lipp et al. 2000). DAG activates TRPC3, C6, C7, but not TRPC4/C5 (Hofmann, Obukhov et al. 1999, Okada, Inoue et al. 1999). IP_3R may exert a positive effect on activation of all TRPCs by competing with Ca^{2+}-CaM for binding to TRPC (Tang, Lin et al. 2001, Zhang, Tang et al. 2001, Vaca and Sampieri 2002). Incidentally, the CIRB site, a conserved motif of about 30 amino acids on proximal C-terminus of TRPC (Tang, Lin et al. 2001, Zhang, Tang et al. 2001, Zhu 2005), is also critical for $G_{i/o}\alpha$ effect on TRPC4 (Jeon, Hong et al. 2012). Also, Ca^{2+} exhibits both positive and negative effects on some TRPC channels (Kinoshita-Kawada, Tang et al. 2005, Ordaz, Tang et al. 2005, Gross, Guzman et al. 2009).

To define components of the PLC pathway critical for TRPC4 activation, I first examined PIP_2. Previously, PIP_2 has been shown to inhibit activation of TRPC4α (Otsuguro, Tang et al. 2008), but prevent desensitization of TRPC4β (Kim, Jeon et al. 2013). Using zebrafish voltage-sensitive phosphatase (DrVSP) to reduce PIP_2 content without a concomitant hydrolysis, I observed a marked depression upon phosphatase activation for TRPC4β currents evoked by both DAMGO and DAMGO + CCh (**Fig. 17**), suggesting that $G_{i/o}$-mediated TRPC4β activation also depends on PIP_2. Therefore, either PIP_2 itself or its hydrolysis product(s) may be essential for continued TRPC4β activation.

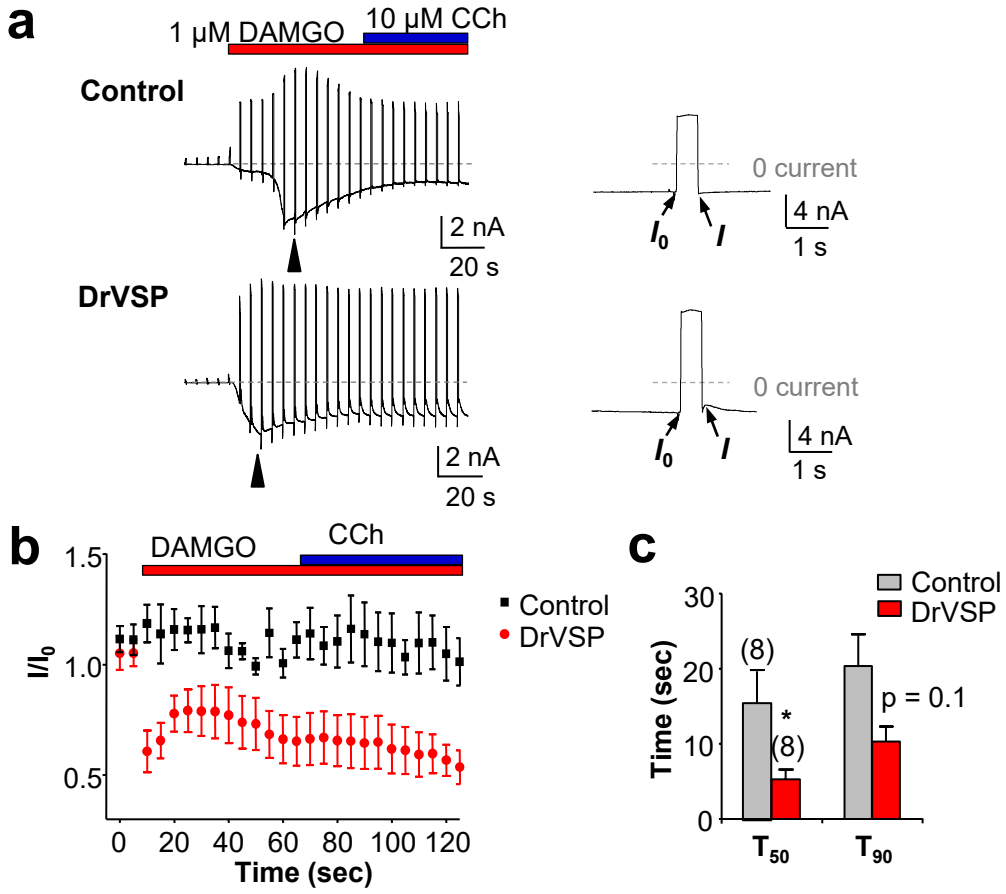

Figure 17. PIP_2 depletion suppresses TRPC4 activation under maximal $G_{i/o}$–stimulation

Stable HEK293 cells co-expressing μOR and TRPC4β were transiently transfected with either a control vector or cDNA encoding zebrafish voltage-sensitive phosphatase (DrVSP). Pipette solution had 0.05 mM EGTA and no added Ca^{2+}. **a.** Cells were held at -60 mV while depolarization pulses (100 mV, 0.5 sec) were applied every 5 sec. DAMGO (1 μM) and CCh (10 μM) were applied as indicated. Note the decrease in current amplitude immediately following each pulse in the DrVSP-expressing cell. Sections pointed by the arrowheads are expanded on left with I_0 (current before pulse) and I (current after pulse) indicated. No current depression was detected in control cells or before DAMGO application in DrVSP-expressing cells. **b.** Time courses of I/I_o for control and DrVSP-expressing cells before and during stimulation by DAMGO ± CCh. n = 6 each. **c.** Summary of T_{50} and T_{90} by DAMGO. Although T_{90} did not reach statistical significance, T_{50} values are different. The near doubling of T_{90} *vs* T_{50} in DrVSP-expressing cells indicates monophasic current development, whereas in controls T_{50} and T_{90} values are close as both occurred during the fast rising phase.

Noticeably, repeated PIP_2 dephosphorylation by DrVSP abolished the slow phase of the biphasic response to DAMGO (**Fig. 17a**). T_{90} was shortened but did not reach statistical significance ($p = 0.1$); however, T_{50} was significantly shorter with DrVSP (**Fig. 17c**), suggesting an acceleration of the initial phase and a likely slow down of the rapid rising phase.

Thus, reducing PIP_2 may help initial current development. To test this possibility, I conducted weak $G_{i/o}$ stimulation using 30 nM DAMGO, which was insufficient to elicit current in control cells. With DrVSP, the same stimulation induced TRPC4β current (**Fig. 18**). Similarly, dephosphorylating PIP_2 with rapamycin-induced membrane translocation of yeast inositol polyphosphate 5-phosphatase, Inp54p (Komatsu, Kukelyansky et al. 2010) also facilitated TRPC4β activation by weak μOR stimulation (**Fig. 19**).

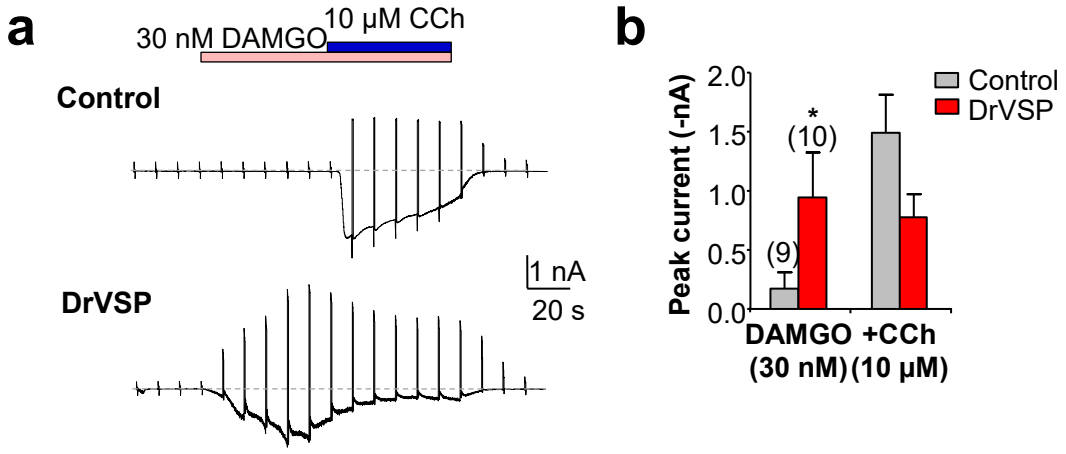

Figure 18. PIP_2 depletion facilitates TRPC4 activation under subthreshold $G_{i/o}$–stimulation

a. Sub-threshold DAMGO concentration (30 nM) activated TRPC4β currents in DrVSP-expressing but not control cells. Subsequent addition of CCh (10 μM) led to robust current development in the control cell. Depolarization pulses were applied at 10 sec intervals. **b.** Summary of peak currents at -60 mV for experiments illustrated in **a**. * $p < 0.05$ *vs* controls by *t* test.

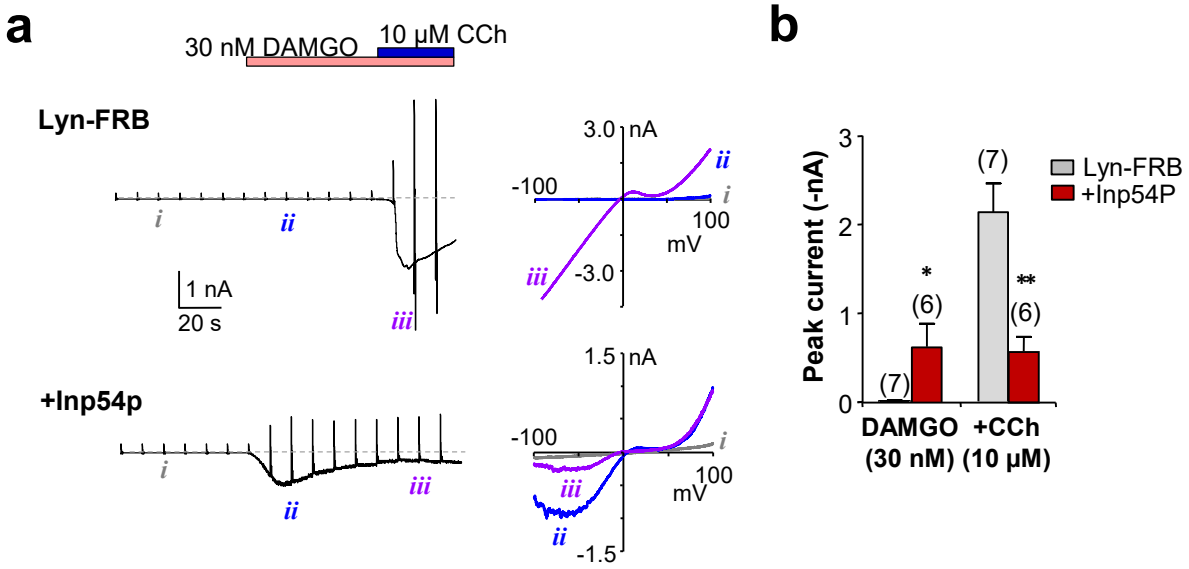

Figure 19. PIP_2 depletion via Inp54P facilitates TRPC4 activation

Stable HEK293 cells co-expressing µOR and TRPC4β were transiently transfected with cDNA for Lyn-FRB alone (as a control) or those for Lyn-FRB and CFP-FKBP-Inp54p together (to allow rapamycin-dependent plasma membrane translocation of Inp54P). Rapamycin (1 µM) was applied extracellularly 5 min before and maintained during whole-cell recordings. Pipette solution contained 0.05 mM EGTA with no added Ca^{2+}. **a.** Representative whole-cell currents in response to a sub-threshold concentration of DAMGO (30 nM) and subsequent addition of CCh (10 µM) in a control cell (*upper panel*) and a cell in which endogenous PIP_2 level had been decreased via dephosphorylation by Inp54p (*lower panel*). I-V curves obtained from the voltage ramps at the indicated time points shown to the right of the time courses revealed typical TRPC4-like I-V relationship. **b.** Summary (means ± SEM) of peak currents at -60 mV evoked by 30 nM DAMGO and after subsequent addition of 10 µM CCh. Note, reducing PIP_2 content by Inp54p not only enhanced the probability of TRPC4β activation by weak $G_{i/o}$ stimulation with the low concentration of DAMGO but also decreased the overall current amplitude evoked by the co-stimulation of $G_{i/o}$ and $G_{q/11}$ pathways (DAMGO + CCh). * $p < 0.05$, ** $p < 0.01$ *vs* control by unpaired *t* test. Numbers of cells are shown in parentheses.

Summary III: Within the mechanism of PLC stimulation, which enhances the probability and kinetics of TRPC4 activation, the depletion of PIP_2 is an essential step. PIP_2 exerts a tonic inhibition on the channel. Therefore, activation of PLC releases PIP_2 inhibition on TRPC4 - facilitating the activation of channel. However, PIP_2 also supports TRPC4 function.

3.2.3 Ca^{2+} improves the probability but not rate of $G_{i/o}$–mediated TRPC4 activation

The need for PIP_2 to support TRPC4 current could reflect a dependence on its breakdown product(s), among which IP_3R activation and $[Ca^{2+}]_i$ rise have been shown to support TRPC4/C5 function (Venkatachalam and Montell 2007). To determine if IP_3R are involved in TRPC4 activation, I applied IP_3R inhibitor, heparin (3 mg/ml), through intracellular dialysis and found that most (7/10) cells failed to respond to DAMGO and subsequent application of CCh (10 μM) (**Fig. 20a-c**).

However, addition of Ca^{2+} ionophore, IM (10 μM), rescued the response, with peak currents similar to that activated by DAMGO in controls (**Fig. 20b, c**). IM causes ER Ca^{2+} release without activating IP_3R. At 10 μM, it also causes Ca^{2+} influx. Thus, increasing $[Ca^{2+}]_i$ by IM bypassed the IP_3R requirement for TRPC4β activation. These results suggest that IP_3R-mediated ER Ca^{2+} release is an important part of the $G_{q/11}$-PLC pathway for TRPC4 activation.

A small number of heparin-treated cells (3/10) responded to DAMGO with peak amplitudes comparable to controls (**Fig. 20c**). This could arise from either an incomplete block of IP_3R or IP_3R-independent $[Ca^{2+}]_i$ rise. Presumably, a triggering $[Ca^{2+}]_i$ rise provided by IP_3R or other means could open a few TRPC4β channels, which would be followed by opening of all channels in the cell through a positive-feedback mechanism due to the Ca^{2+} permeability of these channels. This strong cytosolic Ca^{2+} dependence is supported by the finding that increasing the intracellular Ca^{2+} buffering strength by higher concentrations of EGTA in the patch pipette decreased the probability of DAMGO-evoked TRPC4β whole-cell currents (**Fig. 14d,e**). In addition, increasing the EGTA concentration in the pipette solution also abolished DAMGO-evoked TRPC4β currents in outside-out patches (**Fig. 21a, b**).

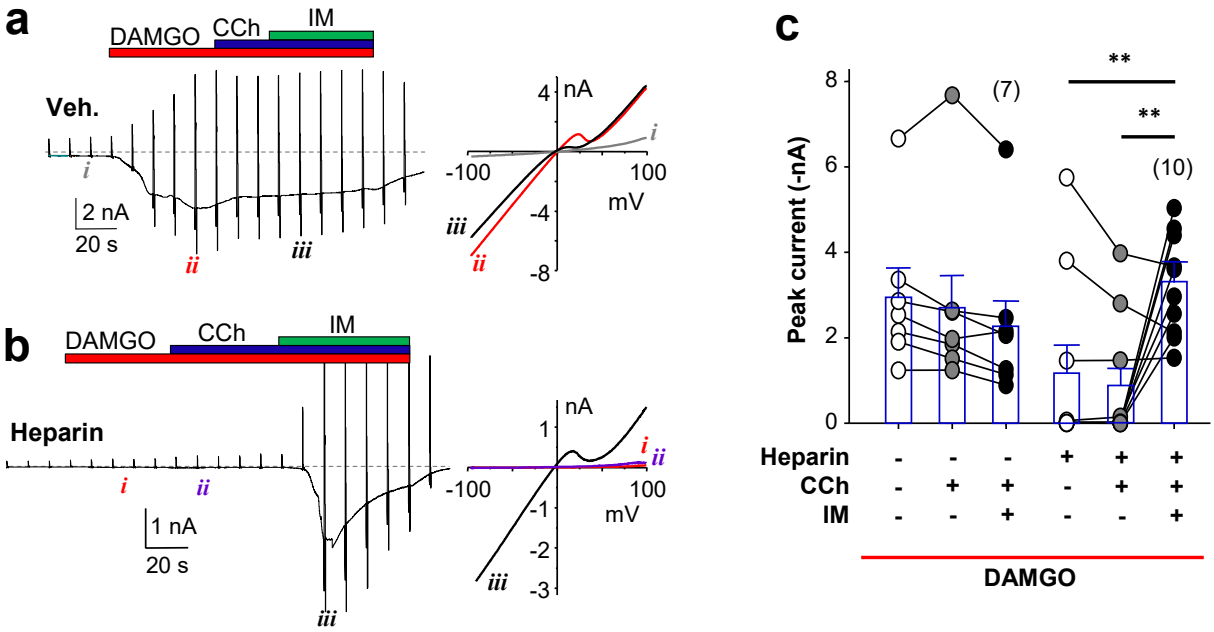

Figure 20. IP_3R-mediated Ca^{2+} release provides triggering Ca^{2+} to initiate TRPC4 activation

All cells stably co-expressed TRPC4β and μOR. **a-c**. Heparin suppressed the activation of TRPC4 by DAMGO ± CCh. Vehicle (Veh., **a**) or heparin (3 mg/ml, **b**) was infused into cells by pipette dialysis for > 5 min before DAMGO (1 μM), CCh (10 μM) and IM (10 μM) were applied extracellularly. Whole-cell currents and I-V curves showed lack of or very weak response to DAMGO and DAMGO + CCh in a heparin-treated cell, but addition of IM rescued the response (**b**). **c.** Peak currents at -60 mV induced by DAMGO ± CCh or IM as indicated for individual cells treated or not by heparin. Note 3 cells were not inhibited by heparin. Blue boxes and bars show means ± SEM. Cell numbers are shown in parentheses. ** $p \leq 0.01$, by ANOVA.

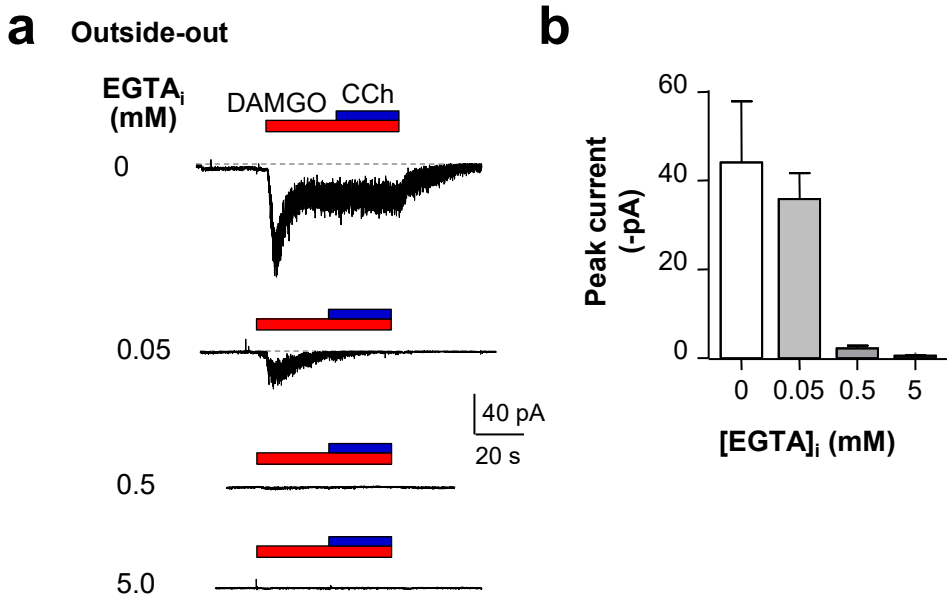

Figure 21. Ca^{2+} regulates DAMGO evoked TRPC4 currents

Strength of the intracellular Ca^{2+} buffer strongly affected DAMGO-evoked TRPC4 activation in outside-out patches. **a.** DAMGO (1 μM)-evoked activation of TRPC4 currents were gradually suppressed by increasing the EGTA concentration in the pipette solution, in which no Ca^{2+} was added. **b.** Summary data (means ± SEM) for DAMGO-evoked peak currents in outside-out patches at -60 mV (**b**). n = 5 – 7. Note, unlike the whole-cell currents shown in **Fig. 14 d,e,** CCh (10 μM) did not facilitate the outside-out currents at 0.5 mM EGTA.

Also, DAMGO evoked very small currents in whole-cell and no current in outside-out patches when Ca^{2+} was removed from the bath solution (**Fig. 22a, b**), showing the importance of continued Ca^{2+} influx to support $G_{i/o}$ -mediated TRPC4 currents. The strong extracellular Ca^{2+} dependence was also seen in the presence of IM (either 1 or 10 μM) (**Fig. 22c,d**). In this case, despite the $[Ca^{2+}]_i$ increase induced by IM through mobilization of ER Ca^{2+} store, while $G_{i/o}$ signaling was activated by DAMGO (30 nM), sizeable biphasic TRPC4 current was not developed until Ca^{2+} (2 mM) was added to the bath solution.

In **Fig. 14b**, **d**, CCh only increased currents in cells that failed to respond to DAMGO alone, suggesting that the $G_{q/11}$-PLC pathway might provide the triggering Ca^{2+} via IP_3R-mediated ER Ca^{2+} release. To examine if a triggering $[Ca^{2+}]_i$ rise was sufficient for TRPC4 activation, we treated DAMGO-irresponsive (*Grp II*) cells with IM. All cells responded to IM, with the peak amplitudes similar to that evoked by DAMGO in *Grp I* cells (**Fig. 23b, d**). By contrast, neither IM alone nor IM + CCh induced discernible TRPC4β current (**Fig. 23c, d**). Subsequent application of DAMGO to these cells gave robust currents, with peak amplitudes similar to cells stimulated by DAMGO + IM irrespective to the sequence of drug application (**Fig. 23d**). These results reinforce the idea that with $G_{i/o}$ stimulation a triggering $[Ca^{2+}]_i$ rise is also necessary for TRPC4 activation. However, currents induced by DAMGO + IM still exhibited biphasic kinetics, with T_{90} significantly longer than if CCh was included in the stimulation cocktail (**Fig. 23c, e**), suggesting that IM treatment, or $[Ca^{2+}]_i$ rise, did not completely reproduce the effect of $G_{q/11}$-PLC stimulation for TRPC4 activation.

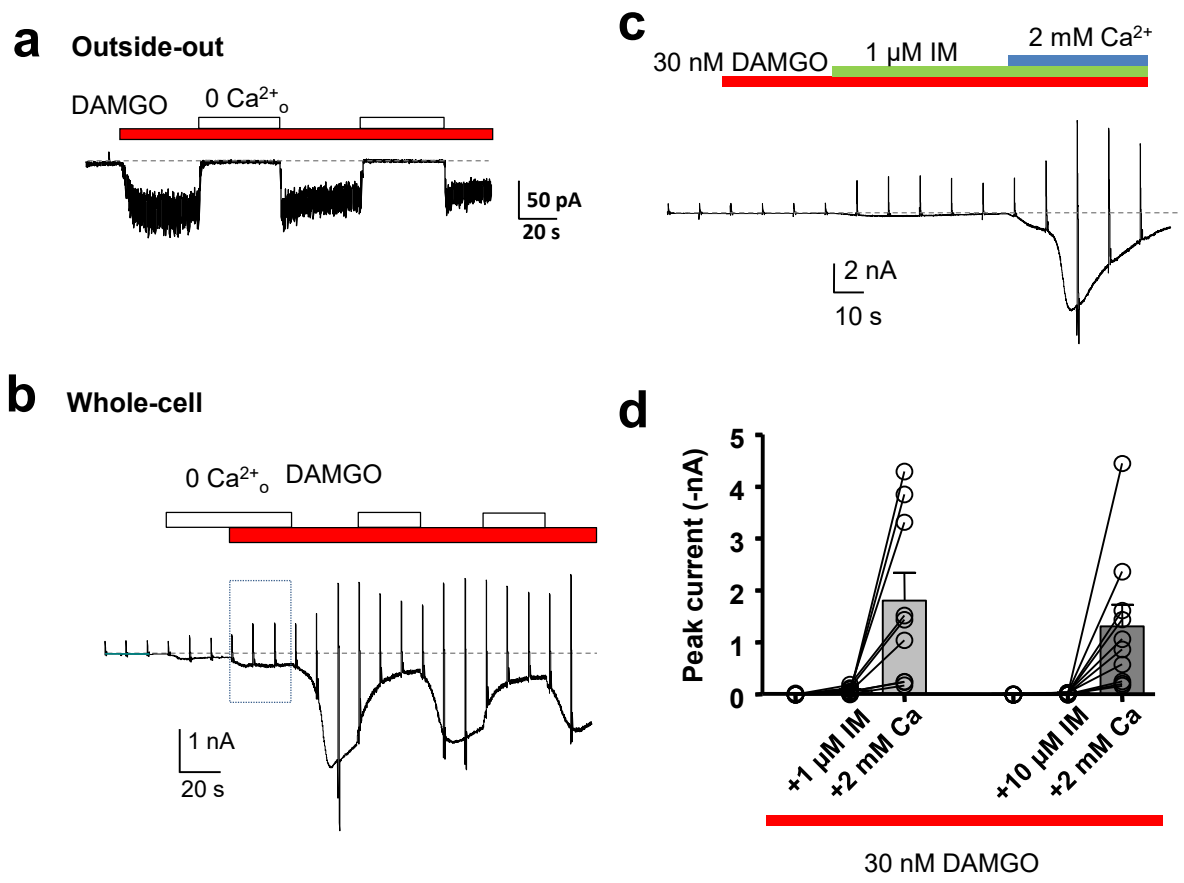

Figure 22. Ca^{2+} influx supports continued TRPC4 activation

Removal of extracellular Ca^{2+} strongly suppressed DAMGO-evoked TRPC4 currents in outside-out (**a**) and whole-cell (**b**) patches. The pipette solution contained 0.05 mM EGTA and no added Ca^{2+}. A Ca^{2+}-free extracellular solution containing 0.2 mM EGTA with no added Ca^{2+} (0 Ca^{2+}) replaced the regular extracellular solution containing 2 mM Ca^{2+} at the indicated time periods while DAMGO (1 µM) was applied. The current decrease in 0 Ca^{2+} indicates a strong requirement for a continuous supply of Ca^{2+}, via Ca^{2+} influx, to maintain TRPC4 activity. Note that TRPC4 whole-cell current was weakly activated by DAMGO in 0 Ca^{2+} (dotted rectangle in **b**), but it reached maximal activation only in the presence of external Ca^{2+}. **c, d**, In the absence of extracellular Ca^{2+}, addition of either 1 µM or 10 µM IM was insufficient to facilitate the full TRPC4 activation under subthreshold stimulation of $G_{i/o}$. Only addition of external Ca^{2+} permitted the development of a biphasic current.

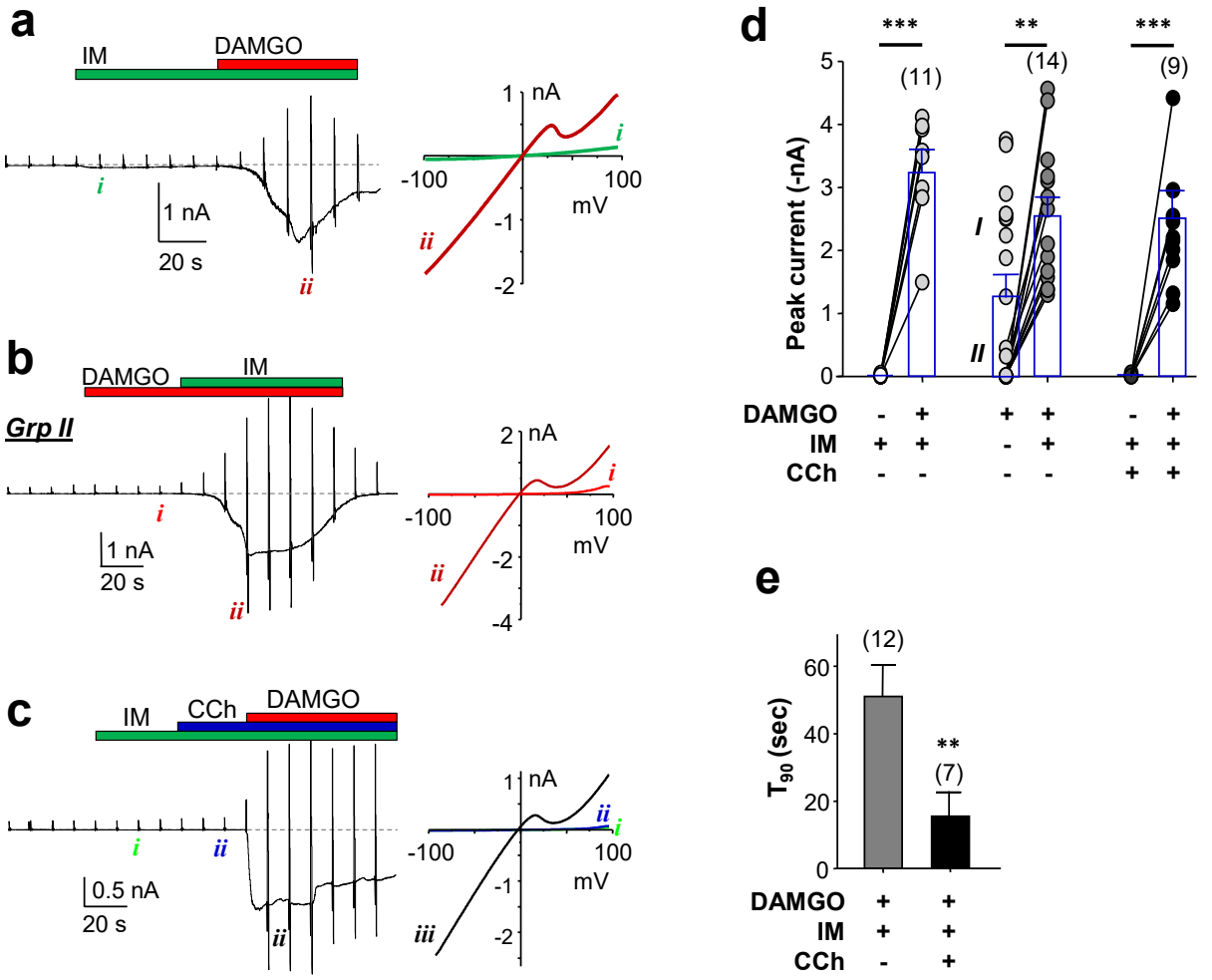

Figure 23. Intracellular Ca^{2+} improves probability but not rate of $G_{i/o}$ -mediated TRPC4 activation

All cells stably co-expressed TRPC4β and μOR. The pipette solution contained 0.2 mM EGTA with no added Ca^{2+}. IM (10 μM) was applied before DAMGO (1 μM) (**a**). In this case, IM caused small increase in current, but the I-V curve was not typical of the TRPC4 currents. A significantly larger current was evoked by stimulation with DAMGO. DAMGO-irresponsive cells (*Grp II*) became activated in presence of IM (**b**), but IM ± CCh failed to elicit current until DAMGO was introduced (**c**). **d.** Peak currents at -60 mV induced by DAMGO, CCh, and IM. Only *Grp II* cells were further treated with IM. **e.** T_{90} for currents evoked by DAMGO + IM ± CCh. Cell numbers are shown in parentheses. ** $p \leq 0.01$, *** $p \leq 0.001$ by *t* test.

To determine the $[Ca^{2+}]_i$ needed to maximally activate TRPC4, we clamped free Ca^{2+} levels in pipette solutions using 10 mM BAPTA which also minimized Ca^{2+} fluctuations during whole-cell recordings. With free $[Ca^{2+}]_i$ clamped to 100 nM, neither DAMGO alone, nor

DAMGO + CCh evoked TRPC4 currents (**Fig. 24a**). Increasing free $[Ca^{2+}]_i$ to > 1 μM allowed current development in response to DAMGO, with maximal current achieved at ~10 μM free $[Ca^{2+}]_i$ (**Fig. 24b-d**). Interestingly, DAMGO-evoked currents became smaller at > 50 μM free $[Ca^{2+}]_i$, indicating a dual dependence on $[Ca^{2+}]_i$ (**Fig. 24d**). Fitting the Ca^{2+}-dependent changes of TRPC4 currents with a biphasic Hill equation (Foskett, White et al. 2007) yielded an EC_{50} of ~12 μM and an IC_{50} of ~28 μM for Ca^{2+}-dependent facilitation and inhibition, respectively, suggesting a very narrow $[Ca^{2+}]_i$ range for TRPC4 activation. Altogether, the above results demonstrate the importance of $[Ca^{2+}]_i$ rise in $G_{i/o}$ -mediated TRPC4 activation; however, Ca^{2+} alone was insufficient to recapitulate the facilitation by PLC on activation kinetics.

Another important observation was that a mere rise in $[Ca^{2+}]_i$ was insufficient to facilitate maximal TRPC4 activation, as 10 μM IM would deplete all intracellular calcium stores, but was insufficient to facilitate activity (**Fig 23a**). Physiological level of extracellular calcium was necessary even in the presence of IM (**Fig 22c, d**) or at ~10 μM free $[Ca^{2+}]_i$ buffered with 10 mM BAPTA (**Fig 24, 25)**, suggesting that a Ca^{2+} influx process is essential for TRPC4 activity. It is possible that this Ca^{2+} influx occurs via TRPC4 itself and is highly spatially localized.

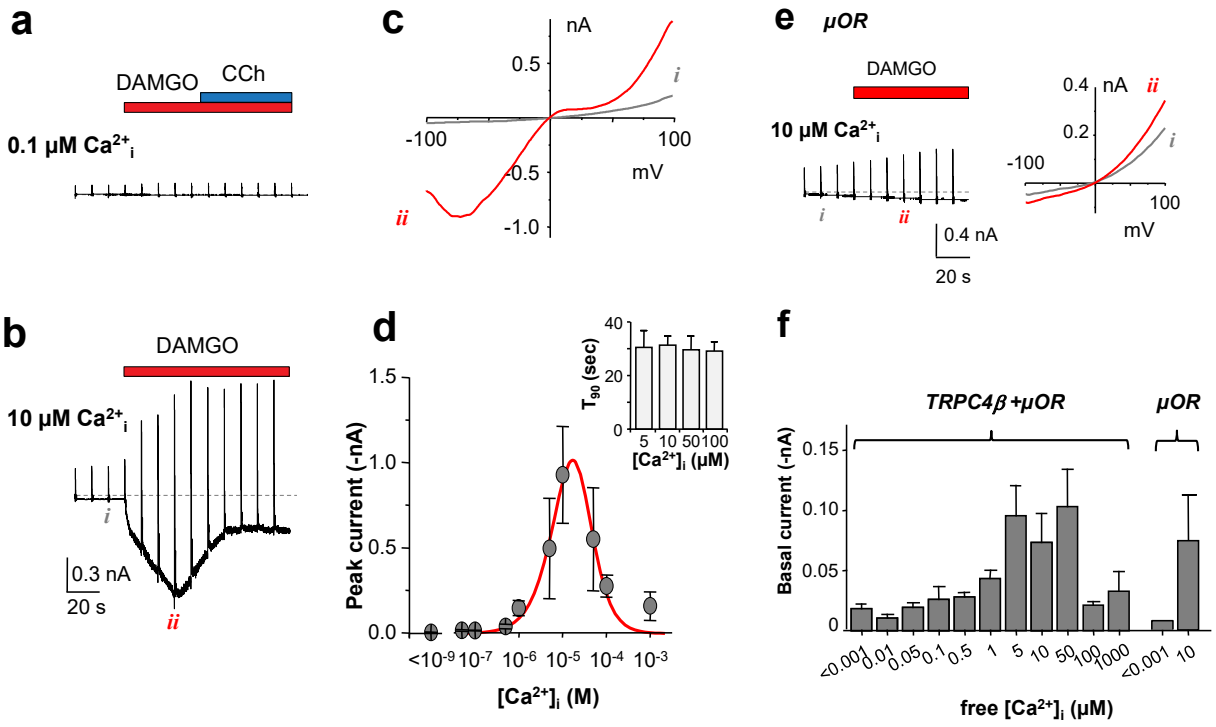

Figure 24. Bimodal regulation of TRPC4 activation by intracellular Ca^{2+}

Whole-cell currents evoked by DAMGO ± CCh in cells dialyzed with pipette solutions containing 10 mM BAPTA with [Ca^{2+}] (concentration of free Ca^{2+}) clamped to 100 nM (**a**) and 10 μM (**b**). I-V curves are shown for basal and DAMGO-evoked currents with $[Ca^{2+}]_i$ clamped at 10 μM (**c**). **d.** Summary of DAMGO-evoked peak currents at -60 mV for cells dialyzed with 10 mM BAPTA and free $[Ca^{2+}]_i$ clamped at indicated levels. Data points (n = 5 - 8) were fitted with the biphasic Hill equation with the expected maximal peak current (P_{Hill}) set to be 2.4 nA, based on the average peak current in response to DAMGO + IM obtained when $[Ca^{2+}]_i$ was allow to fluctuate. The estimated EC_{50} for Ca^{2+} facilitation was 12.2 μM, Hill 1.30; the estimated IC_{50} for Ca^{2+} inhibition was 28.3 μM, Hill -1.68. Inset shows T_{90} of DAMGO-evoked currents with [Ca^{2+}] in the pipette solution clamped as indicated. Extracellular calcium was 2 mM. **e**, Negative control with a cell that expressed μOR only and the pipette [Ca^{2+}] clamped at 10 μM by 10 mM BAPTA. The leak current developed under these conditions did not have the typical I-V relationship of the TRPC4 currents. **f**, Basal currents at -60 mV in cells that stably expressed TRPC4β + μOR or just μOR dialyzed with pipette solutions containing indicated free [Ca^{2+}]'s clamped by 10 mM BAPTA. For TRPC4β/μOR cells, data were from same cells shown in **d**. For μOR only cells, n = 4 each for <0.001 μM Ca^{2+} and 10 μM Ca^{2+}. The results suggest that the enhanced basal currents at high free [Ca^{2+}]'s are unrelated to TRPC4.

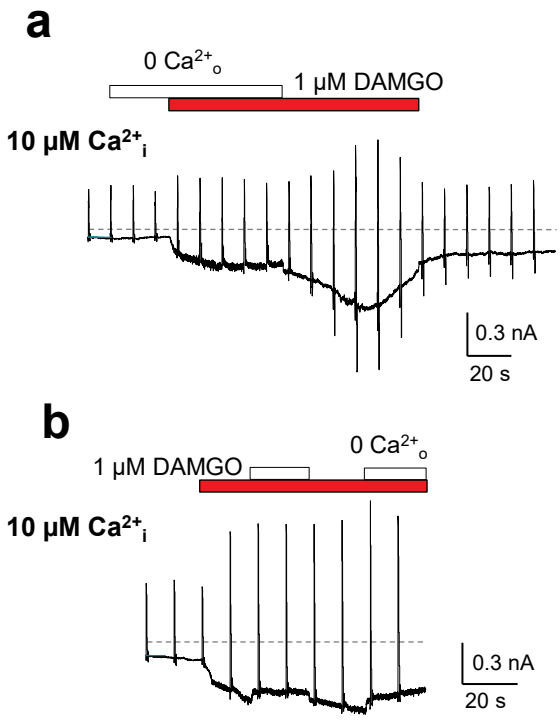

Figure 25. Dependence of TRPC4 currents on extracellular Ca^{2+} while $[Ca^{2+}]_i$ was clamped at 10 μM by BAPTA

a & **b,** The pipette solution had 10 μM free Ca^{2+} buffered by 10 mM BAPTA. Under whole-cell mode, DAMGO (1 μM) was applied either in the Ca^{2+}-free (**a**) or Ca^{2+}-containing (**b**) extracellular solution as in **Fig. 22b**. The solutions were then exchanged as indicated. Note the clear increase in current amplitude upon reintroduction of the extracellular Ca^{2+}, although the magnitude was smaller than with the 0.05 mM EGTA buffer as shown in **Fig. 22b**. The removal of extracellular Ca^{2+} also resulted in less suppression of DAMGO-evoked current than that shown **Fig. 22b**.

Summary IV: Intracellular Ca^{2+} elevation is necessary for $G_{i/o}$ mediated TRPC4 activation. The Ca^{2+}dependence is biphasic with an EC_{50} of ~12 μM and IC_{50} of 28 μM.

3.2.4 PLCδ1 is involved in TRPC4 activation

Testing other components of the PLC pathway, I found no evidence for IP_3, DAG, or PKC to be involved in facilitating $G_{i/o}$-mediated TRPC4 activation even with the triggering $[Ca^{2+}]_i$ rise induced by IM (**Fig. 26a-c**). Interestingly, using a DAG sensor (Tewson, Westenberg et al. 2012), I detected more robust DAG production induced by DAMGO + CCh in TRPC4β/μOR cells than cells that expressed μOR alone (**Fig. 26d**), indicating that TRPC4β also strongly enhanced PLC activity. A likely way for TRPC4 to enhance PLC function was by maintaining elevated $[Ca^{2+}]_i$ through Ca^{2+} influx since most PLC isoforms are Ca^{2+} sensitive and some directly activated by Ca^{2+}, e. g. PLCδ (Suh, Park et al. 2008). Thus, although the Ca^{2+} signal generated by PLC provides the initial trigger for TRPC4 activation, the sustained $[Ca^{2+}]_i$ elevation resulting from channel activity also prolongs PLC stimulation, which may further supports continued TRPC4 function.

To test whether a specific PLC isoform is required for TRPC4 activation, I knocked down PLC isoforms typically associated with $G_{q/11}$ and Ca^{2+} signaling in HEK293 cells (Atwood, Lopez et al. 2011) using isoform specific siRNA. Intriguingly, knockdown of PLCδ1 but not PLCδ3, PLCβ1 or PLCβ3 inhibited TRPC4 activation (**Fig. 27a, b**). To confirm the involvement of PLCδ1, I expressed the Ca^{2+}-insensitive, dominant-negative PLCδ1 mutant, E341R/D343R (Murthy, Zhou et al. 2004) and observed a strong inhibition of TRPC4β (**Fig. 28a, b**) and TRPC4α, but not TRPC5 (**Fig. 29**). Conversely, overexpression of wild-type PLCδ1 (but not PLCβ1/β2) significantly reduced T_{90} of DAMGO-evoked TRPC4β current without affecting peak amplitude (**Fig. 28a-c**). These results indicate that Ca^{2+}-dependent PLCδ1 function is not only necessary but also rate limiting for TRPC4 activation.

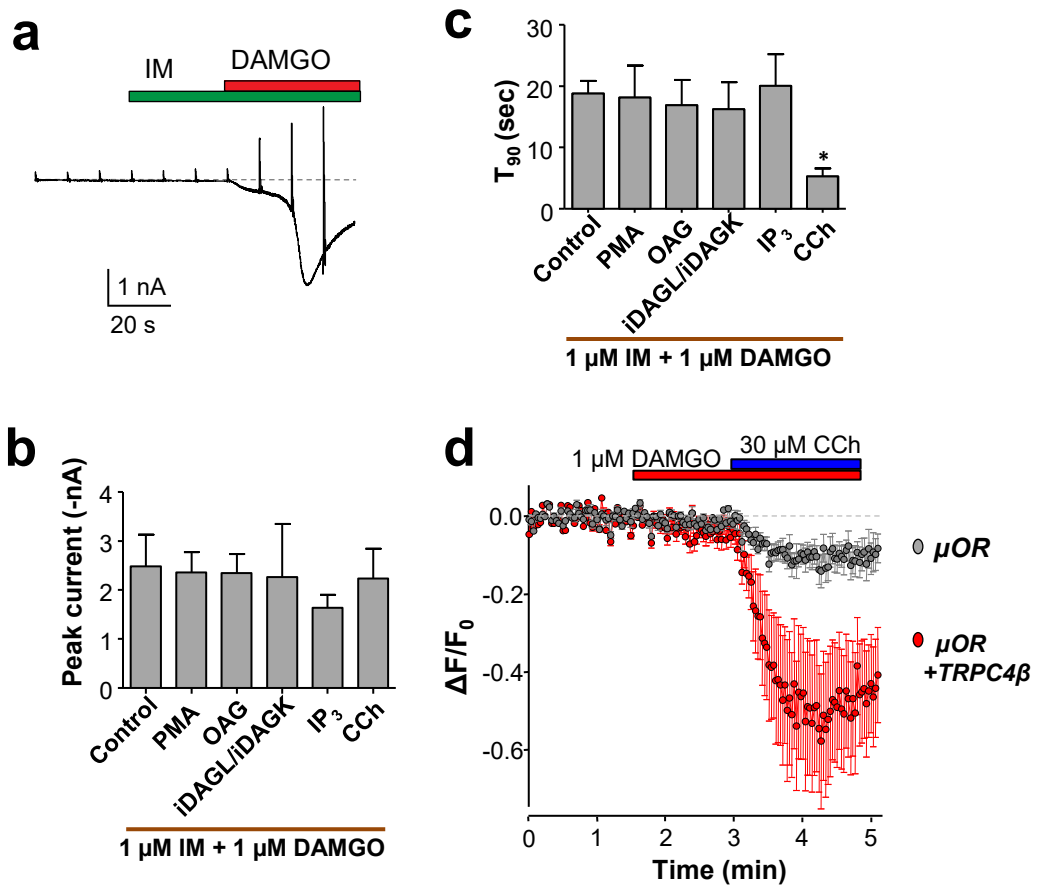

Figure 26. Effects of other components of PIP_2 hydrolysis on $G_{i/o}$ -mediated TRPC4 activation

a-c. All cells stably co-expressed TRPC4β and μOR. Whole-cell currents were recorded (as shown in **a**) with the pipette solution containing 0.05 mM EGTA with no added Ca^{2+}. IM and DAMGO (both at 1 μM) were applied extracellularly as indicated. Together with DAMGO, phorbol-12-myristate-13-acetate (PMA, 1 μM), OAG (50 μM), or CCh (30 μM) were also applied. Alternatively, DAG lipase inhibitor (RHC 80267, 50 μM) and DAG kinase inhibitor (R59 022, 50 μM) were co-applied extracellularly 5 min before- and maintained during- the whole-cell recording (iDAGL/iDAGK), or IP_3 (1 μM) was included in the pipette solution. However, none of these treatments altered the peak currents (at -60 mV) elicited by IM and DAMGO (**b**). Only CCh significantly reduced T_{90} (**c**). Summary data in **b** and **c** are means ± SEM for n = 5 - 7 cells. * $p < 0.05$ by One-way ANOVA followed by Newman-Keuls post-hoc test. **d.** Concomitant stimulation by DAMGO and CCh caused more DAG production in the presence of TRPC4β than in its absence. A fluorescent downward DAG sensor was transiently transfected into stable cell lines that expressed μOR alone or μOR + TRPC4β. DAG production was monitored as a decrease in fluorescence detected using the standard filter set for rhodamine. Cells were stimulated by DAMGO and CCh as indicated. Data are means ± SEM for 14 cells that expressed μOR and 10 cells that co-expressed μOR and TRPC4β.

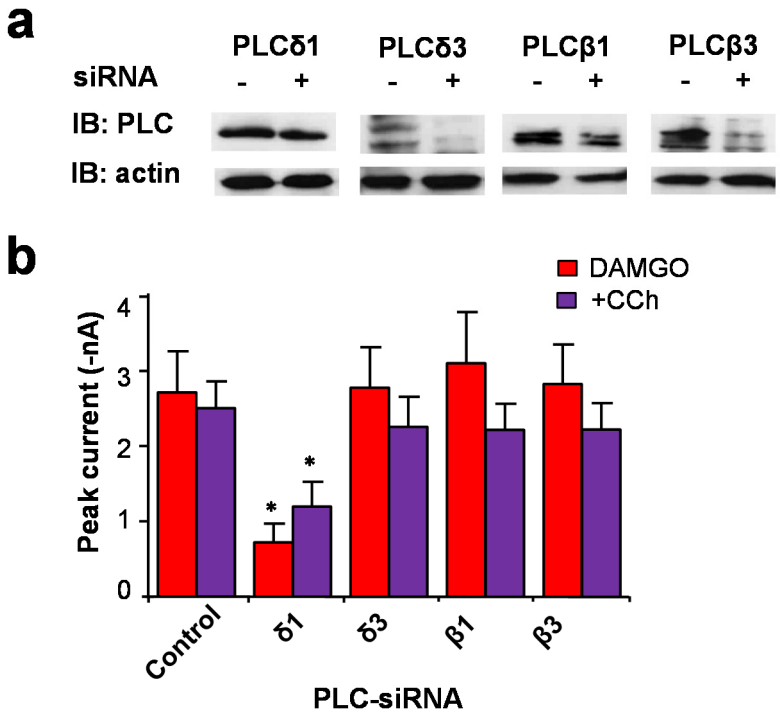

Figure 27. The involvement of PLCδ1 in $G_{i/o}$-mediated TRPC4 activation

a & **b.** siRNA knockdown of PLCδ1 inhibited TRPC4β currents. Stable HEK293 cells co-expressing μOR and TRPC4β were transfected with pEGFP-N1 or pEGFP-N1 + siRNA for PLCδ1, PLCδ3, PLCβ1, or PLCβ3. The transfection was repeated after 48 hrs and cells analyzed 24 hrs later. The knockdown efficiency was analyzed by Western blotting (**a**). DAMGO and CCh-evoked whole-cell currents were measured as in **Fig. 14d** with the pipette solution containing 0.05 mM EGTA and no added Ca^{2+}. Despite the incomplete knockdown, currents evoked by 1 μM DAMGO alone and that with subsequent addition of 10 μM CCh were both significantly decreased by the siRNA for PLCδ1 but not that for other PLC isoforms (**b**). Data are means ± SEM for n = 13 cells for all data points. * $p < 0.05$ by One-way ANOVA followed by Newman-Keuls post-hoc test.

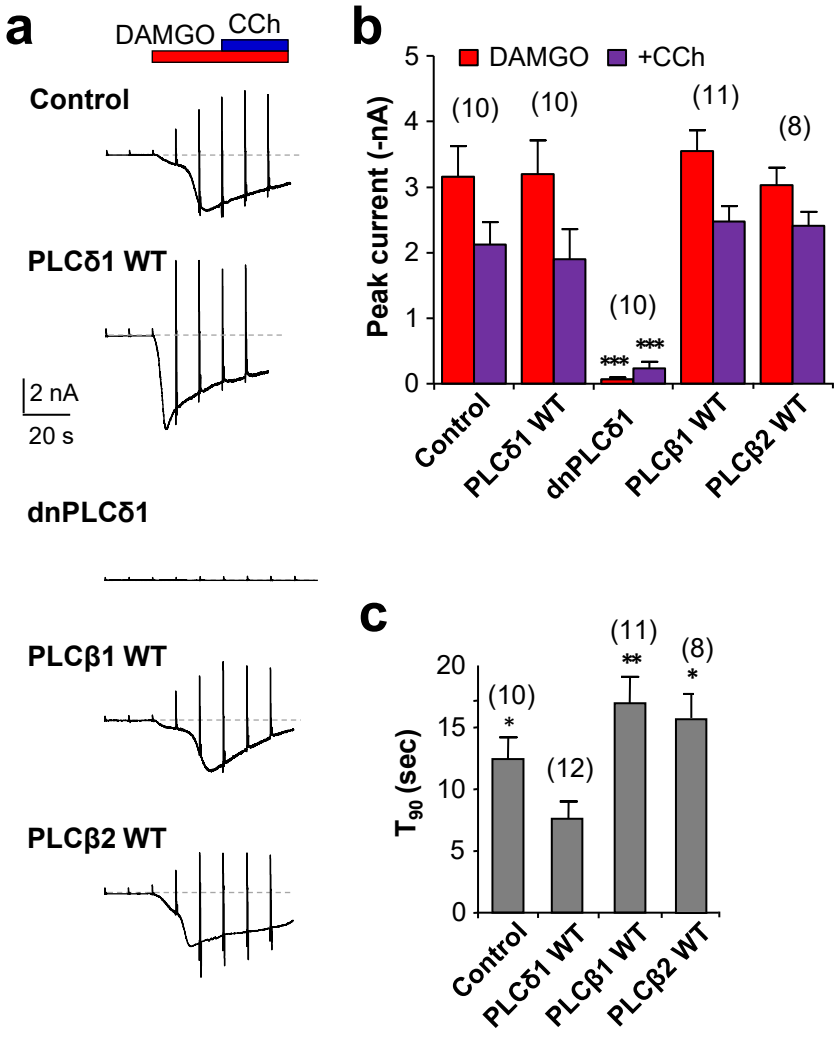

Figure 28. PLCδ1 is necessary for DAMGO-evoked TRPC4 activation

Stable TRPC4β/μOR cells were transiently transfected with either a control vector or cDNA encoding various PLC constructs as indicated. Pipette solution contained 0.05 mM EGTA and no added Ca^{2+}. **a.** Whole-cell currents recorded from control and cells transiently expressing PLCδ1 wild type (WT), dominant-negative PLCδ1 mutant E341R/D343R, PLCβ1 WT, or PLCβ2 WT. DAMGO (1 μM) and CCh (10 μM) were applied as indicated. Note the complete loss of the current with PLCδ1-E341R/D343R mutant and faster rate of DAMGO-evoked current development with PLCδ1 WT compared with PLCβ1/ β2. **b.** Summary of peak currents at -60 mV evoked by DAMGO and with addition of CCh. *** $p < 0.001$ *vs* control by *t* test. **c.** Summary of T_{90} for DAMGO-evoked current at -60 mV, * $p < 0.05$, ** $p < 0.01$ *vs* PLCδ1 WT by *t* test.

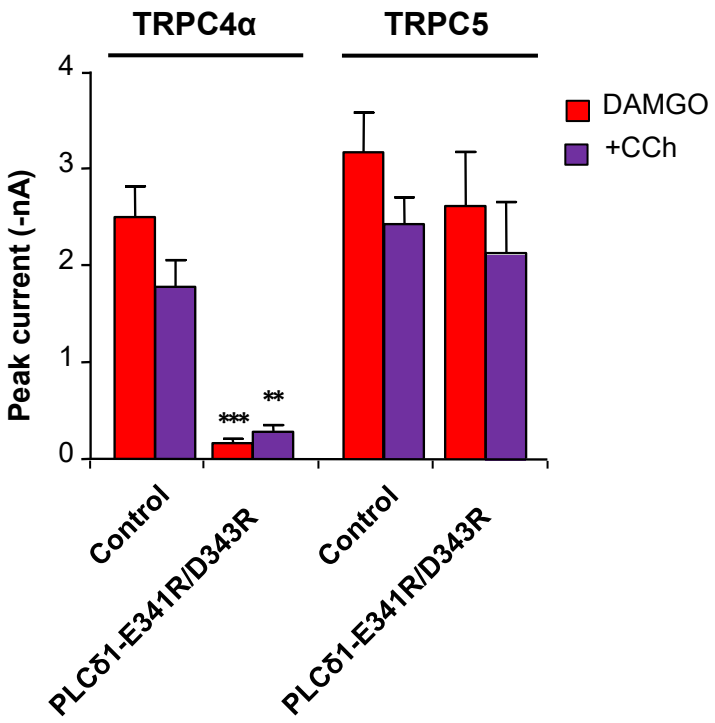

Figure 29. PLCδ1 is necessary for DAMGO-evoked TRPC4α but not TRPC5 activation

The dominant-negative PLCδ1 mutant (E341R/D343R) suppressed TRPC4α but not TRPC5 currents. HEK293 cells stably co-expressing μOR and TRPC4α or TRPC5 were transiently transfected with the control vector (pcDNA3.1) or cDNA for PLCδ1-E341R/D343R. Whole-cell currents were recorded as in **Fig. 28**. Shown are means ± SEM of peak currents at -60 mV for n = 6 - 8 cells. ** $p < 0.01$, *** $p < 0.001$ *vs* corresponding controls by unpaired *t* test.

PLCδ1 has been shown to be inhibited by RhoA (Hodson, Ashley et al. 1998, Murthy, Zhou et al. 2004). Indeed, when co-expressed, the constitutively active mutant of RhoA (L63) strongly inhibited TRPC4β (**Fig. 30a, b**). By contrast, expression of a dominant-negative RhoA mutant (N19) or RhoA-suppressing C3 exoenzyme accelerated the rate of TRPC4β activation without affecting peak amplitude (**Fig. 30a, b, c**), suggesting that RhoA inhibition of PLCδ1 might underlie the slow kinetics of $G_{i/o}$ -mediated TRPC4 activation. Importantly, inhibition by RhoA-L63 was reversed by co-expression of a constitutively active PLCδ1 mutant (δ1-ΔXY) (Hicks, Jezyk et al. 2008) (**Fig. 30a, b)**, demonstrating PLCδ1 as the specific target of RhoA in the context of TRPC4 activation. As controls, we verified that the PLCδ1 and RhoA mutants affected neither TRPC4β surface expression (**Fig. 31a**), nor CCh-stimulated Ca^{2+} store release (**Fig. 31b, c**), indicating that $G_{q/11}$-PLCβ pathway and TRPC4β trafficking remained intact under these conditions.

To test isoform specificity of PLCδ dependent facilitation, I coexpressed wild-type PLCδ1, PLCδ3 or PLCδ4 isoforms with and without the dn-PLCδ1 mutant E341R/D343R (**Fig. 32**). All three isoforms showed unique effects on TRPC4 peak currents and kinetics. While the peak currents were similar for PLCδ1 and PLCδ3 overexpressing cells, the time-to peak was dramatically reduced with PLCδ3. Both peak currents and rise-times were suppressed with overexpression of PLCδ4 (**Fig 32a-f**). In the presence of coexpressed dn-PLCδ1, overexpression of WT-PLCδ1 partially rescued DAMGO-evoked currents. Coexpression of PLCδ3, but not PLCδ4, also partially rescued DAMGO-evoked currents but to a lesser degree than PLCδ1. It is likely that PLCδ3 can partially mimic the effect of PLCδ1; however the strong inhibition seen with coexpression of PLCδ4 could either arise from the sequestration of PLCδ4 at the nucleus or

by PLCδ4 behaving as a dominant negative – sequestering PIP_2 at the plasma membrane, but unable to enzymatically act on TRPC4.

Next, I examined whether, similar to the facilitation provided by PLCβ activation, other PLC pathways (for example, PLCγ) could also facilitate $G_{i/o}$-mediated activation of TRPC4. Under subthreshold levels of $G_{i/o}$ activation with 30 nM DAMGO, activation of epidermal growth factor receptor (EGFR) facilitated TRPC4β activation, where subsequent addition of CCh did not cause any further increase (**Fig. 33a, b**). The current, however, was still dependent on the activation of PLCδ1 because it was abolished by the expression of dn-PLCδ1, emphasizing the critical role of PLCδ1 in $G_{i/o}$-TRPC4 activation. Stimulation of EGFR alone did not activate TRPC4β (**Fig. 31c**). However, it appeared to increase the rate of TRPC4β activation by stimulation of μOR with DAMGO, similar to that by CCh acting via $G_{q/11}$-PLCβ signaling. Therefore, facilitation of the PLCδ1-dependent, $G_{i/o}$-mediated, TRPC4 activation could be a general property of all PLC isoforms.

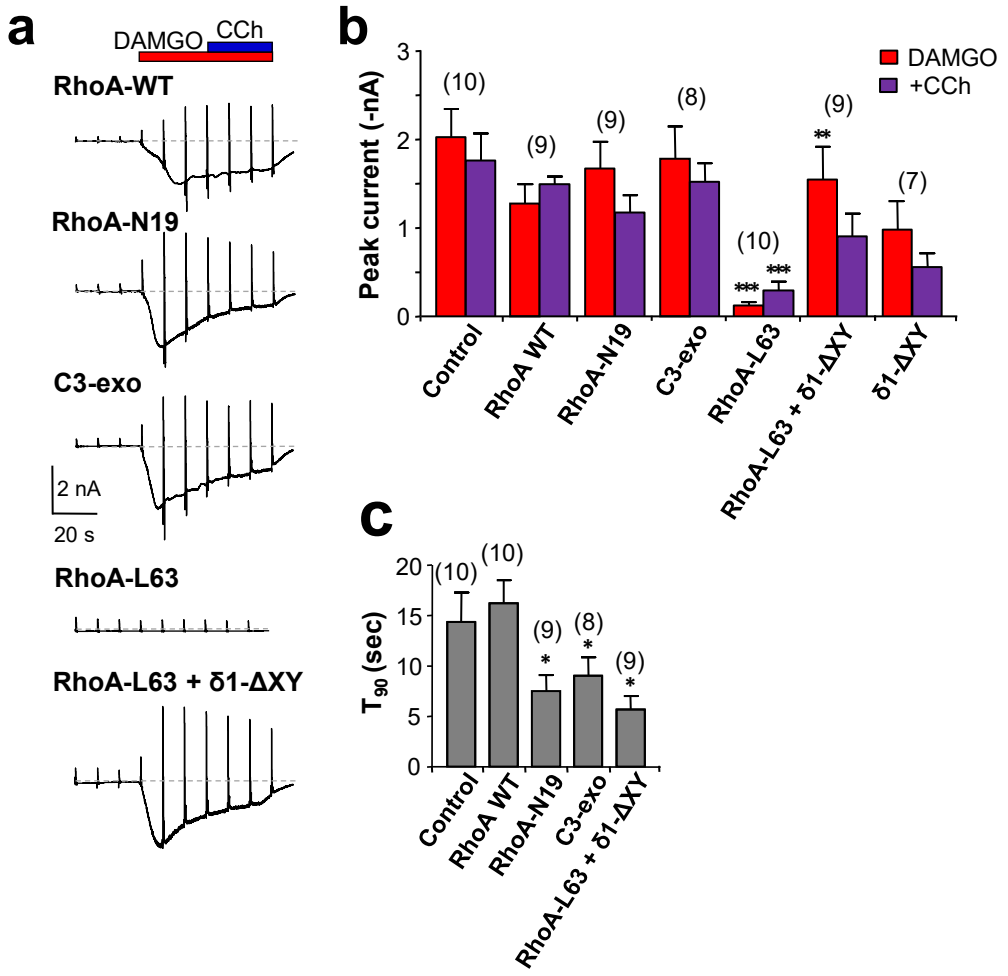

Figure 30. RhoA modulates PLCδ1's effect on TRPC4 activation

a. Whole-cell currents recorded from control and cells transiently expressing RhoA WT, dominant-negative RhoA mutant (RhoA-N19), RhoA inhibiting enzyme C3 exoenzyme (C3-exo), constitutively active RhoA mutant (RhoA-L63), or RhoA-L63 together with constitutively active PLCδ1 mutant (δ1-ΔXY). RhoA-N19 and C3-exo abolished biphasic current development induced by DAMGO while RhoA-L63 eliminated TRPC4β current, which was rescued by δ1-ΔXY. **b** & **c.** Summary of peak currents at -60 mV evoked by DAMGO and with addition of CCh (**b**) and T_{90} for DAMGO-evoked current at -60 mV (**c**). *** $p < 0.001$ *vs* control and $^{\#\#}$ $p < 0.01$ *vs* RhoA-L63 alone in **b** and * $p < 0.05$ *vs* control in **c,** by t-test.

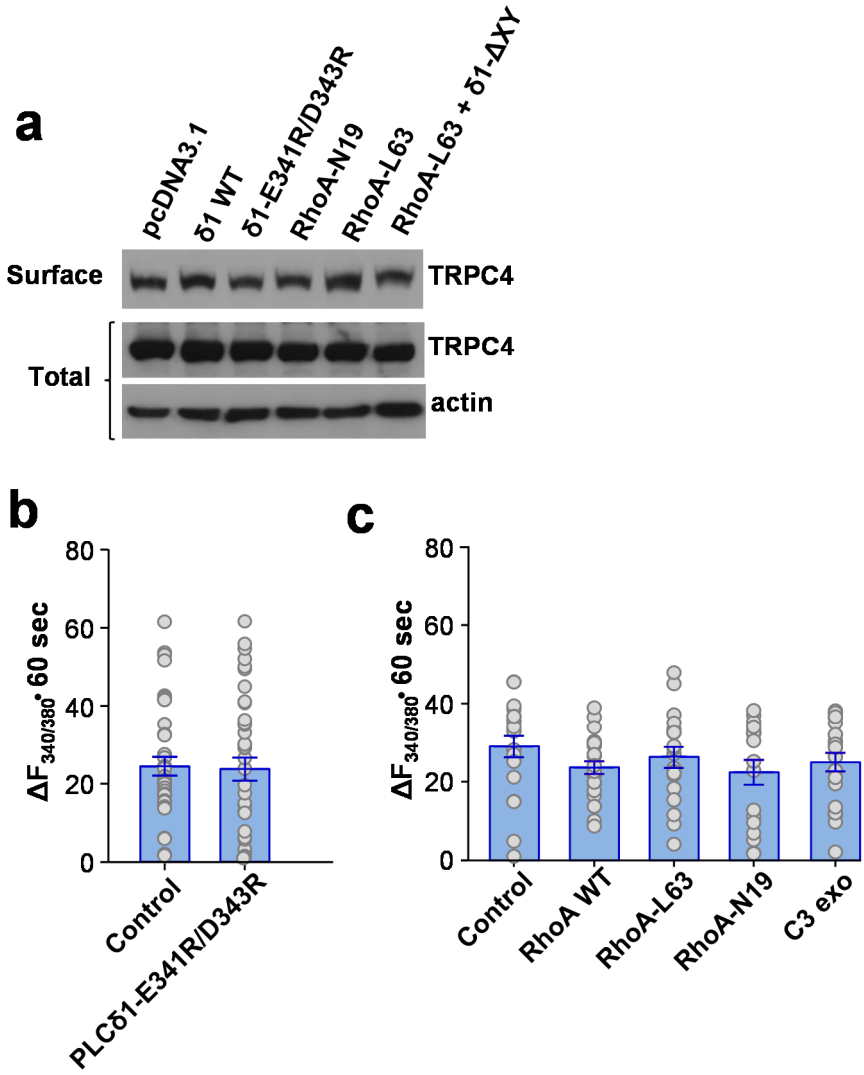

Figure 31. TRPC4 surface expression and store release is unmodified by PLCδ1 regulation

a. Cell surface expression of TRPC4β determined by surface biotinylation. TRPC4 in biotinylated (surface) fractions and in total proteins was determined by Western blotting. Actin was used as loading control. Transfection efficiency was ~80% as evaluated by GFP. The expression of indicated proteins in the stable cell line did not alter surface and total expression levels of TRPC4β. **b** & **c**. Overexpression of PLCδ1 (**b**) and RhoA (**c**) mutants did not affect $G_{q/11}$-PLCβ activation, as revealed by CCh-evoked store Ca^{2+} release. Stable HEK293 cells co-expressing μOR and TRPC4β were transiently transfected with pEGFP-N1 plus the control vector (pcDNA3.1) or the indicated cDNA constructs, seeded on glass coverslips and loaded with Fura-2. Cells were imaged in a Ca^{2+}-free external solution (with 0.2 mM EGTA) for fluorescence ratio changes when excited alternately at 340 and 380 nm and challenged with CCh (30 μM). Shown are integrated fluorescence ratio (F340/380) changed elicited by CCh for individual cells over a 60-sec period (area under the curve). The blue boxes and bars show means ± S.E.M. for n = 3 coverslips each with 10 - 30 cells per condition.

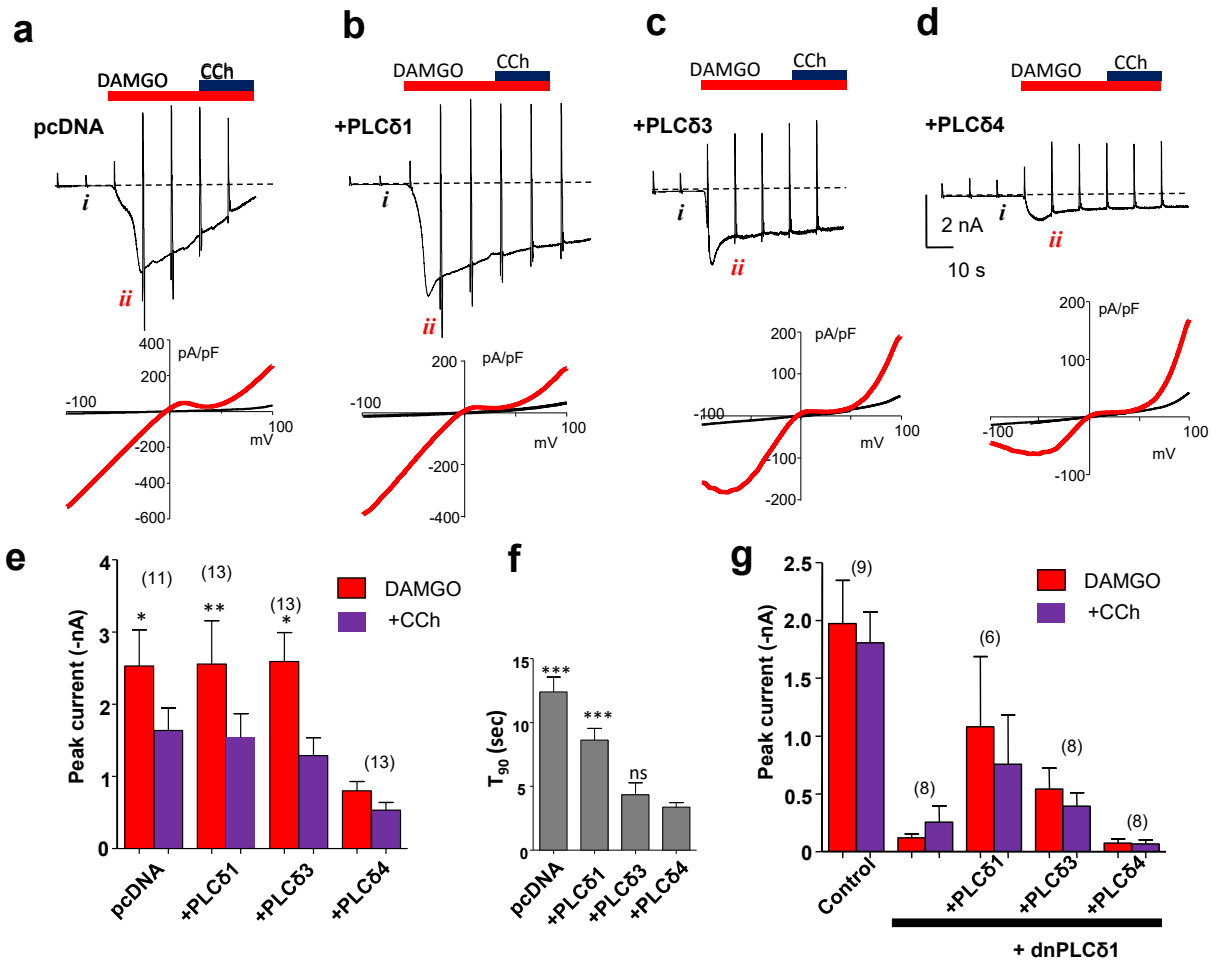

Figure 32. PLCδ isoforms have unique effects on $G_{i/o}$-mediated TRPC4 activation and reversal of dn-PLCδ1-induced inhibition

a-d. Representative whole-cell current traces (*upper*) and I-V curves (*lower*) recorded from stable μOR and TRPC4β co-expressing cells transiently transfected with an empty vector (**a**), human PLCδ1 (**b**), PLCδ3 (**c**), PLCδ4 (**d**). Recording conditions are as in **Fig. 28**. **e & f.** Summary of peak currents evoked by DAMGO and with addition of CCh (**e**) and T_{90} for DAMGO-evoked current at -60 mV (**f**). **g.** Similar experiments as in **a-e,** but cells were also transiently expressed dn-PLCδ1 mutant (E341R/D343R) where indicated. Summary of peak currents at -60 mV evoked by DAMGO and with addition of CCh are shown as means ± SEM. The number of cells are shown in parentheses.

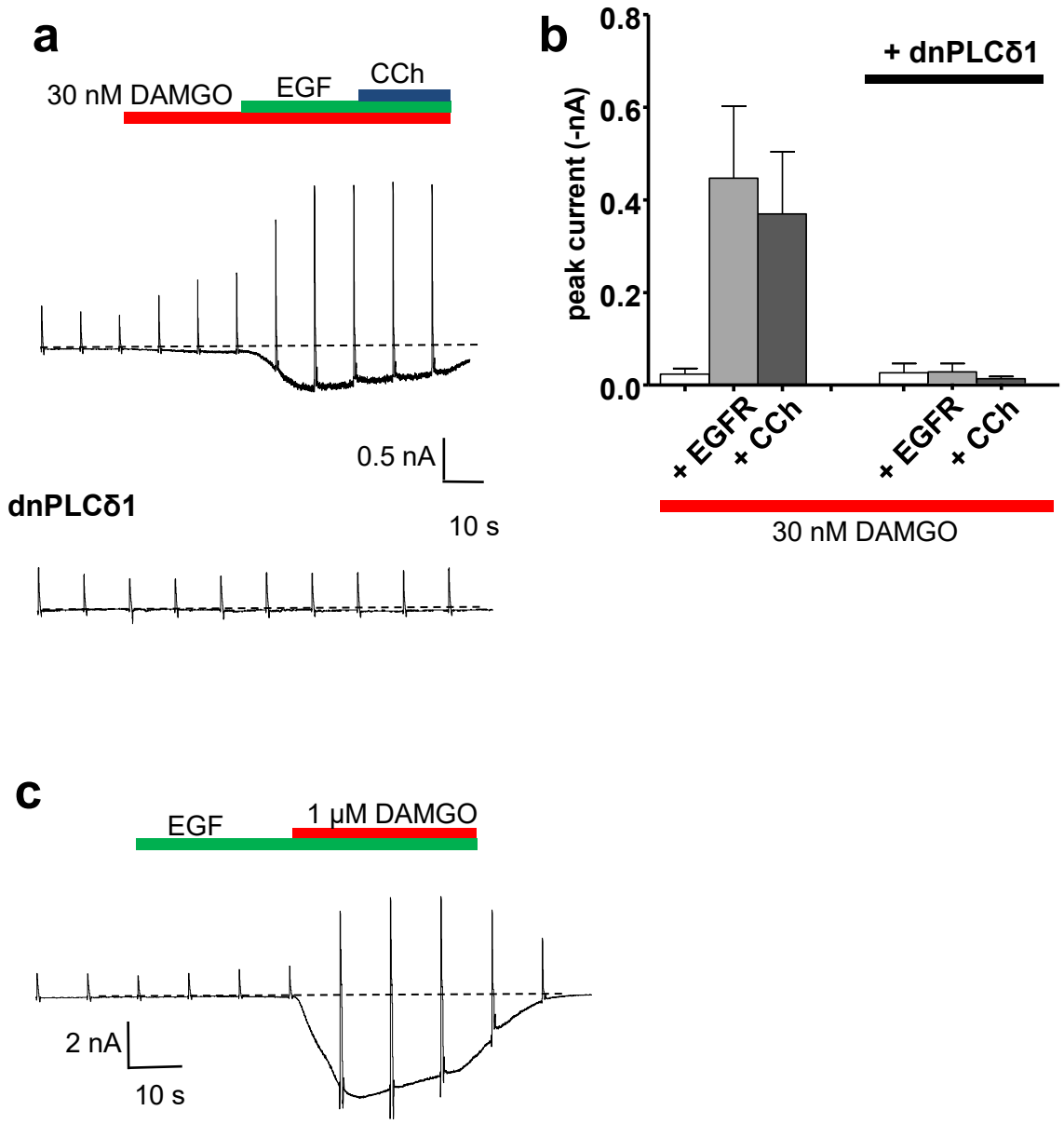

Figure 33. PLCγ facilitates $G_{i/o}$-mediated TRPC4 activation in a PLCδ1-dependent manner

All cells stably co-expressed TRPC4β and μOR. Whole-cell currents were recorded with the pipette solution containing 0.05 mM EGTA with no added Ca^{2+}. Cells were starved for 4 hours before experiments, by incubation in ECS at 37 °C to prevent EGFR desensitization induced by factors present in the culture medium. During experiments 50 ng/mL EGF was added after solubilization in ECS and applied via gravity driven perfusion as indicated. **a**. Below threshold activation by DAMGO (30 nM) was facilitated by EGF (*upper panel)* but was suppressed by overexpression of the dn-PLCδ1 mutant (*lower panel*). **b**. Summary data (means ± S.E.M.) of peak current at -60 mV for (**a**), n = 6 cells. * $p < 0.05$ by paired t-test. **c.** Treatment with EGF

alone did not result in TRPC4-like currents but accelerated the rate of DAMGO (1 μM)-evoked currents.

Summary V: PLCδ1 is a component downstream to intracellular Ca^{2+} elevation that is necessary for $G_{i/o}$ mediated TRPC4 activation. The activation of other PLC isoforms – PLCβ and PLCγ likely facilitates the action of PLCδ1 on TRPC4 through the increase of intracellular Ca^{2+}.

3.3 Discussion

Although TRPC channels are commonly thought as receptor-operated channels gated by PLC signaling, I show here that the $G_{q/11}$-PLCβ pathway may not be essential for TRPC4 activation. Rather, the channel requires $G_{i/o}$ proteins for activation and exhibits an unexpected dependence on PLCδ1, making it a coincidence detector of $G_{i/o}$ and PLCδ1 signaling. PIP_2 is both a substrate and a membrane docking site of PLCδ1 while Ca^{2+} is the main activator (Cifuentes, Honkanen et al. 1993, Essen, Perisic et al. 1996). Also, PLCδ1 is directly inhibited by the small GTPase, RhoA (Hodson, Ashley et al. 1998). Therefore, PLCδ1 appears to be central for the PIP_2 and Ca^{2+} dependence of TRPC4 activation. By inhibiting PLCδ1, endogenous RhoA likely contributes to the biphasic kinetics of $G_{i/o}$-activated TRPC4 current. Thus, disrupting RhoA function can accelerate channel activation. The specific effect of RhoA on PLCδ1 was confirmed by the finding that inhibitory effect of constitutively active RhoA mutant on TRPC4 activation was reversed by the constitutively active mutant of PLCδ1. Intriguingly, inhibiting PLCδ1 with either the active RhoA mutant or a dominant-negative PLCδ1, or reducing PLCδ1 expression by siRNA-mediated knockdown, abolished the effect of not only $G_{i/o}$, but also that of $G_{i/o}$ and $G_{q/11}$ co-stimulation, implicating a unique role of PLCδ1 that cannot be substituted by $G_{q/11}$-PLCβ. Thus, other than PIP_2 hydrolysis, there may be more intimate coupling and/or interaction between

PLCδ1 and TRPC4. The lack of effect of PLCδ1 inhibition on TRPC5 activation further argues for the coupling specificity.

Although PIP_2 has been reported to have both positive and negative effects on TRPC channels (Lemonnier, Trebak et al. 2008, Otsuguro, Tang et al. 2008, Trebak, Lemonnier et al. 2009, Kim, Jeon et al. 2013), the mechanism of its action remains mysterious. Studies with DAG-sensitive TRPC3/C6/C7 channels have revealed a strong dependence on PIP_2 itself to maintain channel activity, in addition to serving as a substrate for DAG production (Imai, Itsuki et al. 2012, Itsuki, Imai et al. 2012, Itsuki, Imai et al. 2014). Similarly, increasing PIP_2 levels attenuated desensitization of TRPC4β and TRPC5 (Kim, Kim et al. 2008, Kim, Jeon et al. 2013). Since PLCδ1 plays an essential role in TRPC4 activation, the substrate dependence may be explained by the fact that membrane translocation of PLCδ1 requires PIP_2 (Cifuentes, Honkanen et al. 1993). However, this may not be applicable to other TRPCs, including the closely related TRPC5, which is not dependent on PLCδ1.

PIP_2 may also exert its action by physically interacting with TRPC4 channel complex. Although it was shown that PIP_2 bound to the C-terminal region present in TRPC4α but not in TRPC4β (Otsuguro, Tang et al. 2008), it may also interact with TRPC4/C5 in a Ca^{2+}-dependent manner through SESTD1, a protein that binds to the CIRB site (Miehe, Bieberstein et al. 2010). However, both modes of interactions have been linked to channel inhibition. I show here that dephosphorylating PIP_2 facilitated TRPC4β activation, indicating the presence of a tonic inhibition by PIP_2 on not only TRPC4α but also TRPC4β. Combining previous results, our data suggest two forms of PIP_2 inhibition on TRPC4: one unique to TRPC4α and another common to both, since α incorporates the entire sequence of the β isoform (Otsuguro, Tang et al. 2008). In the previous study, the TRPC4α specific inhibition was uncovered with $G_{i/o}$ and $G_{q/11}$ co-

stimulation when the phospholipid content was elevated using exogenous PIP_2 (Otsuguro, Tang et al. 2008). Thus, with [PIP_2] elevated, $G_{q/11}$-PLCβ stimulation disrupted inhibition of TRPC4β, but not TRPC4α suggesting a lower affinity PIP_2 interaction at the common site than the unique site, which would be consistent with the conditions used in the current study to reveal PIP_2 inhibition on TRPC4β, i.e. weak $G_{i/o}$ and no $G_{q/11}$-PLCβ stimulation. Thus, one way that receptor stimulation causes TRPC4 activation is to reduce PIP_2.

The downstream factor from PIP_2 hydrolysis that supports TRPC4 activation appears to be Ca^{2+}. Since continued $[Ca^{2+}]_i$ rise can also be maintained by Ca^{2+} influx through open TRPC4 channels, the reliance on PIP_2 to produce a Ca^{2+} signal could be extraneous except for generating an initial trigger. As micromolar $[Ca^{2+}]_i$ is needed for TRPC4 activation and the channel is also inhibited by slightly higher $[Ca^{2+}]_i$, the dynamics of $[Ca^{2+}]_i$ change must be critical. With low EGTA concentrations that allow $[Ca^{2+}]_i$ to fluctuate, peak currents were about 2-fold higher than when $[Ca^{2+}]_i$ was clamped to 10 μM by BAPTA, supporting the importance of spatiotemporal dynamics of Ca^{2+} in TRPC4 regulation. Yet, Ca^{2+} alone did not recapitulate the effect of CCh on activation kinetics, suggesting involvement of additional components of PLC signaling in TRPC4 gating. I did not find any effect of IP_3, DAG and PKC on amplitude or kinetics of IM+DAMGO-evoked TRPC4β current**.** Rather, my data suggest that the rate-limiting step is PLCδ1 activation, on which both Ca^{2+} and PIP_2 may converge to control channel gating. PIP_2 hydrolysis and Ca^{2+} signals generated from PLCδ1 activity could further enhance channel opening. Altogether, the PLCδ1-TRPC4 duet forms a self-reinforcing loop for continued channel activation in a Ca^{2+}- and PIP_2-dependent fashion. The system requires $G_{i/o}$ activation, with $G_{q/11}$-PLCβ (or other PLC, such as PLCγ) acting as an accelerator and RhoA as a brake (**Fig. 34**).

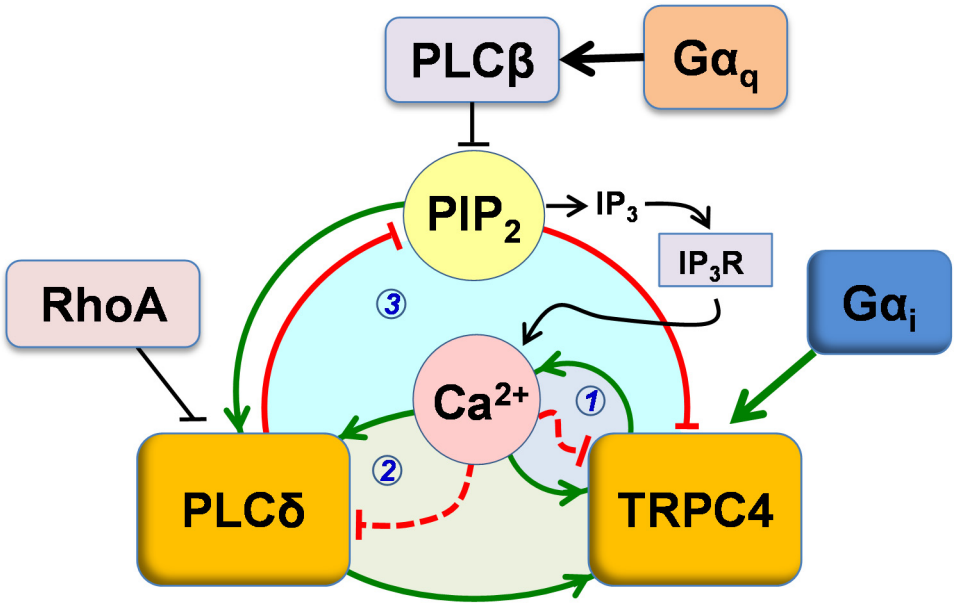

Figure 34. Model of the PLCδ1-TRPC4 self-reinforcing system

Positive and negative effects necessary for TRPC4 activation are indicated in green and red lines, respectively. Non-essential, modulatory effects are indicated in black. In addition to activating PLCδ1, Ca^{2+} might directly enhance channel function, based on previous work with TRPC5. Therefore, at least 3 self-reinforcing loops exist to sustain TRPC4 activity in the presence of $G_{i/o}$ stimulation: positive feedback between Ca^{2+} and TRPC4 (1), PLCδ1, Ca^{2+} and TRPC4 (2), a double negative effect between PLCδ1, PIP_2 and TRPC4 which is continuously supported by Ca^{2+} that links TRPC4 function to PLCδ1 activation (Chatzigeorgiou, Yoo et al. 2010). The system is facilitated by $G_{q/11}$-PLCβ pathway which provides the Ca^{2+} signal for PLCδ1 activation and helps lower the barrier of channel gating by reducing PIP_2. It is negatively regulated by RhoA through inhibiting PLCδ1 and high Ca^{2+} levels, which may inhibit either TRPC4 or PLCδ1, or both (dashed lines).

Because of the dual regulation by both Ca^{2+} and PIP_2, the system should also be very sensitive to signaling processes that alter the levels of these intracellular messengers, making TRPC4 a versatile sensor and integrator of diverse transmitter inputs, critical for its functions in neurons and muscles. Interestingly, persistent TRPC4 activation was observed in lateral septal neurons exposed very briefly to an mGluR agonist in a manner dependent on $[Ca^{2+}]_i$ changes and voltage-gated Ca^{2+} channel activation (Tian, Thakur et al. 2013), adding another variable in native

cells where membrane depolarization and Ca^{2+} entry via voltage-gated channels can be critical for TRPC4 function. Moreover, interplay among $G_{i/o}$, PLCδ1, and Ca^{2+} entry channels has been documented in rabbit gastric smooth muscle where activation of $G_{i/o}$ -coupled receptors caused delayed activation of PLCδ1 in a manner thought to depend on SOCE and inhibited by RhoA (Murthy, Zhou et al. 2004). However, the pharmacology used and presence of TRPC4 in these cells (Lee, Jun et al. 2005) would argue that the entry channel was formed by TRPC4. Therefore, not only does PLCδ1 support TRPC4 activation, but also TRPC4 function enhances PLCδ1 activity. The positive feedback loops formed by this system should have strong implications to its function as an environmental and stress sensor in the gastrointestinal (GI) tract (Tsvilovskyy, Zholos et al. 2009), cardio-pulmonary vasculature (Tiruppathi, Freichel et al. 2002, Tiruppathi, Minshall et al. 2002), and neurons (Munsch, Freichel et al. 2003, Phelan, Mock et al. 2012).

Chapter 4

Calmodulin has a dual action on TRPC4β activity

4.1 Introduction

In the previous chapter, I demonstrated that $G_{i/o}$-medicated TRPC4 activation was bi-directionally regulated by intracellular Ca^{2+}. Although the Ca^{2+}-dependence of PLCδ1 may explain, to a large extent, the Ca^{2+} requirement that supports the reinforcing positive feedback loop between PLCδ1 and TRPC4, there remains a possibility that other Ca^{2+} targets also participate in the regulation of channel function. CaM can bind to TRPC4α at four sites (one at the N terminus and three at the C terminus) and TRPC4β at two sites (one at the N terminus and one at the C terminus). The common site at the C-terminus is the CIRB domain, which is conserved in all TRPC isoforms and interacts with CaM in a Ca^{2+}-dependent manner (Tang, Lin et al. 2001, Zhu 2005). In the presence of Ca^{2+}, the interaction between IP_3R and TRPC is inhibited by CaM. Additionally, it had been shown that in inside-out patches TRPC4-like activity was facilitated in the presence of the CaM inhibitor, calmidazolium. However, it remains unclear whether CaM inhibits only TRPC4 function, or if it has other effects on the channels, and to what extent the CIRB domain contributes to these effects. Here, I tested the hypothesis that a part of the Ca^{2+} dependent facilitation and/or inhibition of TRPC4 activation may arise from the regulation of TRPC4 by Ca^{2+}-CaM.

4.2 Results

4.2.1 Pharmacological inhibition of CaM modulates TRPC4 currents bimodally

Pharmacological inhibition of endogenous CaM in HEK293 cells using ophiobolin A (Oph-A) or calmidazolium (CMZ) perfused through the patch pipette resulted in a facilitation of the $G_{i/o}$ -mediated TRPC4β response activated by a weak stimulation of μOR (with 30 nM DAMGO) (**Fig. 35**). This suggested that CaM has an inhibitory effect on the activation of TRPC4. In contrast, when high doses of DAMGO and CCh were used to maximally activate the channel, the CaM inhibitors resulted in a partial inhibition of the peak TRPC4 current. This result suggested that either Ca^{2+}-CaM contributes towards full activation of TRPC4 or that CaM inhibitors have a non-specific effect that reduces the peak TRPC4 response.

4.2.2 Disruption of CaM binding to TRPC4β C terminus facilitates channel activation

To identify the site of action of CaM as well as to eliminate the possibility that the effects on TRPC4 were a result of non-specific reactions of CaM inhibitors, I used a TRPC4β mutant where the CIRB domain has been modified so that IP_3R binding is allowed at the domain but the binding of CaM is not (based on X-ray crystallographic data on CaM-TRPC5 interactions from Dr. Jian Yang's lab, Columbia University). The mutated channel protein is referred to as TRPC4β-IRB mutant (or IRB).

Compared to the wild type channel, the IRB mutant was activated more strongly at low concentrations of DAMGO, but showed reduced peak currents in response to the co-stimulation of both $G_{i/o}$ and $G_{q/11}$ pathways by DAMGO and CCh (**Fig 36**), mirroring the dual regulation seen with pharmacological inhibition of CaM. These two sets of experiments suggest that it is indeed the action of CaM on the TRPC4 CIRB domain that regulates channel activity. Interestingly, the

N terminal CaM binding (NCB) site mutant (ΔNCB) which had the binding site deleted, showed a complete ablation of current. At this moment it is not known whether this mutant: 1) renders the channel silent, or 2) prevents channel subunits from assembling into functional tetramers or 3) prevents trafficking of the channel to the plasma membrane.

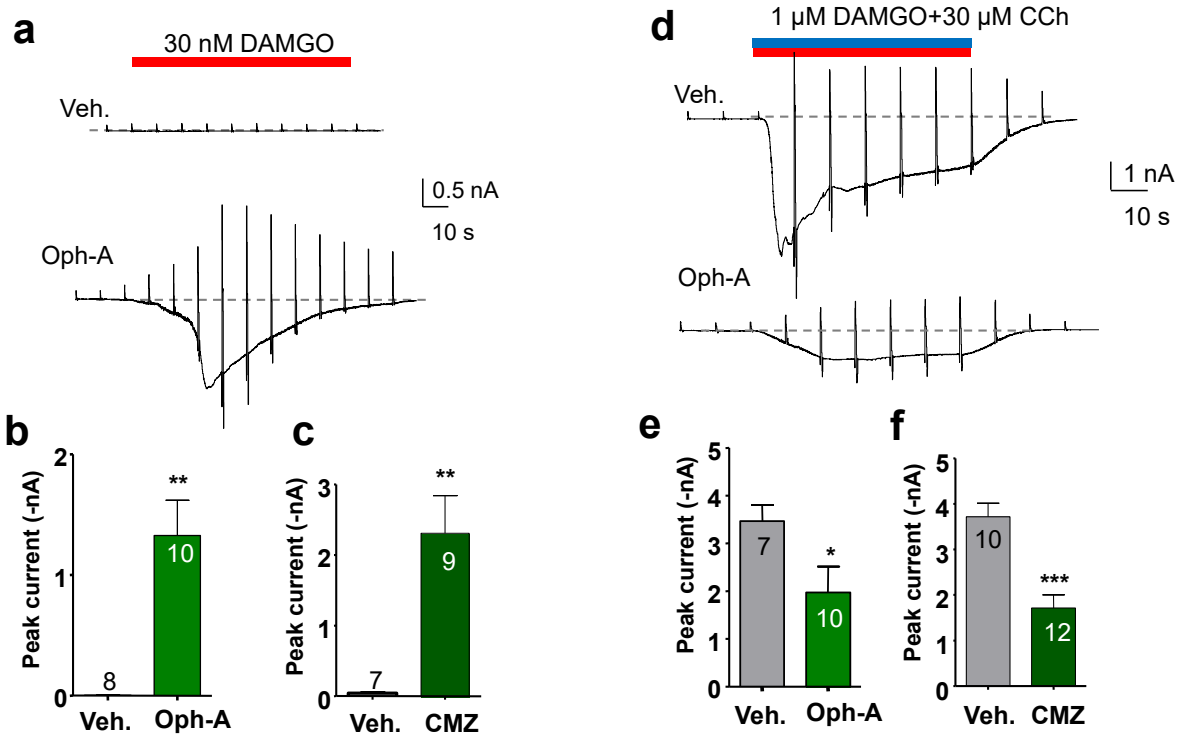

Figure 35. OphA and CMZ modulate TRPC4 currents bimodally

All cells stably co-expressed TRPC4β and μOR. **a-c.** In the whole-cell patch clamp configuration, CaM inhibitor, Oph-A (**a,b**) or CMZ (**c**) (each 10 μM) was infused into the cell through the patch pipette and allowed to dialyze into the cell for 5 minutes. Cells were subsequently stimulated with 30 nM DAMGO. Both CaM inhibitors facilitated TRPC4 activation under application of subthreshold concentrations of DAMGO. **d-f**, Similar to **a-c**, but maximal stimulation of TRPC4 by co-activation of $G_{i/o}$ and $G_{q/11}$ was carried out with 1 μM DAMGO and 30 μM CCh. In this case, the CaM inhibitors suppressed the peak TRPC4 currents. For controls, appropriate amounts of DMSO (solvent used for both Oph-A and CMZ) were added to the patch pipette solution. Summary data (means ± SEM) for DAMGO or DAMGO + CCh-evoked peak currents at -60 mV are shown. Concentration of EGTA in all patch pipette solutions was 0.05 mM with no added Ca^{2+}.

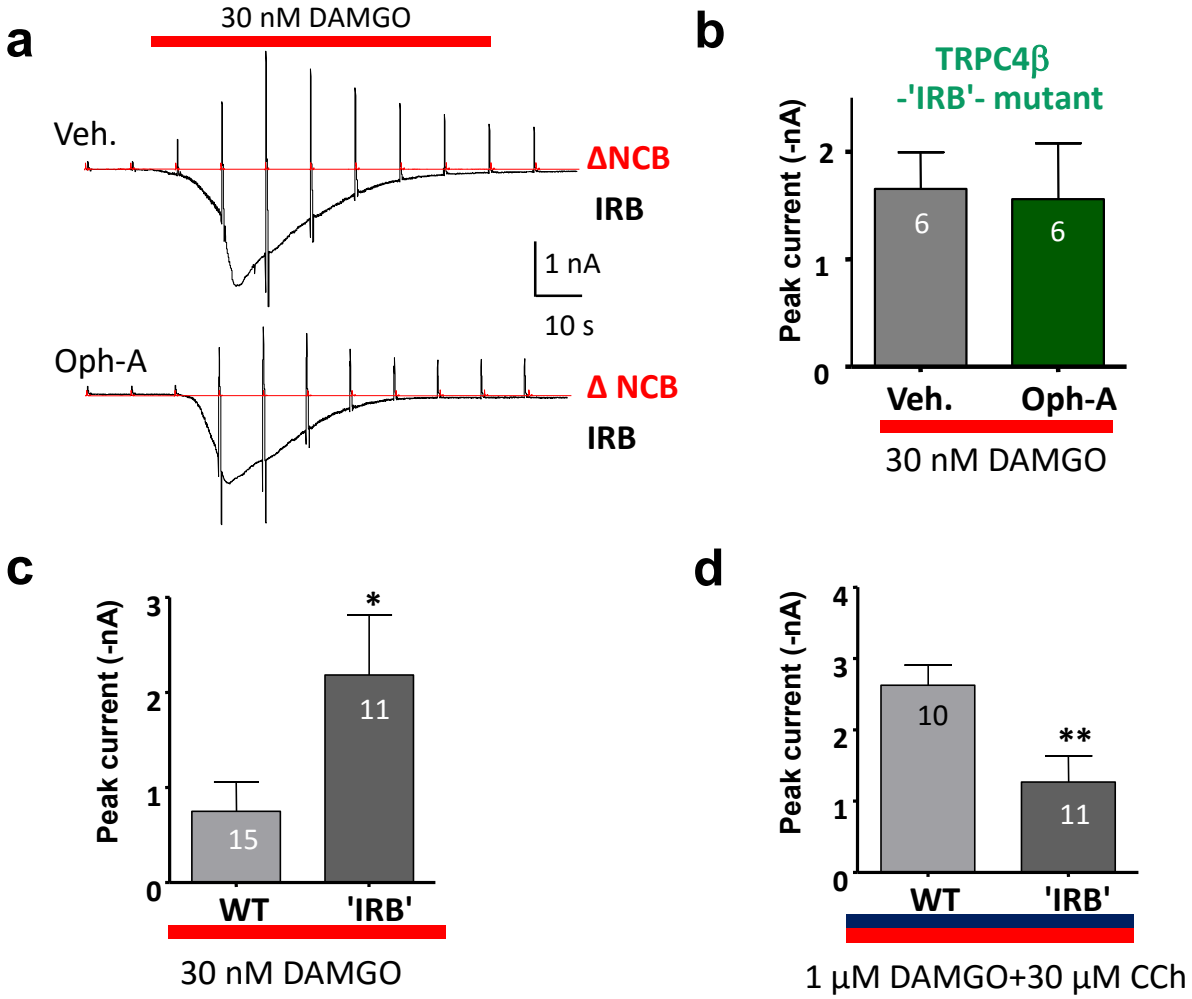

Figure 36. Disruption of CaM binding to TRPC4 CIRB domain facilitates channel activation by weak $G_{i/o}$ stimulation but inhibits the peak currents evoked by strong co-stimulation of both $G_{i/o}$ and $G_{q/11}$ pathways

a & **b.** In cells stably expressing µOR and transiently expressing the TRPC4β C-terminal CaM binding site mutant 'IRB', a subthreshold concentration of DAMGO (30 nM) showed similar levels of activation in the absence and presence of Oph-A. In comparison with cells transiently expressing wild type TRPC4β, the IRB mutant showed higher peak currents in response to 30 nM DAMGO. Note, cells transiently expressing TRPC4β showed weak response to 30 nM DAMGO, unlike the lack of response seen in cells stably expressing this channel under the same conditions (**Fig 35**). This might be due to the higher expression levels with transient transfection. Similar to **figure 35d-f**, under maximal stimulation by DAMGO and CCh, the IRB mutant showed suppressed peak currents in comparison with cells transiently expressing the wild type channel. Summary data (means ± SEM) for DAMGO or DAMGO + CCh-evoked peak currents at -60 mV are shown. Concentration of EGTA in all patch pipette solutions was 0.05 mM with no added Ca^{2+}.

4.2.3. Ca^{2+} binding defect mutants of CaM alter TRPC4 response to $G_{i/o}$ stimulation

Next, I examined whether a modification of the Ca^{2+} binding sites of CaM would alter the response of TRPC4 to $G_{i/o}$ and/or $G_{q/11}$ stimulation, based on the previous finding that certain CaM mutations selectively impair its association with the TRPC4 C terminal CIRB domain (Zhu 2005). Of these, the EF3 mutant, where a single amino acid substitution (Glu104 to Ala) renders it ineffective to bind to Ca^{2+} at this site, was shown to be least affected for binding to TRPC4 CIRB domain in comparison with other CaM mutants, such as Glu31Ala (EF1), Glu67Ala (EF2), or Glu140Ala (EF4) or double mutants EF1,2 and EF3,4. Similarly, although the CIRB domains of TRPC1 and TRPC5 (but not TRPC2, 3, 6) also showed high affinities to the EF3 mutant, the TRPC5 CIRB domain showed even higher affinity to EF4 and EF3,4 mutants (Zhu 2005), which may account for differential modulation of TRPC4 and TRPC5 by CaM.

In whole-cell recordings, overexpression of the CaM EF3 mutant but not the EF3,4 mutant led to a facilitation of the TRPC4 current development in response to subthreshold stimulation of μOR by DAMGO (**Fig. 37a**). However, there was no significant change in the peak currents in response to maximal stimulation of $G_{i/o}$ and $G_{q/11}$ signaling (**Fig. 37b**). The facilitation seen with the EF3 mutant, but not the EF3,4 mutant, mirrors the difference in binding seen with the TRPC4 CIRB domain, where EF3 binds to the TRPC4 CIRB domain but EF3,4 does not (Zhu 2005). As the CaM EF3,4 mutant does not bind to TRPC4, its overexpression was not expected to impact channel function as it would be unable to compete with the endogenous CaM to exert any effect. On the other hand, the overexpressed EF3 can compete with endogenous CaM and occupy the binding site, but in a different configuration because of the loss of Ca^{2+} binding to the 1^{st} EF hand at the C-lobe. It is well known that CaM C-lobe binds to Ca^{2+} with high affinity (Linse, Helmersson et al. 1991) and is most likely Ca^{2+} bound under resting $[Ca^{2+}]_i$. Therefore, the C-lobe

binding to TRPC4 may present an inhibitory action on channel opening, which was crippled by disrupting Ca^{2+} binding to CaM EF3, in the TRPC4β-IRB mutant or by treatment with CaM antagonist. On the other hand, the N-lobe of CaM, which binds to Ca^{2+} with low affinity, may be involved in enhancing TRPC4 function. Because this interaction requires high $[Ca^{2+}]_i$, it is more apparent when the channels are strongly activated. This interaction was not disrupted by the mutation at EF3 of CaM, but abolished by the TRPC4β-IRB mutant or treatment with CaM antagonist. Therefore, the decrease in TRPC4 peak currents in response to maximal stimulation was only detected under the two later conditions, but not when CaM EF3 mutant was overexpressed. These results indicate that CaM regulates channel activity through binding to the C-terminal CIRB site where binding conformations change in response to elevation of $[Ca^{2+}]_i$, such that at low resting $[Ca^{2+}]_i$, CaM C-lope binding inhibits channel opening whereas upon $[Ca^{2+}]_i$ rise, the N-lobe binding facilitates channel opening. This dynamic change in CaM conformation explains the bimodal effects of CaM on TRPC4 channel function.

Summary VI: CaM regulates $G_{i/o}$ mediated TRPC4 activation. At low resting $[Ca^{2+}]_i$ (likely Ca^{2+} bound at the C-loop), CaM posts an inhibition on TRPC4 activation. At high $[Ca^{2+}]_i$ (likely Ca^{2+}bound at both N- and C-loops), CaM facilitates TRPC4 activation. The dual effects of CaM was revealed by the use of CaM antagonists and the CIRB domain mutant of TRPC4β for which CaM binding to its C terminus is prevented.

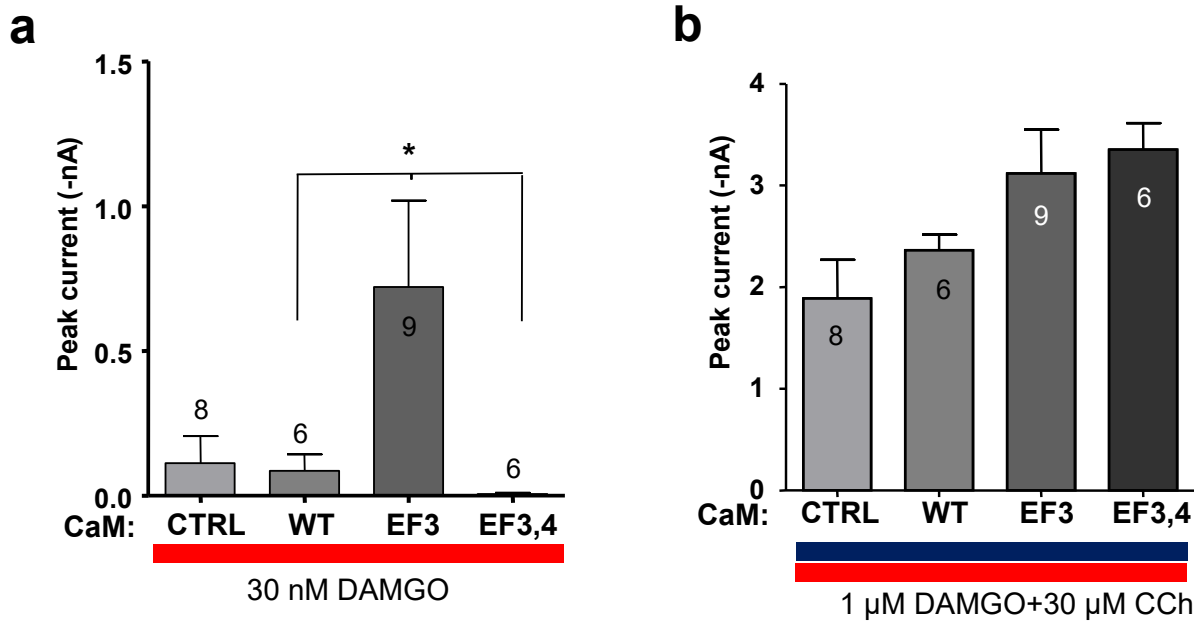

Figure 37. CaM mutants have differential effects on TRPC4

All cells stably co-expressed TRPC4β and μOR. Wild type CaM or CaM mutants in pcDNA3.1 were transiently transfected and cells were recorded by whole-cell patch clamping after 16-24 hours. Summary data (means ± SEM) for DAMGO or DAMGO + CCh-evoked peak currents at -60 mV are shown. Concentration of EGTA in all patch pipette solutions was 0.05 mM with no added Ca^{2+}.

4.3. Discussion

Although Ca^{2+}-CaM binding to TRPCs have been demonstrated long before (Zhu 2005), exactly how such interactions affect the channel function remains largely unexplored. TRPC4 is particularly complex with respect to CaM regulation because of the presence of multiple CaM-binding sites. Therefore, I decided to focus on TRPC4β as it contains two less CaM-binding sites than TRPC4α and therefore allows a better opportunity of dissecting the site-specific regulation. In addition, the availability of crystallographic structure of Ca^{2+}-CaM-bound TRPC5 CIRB domain makes it possible to predict the critical residues in TRPC4β CIRB domain involved in

coordinating the interaction with CaM, allowing specific disruption of CaM binding to this domain with minimal unintended effect on other regulatory functions. Intriguingly, the CIRB mutant appears to be responsible for both the tonic inhibition on channel activation by $G_{i/o}$ signaling and the potentiation of channel function in response to strong stimulation. That both of these effects are mediated by CaM, was demonstrated by the observation that pharmacological inhibition of CaM had almost identical consequences as disrupting CaM binding to the TRPC4β CIRB domain. Furthermore, the dual effects of CaM can most likely be explained by C-lobe binding to the CIRB site under resting $[Ca^{2+}]_i$, while the elevation of which due to the TRPC4 channel function itself and/or other $[Ca^{2+}]_i$ rising mechanisms recruit the N-lobe to alter CaM interaction at this critical motif to enhance channel function. This novel mechanism of Ca^{2+}-CaM regulation on TRPC4 warrants additional investigation.

Unlike the CIRB site, little is known about how CaM binds to the N-terminal CaM binding (NCB) site of TRPC4. Since no crystal structure is available for this domain, it has been difficult to design strategies to selectively disrupt CaM binding at the NCB site. So far, all attempts targeting the NCB domain have rendered TRPC4β non-functional. Therefore, the NCB site appears to be critical for channel function and/or assembly and/or trafficking. It would require additional work to sort out these possibilities. One of the additional CaM-binding sites of TRPC4α has a very low affinity for Ca^{2+} (~600 nM) compared to the CIRB domains of all TRPCs (Tang, Lin et al. 2001). This site therefore might function as a negative regulatory site in the presence of high $[Ca^{2+}]_i$. However, since Ca^{2+}-dependent inhibition was also observed in TRPC4β, the Ca^{2+} dependent inhibition shown in **Fig. 24d** has to be intrinsic to both TRPC4α and C4β, arguing for a more finite regulation by the extra CaM-binding site in TRPC4α. Further experimentation and possibly molecular dynamics simulations with a TRPC4C terminus co-crystallized with CaM or

a homology based structure prediction based on the crystallized TRPC5 C terminus, should shed more light on the multimodal regulation of CaM on TRPC4.

Chapter 5

Protons accelerate $G_{i/o}$-mediated TRPC4 activation in a Ca^{2+}-dependent manner

5.1 Introduction

In **Chapter 3**, I have shown that $[Ca^{2+}]_i$ rise enhanced the probability, but not the rate, of whole-cell current development of TRPC4β in response to stimulation of $G_{i/o}$ proteins via μOR activation, indicating that the Ca^{2+} signal alone cannot completely recapitulate the effect of $G_{q/11}$-PLCβ stimulation via endogenous muscarinic receptors. Considering the factors of the PLC pathway that may cooperate with Ca^{2+} to facilitate TRPC4 activation, I had examined various products or downstream signals of PIP_2 hydrolysis, including DAG, PKC, and IP_3, but did not observe any obvious effect (See **Ch. 3**). There is one more, but often overlooked, PIP_2 hydrolysis product H^+, which is generated at a molar ratio of 0.8 per substrate and was shown to be critical for activation of TRP and TRPL channels in *Drosophila* photoreceptors (Huang, Liu et al. 2010).

Protons regulate the latency of *Drosophila* TRP channel in response to repeated light stimuli via their effect on the scaffolding protein INAD, which contains five postsynaptic density/discs-large/zonula occludens (PDZ) domains and coordinates the formation of a complex composed of TRP, rhodopsin and PKC. Although an ortholog of INAD does not exist in mammals, another scaffolding protein called NHERF (Na^+/H^+-exchanger regulatory factor) consisting of two PDZ domains has been shown to be associated with TRPC4 and PLCβ (Tang, Tang et al. 2000). This raises the possibility that TRPC4 may also be modulated by intracellular protons in a similar fashion as *Drosophila* TRP channels.

Supporting the modulatory effect of protons on TRPC4 function, the activities of TRPC4 and the closely related TRPC5 were shown to be facilitated by an acidification of the extracellular

solution (Semtner, Schaefer et al. 2007). A mutation of Glu543 located in the P-loop to Gln only eliminated pH potentiation of GTPγS-evoked current but did not completely abolish the pH potentiation of basal TRPC5 current, suggesting the presence of an additional proton sensor(s). As extracellular acidification induces intracellular acidification in HEK293 cells, it is likely that the pH potentiation of TRPC5 and therefore also TRPC4 may occur from the intracellular side. Therefore, I examined whether and how intracellular acidification could affect TRPC4 activation. I focused especially on activation kinetics because this property was unaffected by increasing $[Ca^{2+}]_i$ in the absence of $G_{q/11}$-PLCβ stimulation.

5.2 Results

Again, the stable HEK293 cell line co-expressing TRPC4β and μOR was used for whole-cell voltage clamp recordings. Pipette solutions contained 0.05 mM EGTA and no added Ca^{2+} to allow TRPC4 activation by co-stimulation with DAMGO and IM (both at 1 μM). I used three methods to lower intracellular pH (pH_i). First, pH_i was clamped by a higher HEPES concentration (50 mM) to either 6.5 or 7.2 in the pipette solution. Similar to the standard pipette solution as shown in **Figs. 23a** and **26a**, in the presence of IM, DAMGO evoked a biphasic current development with pH_i clamped to 7.2. However, with pH_i clamped to 6.5, the biphasic current development was eliminated, resulting in a faster activation kinetics than the pH 7.2 pipette solution without a change in the peak current (**Fig. 38a-c**).

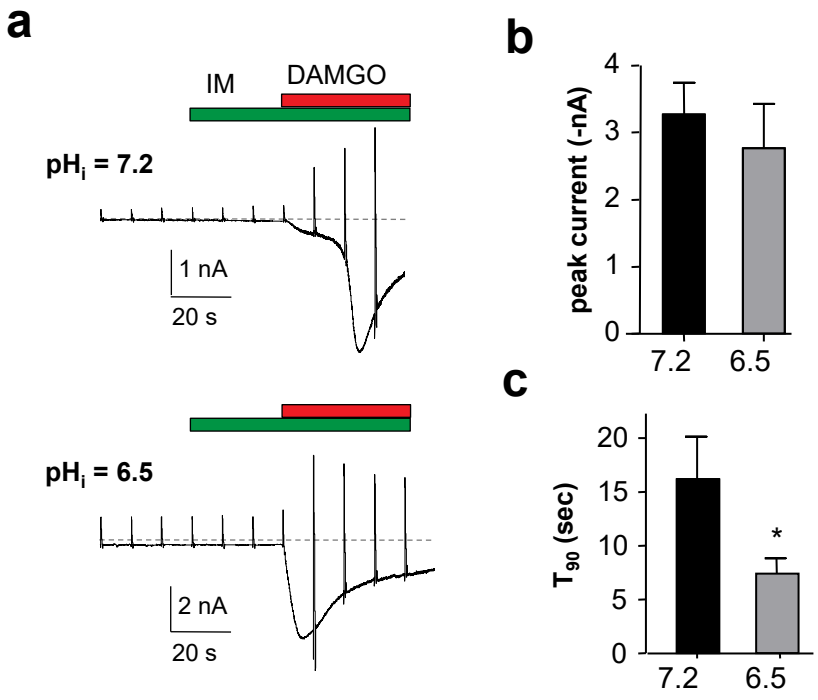

Figure 38. Protons accelerate $G_{i/o}$-mediated TRPC4 activation

For **a-c**, all cells stably co-expressed TRPC4β and μOR and pipette solutions contained 0.05 mM EGTA with no added Ca^{2+}. **a**, Whole-cell currents evoked by DAMGO (1 μM) in the presence of IM (1 μM) in cells dialyzed with pipette solutions having pH buffered to 7.2 (*upper panel*) and 6.5 (*lower panel*) by 50 mM HEPES. Note the faster development of current with pH_i of 6.5. **b** & **c**, Summary (means ± SEM) of peak currents (**b**) and T_{90} (**c**) at -60 mV evoked by DAMGO in the presence of IM. n = 7 for each. * $p \leq 0.05$ by unpaired *t* test.

However, intracellular dialysis does not allow changing pH_i at desired time points and the low pH solution could potentially elicit undesired currents upon making whole-cell - thereby interfering with $G_{i/o}$-mediated TRPC4 currents. Therefore, I used the sodium acetate (NaAc) gradient method (Yuan, Shimura et al. 2003, Niemeyer, Cid et al. 2010) to alter pH_i through bath perfusion while maintaining a constant extracellular pH (pH_o = 7.4). To do this, 5 mM NaAc was included in the pipette solution adjusted to pH 7.4. With the cell held under whole-cell configuration, increasing extracellular NaAc concentration to 7.9, 39.5, or 125.4 mM (with equal molar exchange for NaCl, all at pH 7.4) led to the expected pH_i drop to 7.2, 6.5, or 6.0 according to the formula given in **Chapter 2, page 56**. These pH_i changes were confirmed by imaging fluorescence ratio changes inside the cell with BCECF under the exactly the same conditions used for whole-cell recordings (**Fig. 40a**). With co-stimulation by IM (1 μM), I showed that reducing pH_i to 7.0 markedly decreased T_{90} of DAMGO-evoked TRPC4β current by ~9 s (**Fig. 39c**). Maximal decreases (final T_{90} ranged from 4.4 to 6.1 sec, n = 16) were obtained in the pH_i range of 6.25 to 6.75 (**Fig. 39a,c**). However, T_{90} became much longer at $pH_i < 6.25$, indicating that, mirroring the effect of Ca^{2+}, the pH regulation is also bi-directional, with pH_i 7 to 6.25 being facilitating and $pH_i < 6.25$ being inhibitory. Fitting the data points with a biphasic Hill equation yielded the pH_i of 7.25 for half maximal facilitation and pH_i of 6.09 for half maximal inhibition - for proton effects on the rate of TRPC4 activation (**Fig. 39c**). Remarkably, $[Ca^{2+}]_i$ rise was needed for the proton effects as in the absence of IM, T_{90} remained about constant across the entire pH range tested (**Fig. 39c**). Furthermore, the maximal current amplitudes were unchanged by pH_i or IM (**Fig. 39b**). Therefore, intracellular pH strongly affected the kinetics of $G_{i/o}$-mediated TRPC4β activation when $[Ca^{2+}]_i$ was elevated. While TRPC4α was similarly regulated by pH_i as TRPC4β, TRPC5 only showed facilitation but not inhibition by pH_i, at least until pH 6.0 (**Fig. 39c**).

Moreover, the facilitation effect by pH_i 6.5 on T_{90} was also detected with free $[Ca^{2+}]_i$ clamped to 10 μM by 10 mM BAPTA without IM stimulation (**Fig. 40b**), confirming it is Ca^{2+}, rather than IM, dependent.

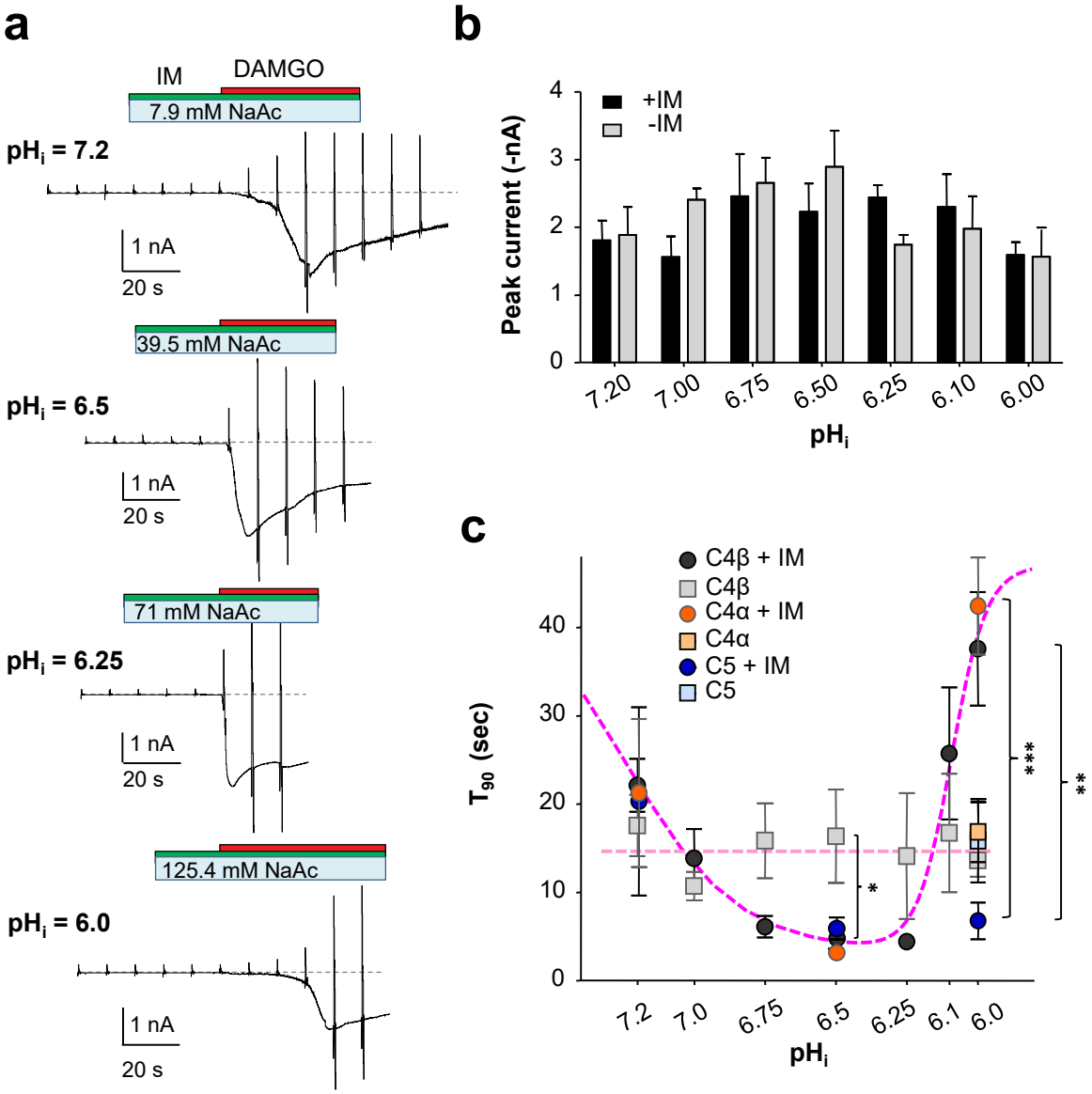

Figure 39. Protons accelerate $G_{i/o}$-mediated TRPC4 activation in a Ca^{2+}-dependent manner

a. Whole-cell TRPC4β currents evoked by DAMGO (1 μM) following the change of pH_i to varying levels by extracellular application of different concentrations of NaAc as indicated. IM (1 μM) was applied to increase $[Ca^{2+}]_i$. The pipette solution contained 5 mM NaAc and was adjusted to pH 7.4. Note the differences in the kinetics of current development with different pH_i. **b**, Summary (means ± SEM) of peak currents at -60 mV evoked by DAMGO in the presence (*black*) and absence (*gray*) of IM with pH_i changed by NaAc to values as indicated. **c**, Summary (means ± SEM) of T_{90} for DAMGO-evoked currents in the presence (*circles*) and absence (*squares*) of IM with pH_i changed by NaAc for cells that stably expressed μOR together with TRPC4β, TRPC4α, or TRPC5 (n = 6-9). Note the lack of inhibition by pH 6.0 for TRPC5. Data for TRPC4β in the presence of IM were fitted with the biphasic Hill equation assuming maximal and minimal T_{90} values of 50 and 3.3 sec. The estimated EC_{50} for pH_i facilitation was 7.25, Hill

2.15; the estimated IC_{50} for pH_i inhibition was 6.09, Hill -7.07. Data for TRPC4β in the absence of IM were fitted with linear regression. * $p \leq 0.05$ for +IM *vs* –IM for TRPC4β, ** $p \leq 0.01$, *** $p \leq 0.001$ *vs* TRPC5 (+IM), by unpaired *t* test.

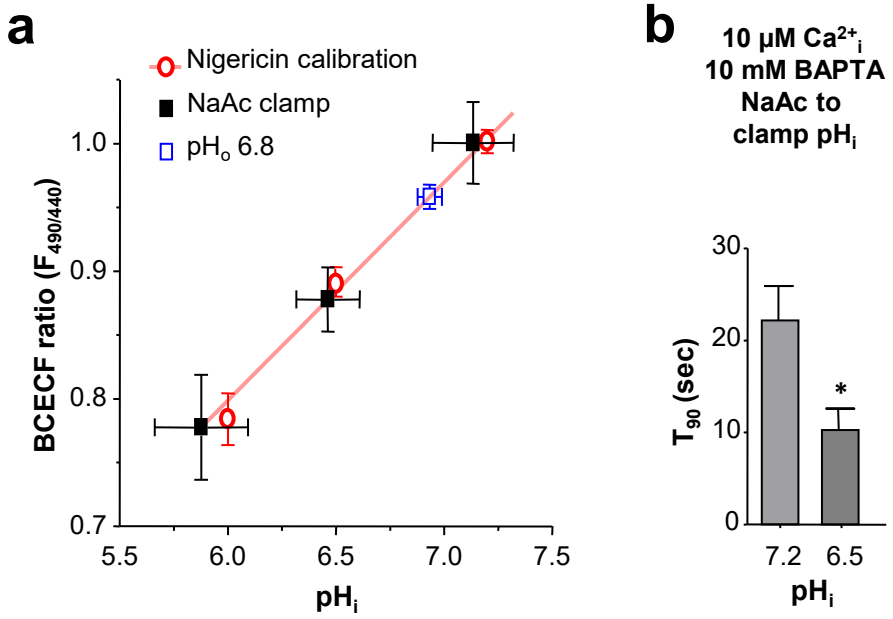

Figure 40. Calibration of intracellular pH (pH_i) changes induced by NaAc gradients

a, Cells stably expressing TRPC4β and µOR were voltage-clamped at -60 mV with the pipette solution that contained (in mM): 140 CsCl, 5 NaAc, 1 $MgCl_2$, 0.05 EGTA, and 10 HEPES, pH 7.4, supplemented with 300 µM BCECF (2',7'-Bis-(2-Carboxyethyl)-5-(and-6)-Carboxyfluorescein; free K^+ salt). The initial bath solution contained (in mM): 140 NaCl, 5 KCl, 2 $CaCl_2$, 1 $MgCl_2$, 10 glucose, and 10 HEPES, pH 7.4. After establishment of the whole-cell configuration and dialysis for > 5 min, the bath was changed to a solution in which an equal molar NaCl was replaced with 7.9, 39.5, or 125.4 mM NaAc (all at pH 7.4) with the expected pH_i drop to 7.2, 6.5, or 6.0 while BCECF fluorescence images were taken at alternating excitations of 440 and 490 nm at 3 sec intervals. At the end of the experiment, the cells were exposed to calibration solutions containing 145 KCl, 2 $CaCl_2$, 1 $MgCl_2$, 10 glucose, and 10 HEPES, supplemented with 10 µM nigericin, with pH adjusted to 7.2, 6.5, and 6.0, and BCECF fluorescence images continuously taken. Background fluorescence intensities were determined using neighboring cells not loaded with BCECF. Background subtracted $F_{490/440}$ ratios from KCl/nigericin calibration (means ± SEM, n = 5 for each pH) were used to generate the standard curve by linear regression fit. pH_i levels (means ± SEM) for NaAc gradients (n = 5 for each condition) were determined from the standard curve and were found to be very close to the predicted values. The blue box represents the BCECF ratio and the calculated pH_i in response to the bath application of the pH 6.8 extracellular solution as used in **Fig. 41** (n = 4). **b**, T_{90} of TRPC4 currents evoked by DAMGO (1 µM) when free $[Ca^{2+}]_i$ was clamped to 10 µM by 10 mM BAPTA and pH_i clamped to 7.2 or 6.5 by the NaAc gradient. pH_i 6.5 still accelerated the current development under these conditions

indicating that intracellular Ca^{2+} rise rather than IM treatment *per se* was involved in cooperating with protons to facilitate TRPC4 activation. n = 9, * $p < 0.05$ by unpaired *t* test.

Third, because extracellular acidification also reduces pH_i (Kettenmann and Schlue 1988), I tested the effect of lowering pH_o on DAMGO-induced TRPC4β activation in the presence of IM. Changing pH_o from 7.4 to 6.8 significantly reduced T_{90} (**Fig. 41a, c**). However, since TRPC4 and C5 activities are enhanced by extracellular protons (Semtner, Schaefer et al, 2007), the effect of pH_o 6.8 could reflect regulation at the extracellular side. To prevent the extracellular effect, I mutated the two critical glutamates, E542 and E543, to glutamines and tested the activation by DAMGO and IM in cells that co-expressed μOR and TRPC4β (E542Q/E543Q). Again, pH_o 6.8 significantly decreased T_{90} as compared to pH_o 7.4 (**Fig. 41b, c**). Moreover, using a pH_i 8.5 pipette solution to counteract the pH_i lowering effect of pH_o, I completely prevented the facilitation by pH_o 6.8 on the mutant channel (**Fig. 41b, c**). For the wild type channel, the pH_i 8.5 solution also partially reversed the facilitation by pH_o 6.8 (**Fig. 41a, c**). Importantly, these manipulations on pH_o and pH_i did not significantly change the peak current (**Fig. 41d**). These results suggest that extracellular protons potentiated TRPC4 activation through both extracellular and intracellular mechanisms.

The above results, thus, suggest that protons are another constituent of PLC activation that cooperates with Ca^{2+} to support $G_{i/o}$-mediated TRPC4 activation. Then preventing the pH_i drop to < 7.0 during co-stimulation of $G_{i/o}$ and $G_{q/11}$ would be expected to slow down channel activation. Buffering pH_i to 8.5 in the pipette solution indeed increased T_{90} of TRPC4β current evoked by co-application of DAMGO (1 μM) and CCh (30 μM) and this effect was more pronounced with the stronger pH buffer by 100 mM HEPES than by the standard 10 mM HEPES (**Fig. 42a, b**). Again, the peak current was not changed by the alkaline pH_i (**Fig. 42c**).

Furthermore, with the optimal pH_i and $[Ca^{2+}]_i$, *Dr*VSP-induced current suppression was significantly decreased (**Fig. 43**), suggesting a reduced dependence on PIP_2 and its products. Altogether, these results suggest that a moderate pH_i decrease due to hydrolysis of PIP_2 is a key component of PLC activation that facilitates $G_{i/o}$-mediated TRPC4β activation.

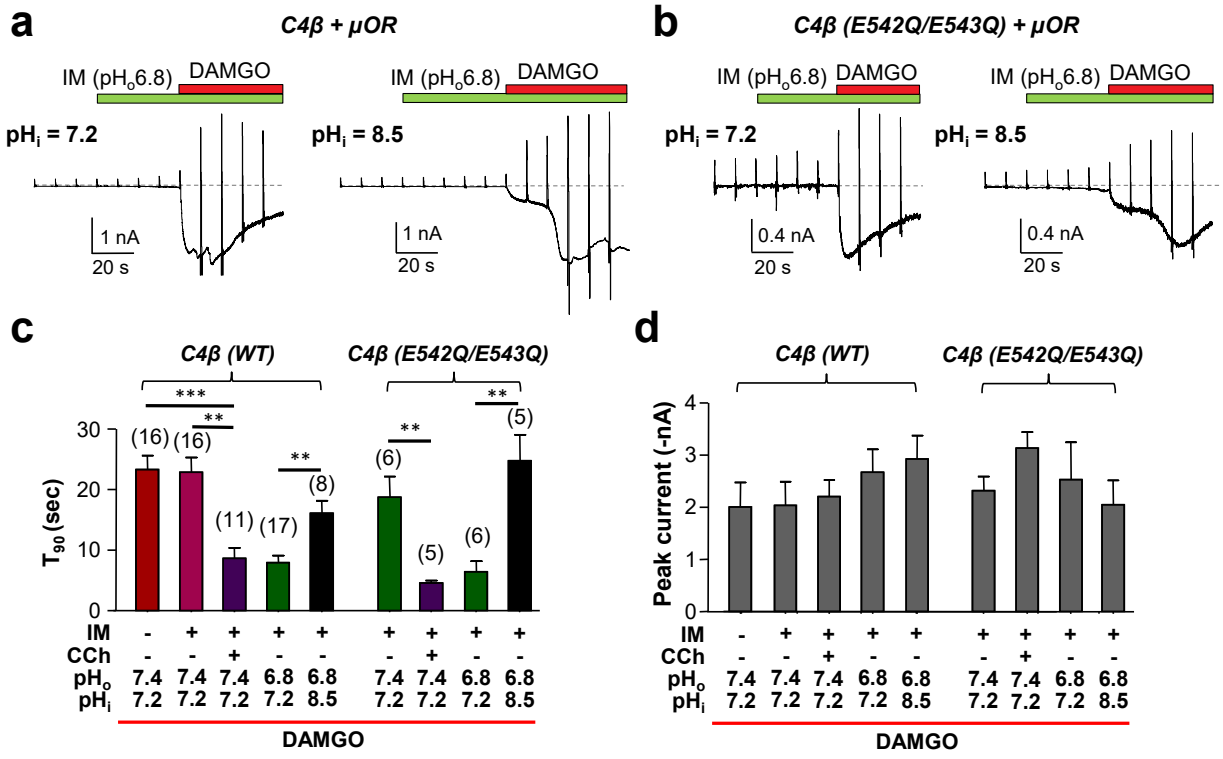

Figure 41. Extracellular acidification accelerates the rate of $G_{i/o}$-mediated activation of TRPC4β and its E542Q/E543Q mutant, and the effect was blocked by intracellular alkalinization

a-d, HEK293 cells stably expressing μOR were transiently transfected with cDNA for wild type (WT) or the E542Q/E543Q mutant of mouse TRPC4β as indicated. Pipette solutions contained 0.05 mM EGTA and no added Ca^{2+} and the pH was buffered at 7.2 or 8.5 with 100 mM HEPES. In the presence of IM (1 μM), whole-cell current development in response to DAMGO (1 μM) was accelerated by lowering extracellular pH (pH_o) from 7.4 to 6.8 for both WT (**a**) and the mutant (**b**) TRPC4β channels when pH_i was buffered at 7.2 (*left panels*). However, raising the pH_i to 8.5 prevented the accelerating effect of pH_o 6.8 (*right panels*). Summaries (means ± SEM) show similar facilitation on T_{90} by pH_o 6.8 as CCh (10 μM), but the effect was reversed by pH_i 8.5 for both WT and the mutant channels (**c**). However, the peak currents at -60 mV were not affected (**d**). ** $p \leq 0.01$, *** $p \leq 0.001$ by unpaired *t* test.

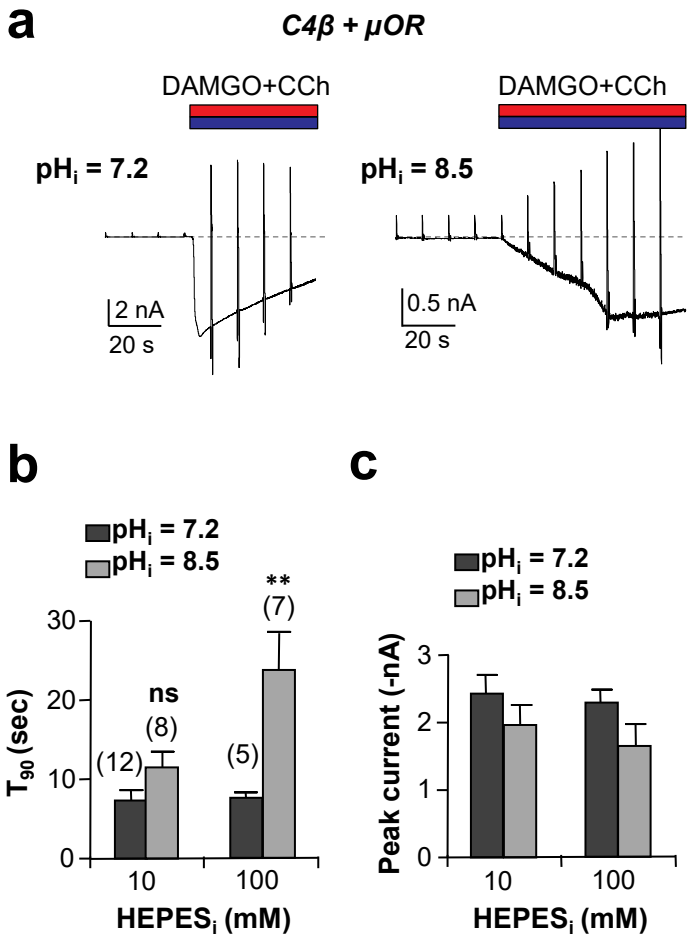

Figure 42. Alkaline intracellular pH slows down TRPC4 activation

a. Whole-cell currents evoked by simultaneous application of DAMGO (1 μM) and CCh (10 μM) in cells that stably co-expressed TRPC4β and μOR. Pipette solutions contained 0.05 mM EGTA and no added Ca^{2+} and the pH was buffered at 7.2 or 8.5 with either 10 or 100 mM HEPES. Shown are example traces with pH_i buffered at 7.2 (*left panel*) and 8.5 (*right panel*) by 100 mM HEPES (**c**) and summaries (means ± SEM) for T_{90} (**b**) and peak currents at -60 mV (**c**) with pH_i buffered at 7.2 or 8.5 with either 10 or 100 mM HEPES as indicated. ** $p < 0.01$, ns, not significant *vs* pH_i = 7.2 by unpaired *t* test. Numbers of cells are shown in parentheses.

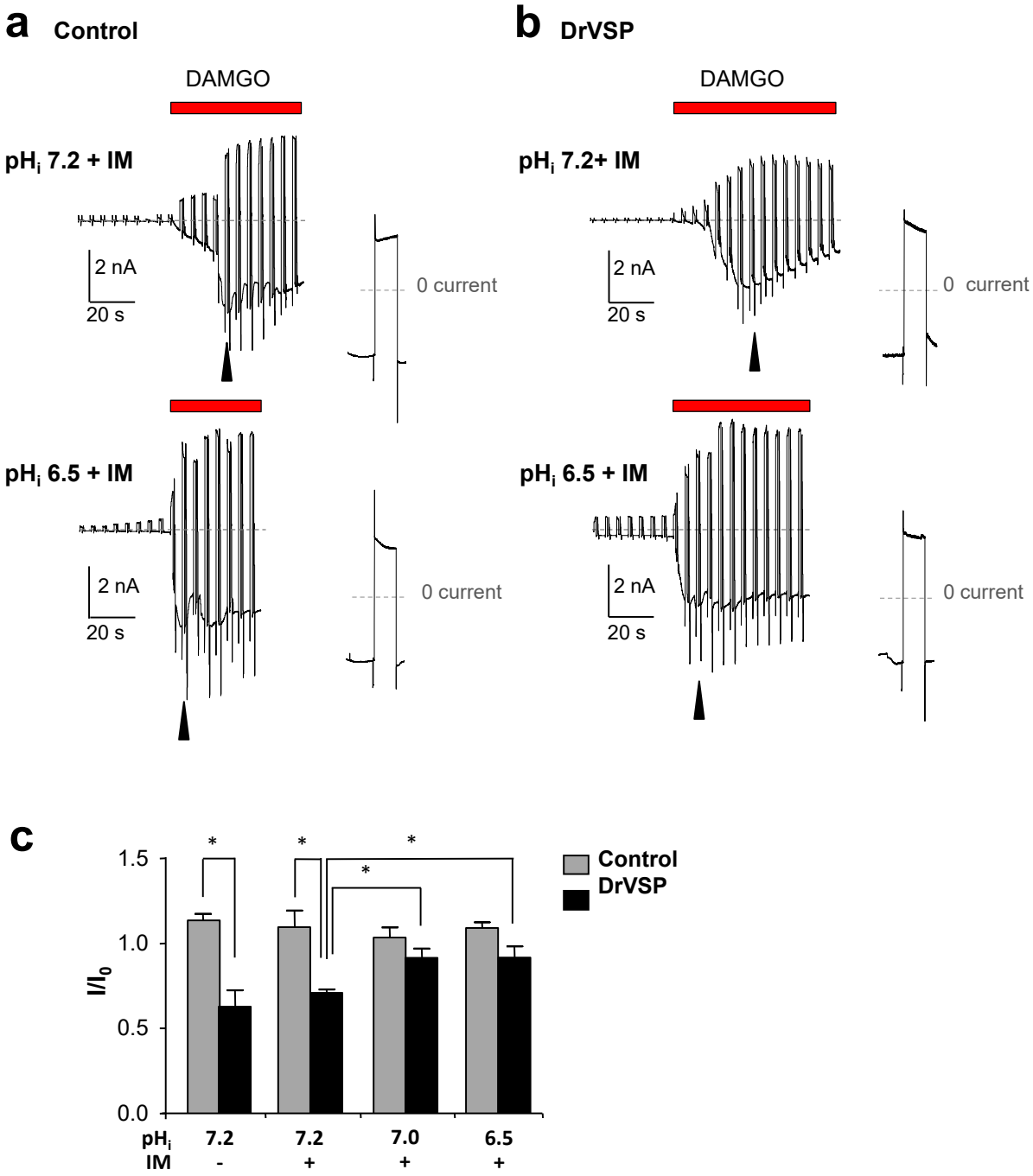

Figure 43. Simultaneous elevations of $[Ca^{2+}]_i$ and $[H^+]_i$ attenuated the PIP_2 dependence

Cells that stably co-expressed TRPC4β and μOR were transiently transfected with either a control vector (**a**) or the cDNA for DrVSP (**b**). The pipette solution contained 0.05 mM EGTA with no added Ca^{2+} and 5 mM NaAc with the initial pH of 7.4. Cells were held at -60 mV and currents continuously recorded while a depolarization pulses to 100 mV for 1 sec was applied every 5 sec. A voltage ramp was added 0.5 sec after each pulse. IM (1 μM) and NaAc (7.9 or 39.5 mM) were applied extracellular to increase $[Ca^{2+}]_i$ and clamp pH_i to 7.2 (*upper panels*) or 6.5

(*lower panels*) 30 sec before DAMGO (1 μM) was added. The sections indicated by the arrowheads are expanded at the left. Note the current depression in DrVSP-expressing cells seen at pH_i 7.2 is diminished at pH_i 6.5. c, Summary of I/I_0. Data are means ± SEM for 4 cells of each condition.* $p \leq 0.05$.

To test whether the proton dependent facilitation required a cystosolic component, I used excised outside-out and inside-out patches. Because the nominally Ca^{2+}-free solutions made using the untrapure water from Milli-Q Water Purification system (EMD Millipore) contain very low Ca^{2+} (<100 nM by Fura-2 measurement), I assessed the Ca^{2+}- and pH-dependence of TRPC4 using intracellular solutions made of (in mM): 140 CsCl, 5 KCl, 1 $MgCl_2$, varying $CaCl_2$, and 50 mM HEPES, with pH adjusted by CsOH to varying levels between 6.0 to 7.2. No Ca^{2+} chelator was added to avoid the complex effect of the chelator on pH and free $[Ca^{2+}]_i$. The extracellular solution was nominally Ca^{2+} free to avoid $[Ca^{2+}]_i$ changes due to Ca^{2+} influx. In outside-out patches excised from cells that expressed TRPC4β and μOR, application of DAMGO (1 μM) elicited macroscopic currents at -60 mV with pH_i ranged from 6.4 to 7.4 and $[Ca^{2+}]_i$ ranged from 1 to 10 μM (**Fig. 44a**). With varying combinations of pH_i and $[Ca^{2+}]_i$, I observed an intersecting bimodal dependence, with maximal currents achieved just below pH_i 7.0 at ~ 10 μM Ca^{2+} (**Fig. 44a, b**). On the other hand, only single channel activities were detected in inside-out patches even with the Ca^{2+} concentration at the cytoplasmic side switched to 10 μM (**Fig. 45**). Lowering the pH_i from 7.2 to 7.0 did not change the activity while lowering it to 6.5 only resulted in inhibition, instead of facilitation (**Fig. 45**). This conflict between the outside-out and inside-out patches could be explained by the difference in the intracellular milieu isolated in the two excised patch techniques – the outside-out patch is typically a larger portion of the membrane and may retain parts of the cytoplasm such as the ER and the cytoskeleton. The inside-out patch is expected to contain fewer cytoplasmic elements. The difference in pH_i dependence therefore may arise from a pH sensitive

cytoplasmic component which is lost in the inside-out configuration. The pH dependent inhibitory process might be more proximal or directly on the channel. The Ca^{2+} facilitation might be accounted for by a direct effect of Ca^{2+} on the channel domains or on CaM which associates with the C –terminus (**Chapter 4**).

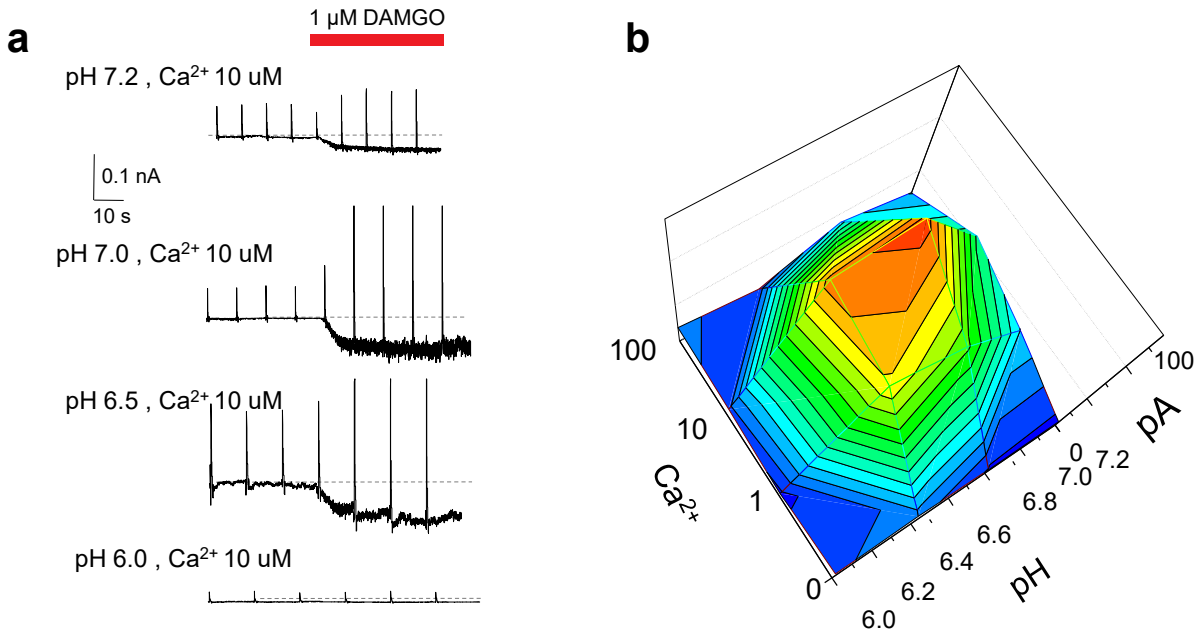

Figure 44. Dependence of macroscopic TRPC4 currents on pH_i and $[Ca^{2+}]_i$ in outside-out patches

In HEK293 cells stably expressing µOR and TRPC4β, outside-out recordings were made with pipette solutions where pH was clamped with 50 mM HEPES and free Ca^{2+} concentrations set without any Ca^{2+} chelator. No Ca^{2+} chelator or Ca^{2+} was added to the external buffer, which gave background levels of nominally free Ca^{2+} to exist in the solution to allow for only the internal Ca^{2+} and pH to influence the currents. **a.** Representative current traces recorded at – 60 mV (applied to the intracellular side – inside the patch pipette) at $[Ca^{2+}]_i$ of 10 µM and varying pH_i as indicated. Note that DAMGO (1 µM) evoked macroscopic currents. **b.** Summary of peak currents (n = 6-8) shows a coincident bimodal dependence – with a narrow range for both pH_i and $Ca^{2+}{}_i$.

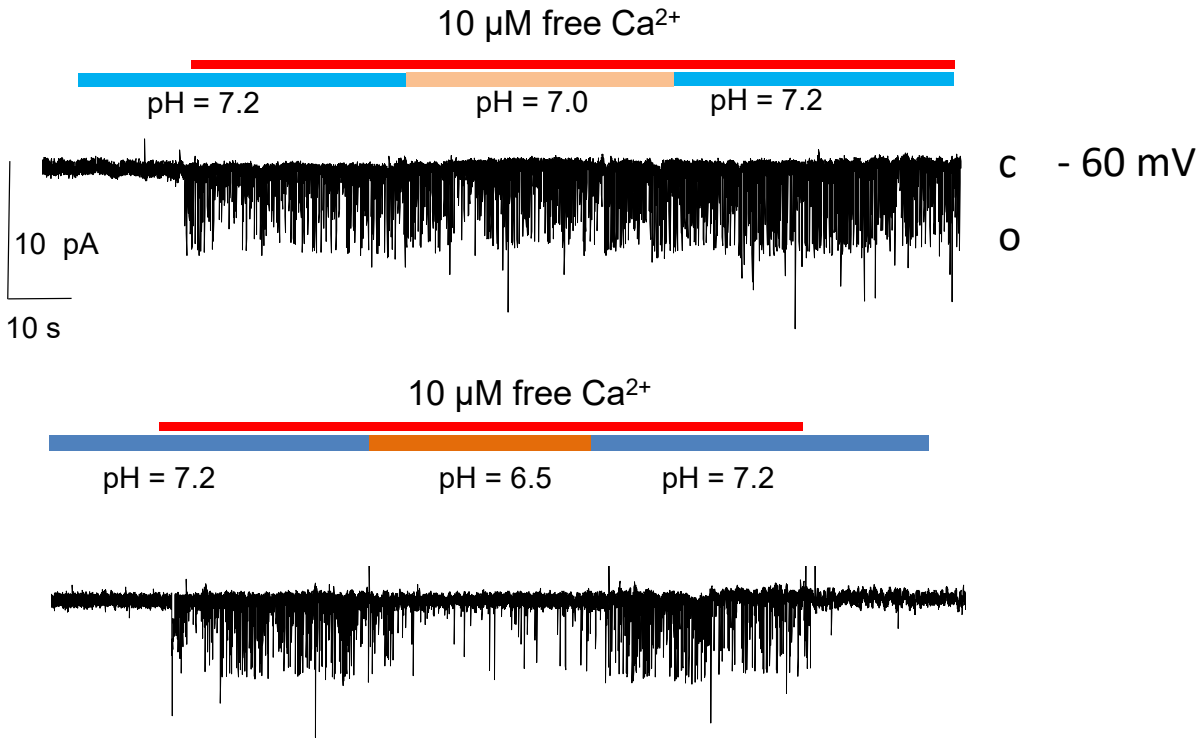

Figure 45. Decreasing pH_i inhibits single channel activity of TRPC4 in inside-out patches

In HEK293 cells stably expressing µOR and TRPC4β, inside-out recordings were made with cytoplasmic solutions where pH was clamped with 50 mM HEPES and free Ca^{2+} concentration set without any Ca^{2+} chelator. DAMGO (10 nM) was added to the patch pipette solution (ECS described in 2.3). The patches were held at -60 mV (at the intracellular side) and solutions were applied to the intracellular side by a gravity driven perfusion system. Application of 10 µM free Ca^{2+} was sufficient to induce maximal single channel activity which was not further enhanced by lowering the pH_i to 7.0 (*upper panel*). However lowering pH to 6.5 inhibited the activity reversibly.

Summary VII: Ca^{2+} and H^+ are two major factors associated with PLC signaling that act in concert with $G_{i/o}$ protein activation to gate TRPC4 channels. H^+ exerts bidirectional (facilitation and inhibition) effects on the channel with narrow concentration ranges, revealing TRPC4 as a finely tuned sensor of coincident $G_{i/o}$ stimulation, cytosolic Ca^{2+} increase and acidification.

5.3 Discussion

In **Chapter 3**, I showed an absolute dependence on triggering Ca^{2+} for $G_{i/o}$-mediated TRPC4 activation. However, in all conditions where $[Ca^{2+}]_i$ was increased alone without a concomitant $G_{q/11}$-PLCβ stimulation, it only supported slow development of $G_{i/o}$-mediated TRPC4 whole-cell currents. Here, I show that this delay was abolished by lowering pH_i, another component of PLC signaling not often discussed. Previously, intracellular protons produced downstream of G_q-PLCβ activation were shown to contribute critically to the activation of related *Drosophila* TRP and TRPL channels (Huang, Liu et al. 2010). Therefore, a drop of pH_i may be a common factor involved in PLC-mediated activation of all TRPC channels. The pH_i effect also has a narrow range and is likely local - as shown by the ability of pH 8.5 internal solution to slow down CCh facilitation when buffered by 100 but not 10 mM HEPES.

The kinetic effect of pH_i in whole-cell mode probably reflects the ability of intracellular protons to lower the Ca^{2+} threshold of TRPC4 activation. Noticeably, in outside-out patches, both Ca^{2+} and H^+ only affected peak current amplitude without any obvious effect on activation kinetics (**Fig. 44**). The slightly acidic pH_i (6.4-6.8) brought down the $[Ca^{2+}]_i$ needed to evoke maximal currents by about 10 fold. To understand how this affects whole-cell current, one has to consider the fact that TRPC4 proteins are present as clusters on the plasma membrane (Plant and Schaefer 2003, Graziani, Poteser et al. 2010). Presumably, the triggering Ca^{2+} only randomly opens channels in a limited number of clusters, which, despite the self-promoting positive feedback effect within the cluster, is insufficient to display obvious whole-cell currents. Ca^{2+} diffusion to neighboring clusters is necessary to generate the global response with robust whole-cell currents. However, Ca^{2+} diffusion in the cytosol is limited and heavily influenced by cytosolic Ca^{2+}-binding proteins and buffers. Thus, the level of Ca^{2+} that reaches the neighboring clusters may only be

able to generate a propagating response at low pH_i, but not the normal pH_i of 7.2. Such a drop in pH_i is normally provided upon stimulation of PLC. In the absence of $G_{q/11}$-PLCβ stimulation by a receptor, other PLC isoforms, e.g. PLCδ, may be recruited by the rising $[Ca^{2+}]_i$ to produce the needed protons. However, this may be another Ca^{2+} diffusion delimited process that happens inefficiently until a threshold (most likely the spatiotemporal summation of Ca^{2+} signals generated from the influx mediated by the few open TRPC4 channels) is reached. This explains the biphasic kinetics of TRPC4 activation induced by DAMGO alone or DAMGO plus IM.

Cytosolic Ca^{2+} increase and acidification are events that typically coincide in the GI smooth muscle cells and the cardio-pulmonary vasculature during ischemic and hypoxic conditions (Ladilov, Schäfer et al. 2000) as well as neurons during brain injury and epileptic attack (Lipton 1999, Pavlov and Walker 2013). A number of studies have shown an upregulation of TRPC4 in hypoxic conditions (Alzoubi, Almalouf et al. 2013, Parrau, Ebensperger et al. 2013) and the involvement of TRPC4 in neuronal death (Phelan, Shwe et al. 2013, Nagarajan, Ning et al. 2014). My results coincide with these findings in suggesting that TRPC4 likely acts as a stress sensor uniquely sensitive to $G_{i/o}$ signaling and acidification.

Chapter 6

Discussion and future directions

TRPC channels are commonly thought to be gated by PLC signaling, but for TRPC4, $G_{i/o}$ proteins are obligatorily involved, making this channel a coincident detector of $G_{i/o}$ and PLC signaling. While $G_{i/o}\alpha$ binding to the C-terminal CIRB domain of TRPC4 protein may be involved for the $G_{i/o}$ effect (Jeon, Hong et al, 2012), this action alone is insufficient to maximally activate the channel. My studies have provided evidence that the TRPC4 activation mechanism consists of multiple steps:

1) Activation of $G_{i/o}$
2) Activation of PLCδ1
3) Increase in intracellular Ca^{2+}
4) Depletion of PIP_2
5) Intracellular acidification

Of these steps, 1 – 3 must obligatorily coincide. Inhibition of any one of these three events completely ablates TRPC4 activity.

6.1 The role of PIP_2

The involvement of PIP_2 is multifaceted: even though the depletion of PIP_2 facilitates the activation (**Chapter 3**), the presence of PIP_2 is necessary (**Fig. 46**). One of the most widely used experimental conditions to strongly deplete PIP_2 is the overexpression of the constitutively active mutant of the $G\alpha_q$ subunit $G_q\alpha$-Q204L (G_qQL). In cells expressing the G_qQL mutant, TRPC4

activity is completely ablated – neither maximal $G_{i/o}$, nor coincident $G_{i/o}$ and $G_{q/11}$ activation produce any TRPC4 current (**Fig 46a,** *top panel*). However, overexpression of the constitutively active PLCδ1 mutant reversed this inhibition suggesting that one of the primary functions of PIP_2 in the TRPC4 activation mechanism might be to deliver PLCδ1 to the plasma membrane and likely into proximity with the channel.

It should be noted that the overexpression of G_qQL does not completely deplete PIP_2 (**Fig. 46c**). Sufficient PIP_2 remains in the membrane or is re-synthesized constantly by the cell - to allow for CCh-stimulated Ca^{2+} store release (**Fig. 46c**), albeit being smaller than cells that did not express G_qQL. Therefore, it is possible that the constitutively active PLCδ1 mutant needs a minimal amount of PIP_2, which may be supplied by the residual or regenerated PIP_2, to translocate to the membrane and also possibly to perform the function necessary for TRPC4 activation. The association of PIP_2 with the PLCδ1 enzyme in this scenario would then hydrolyze the PLC (or TRPC4) bound PIP_2 and then TRPC4 would be facilitated/activated by a PIP_2 hydrolysis product. However, PIP_2 may also act merely as a translocation agent to facilitate a direct coupling of PLCδ1 or a downstream intermediary with TRPC4. In this scenario the hydrolysis of PIP_2 would not be necessary for the action of PLCδ1 on TRPC4.

The overexpression of the constitutively active mutant of PLCβ2 or the application of the strongly facilitatory condition of reduced pH_i and elevated calcium was insufficient to reverse the G_qQL-PIP_2 depletion induced inhibition. To verify whether PLCδ1 needs to interact with the channel directly or to the membrane to perform its function, co-precipitation assays to examine physical association between TRPC4 and PLCδ1 could be performed. In addition, membrane targeting of PLCδ1 by introducing either a myristoyl chain binding motif to PLCδ1 or additional

PH domains which may exaggerate PLCδ1 targeting to PIP_2 rich membrane regions is also expected to facilitate TRPC4 activation.

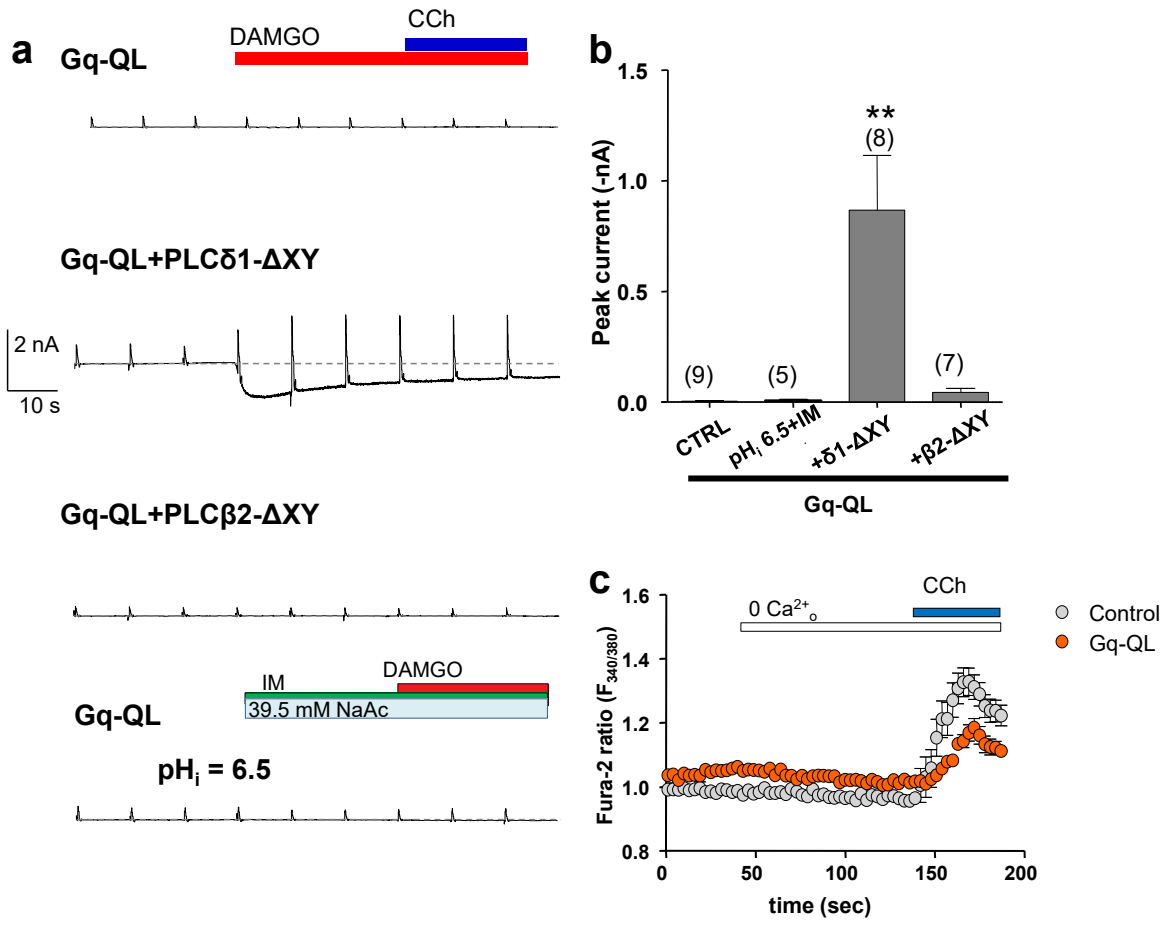

Figure 46. Reversal of PIP_2 depletion induced TRPC4 inhibition by constitutively active PLCδ1

a, Representative whole-cell current traces evoked by DAMGO (1 μM) and DAMGO plus CCh (10 μM) in cells that stably co-expressed TRPC4β and μOR, and transiently transfected with human G_qQL without or with PLCδ1-ΔXY or PLCβ2-ΔXY as indicated. Pipette solutions contained 0.05 mM EGTA and no added Ca^{2+}. **b**, Summary data (means ± SEM) for DAMGO evoked peak currents at -60 mV are shown. **p < 0.01 *vs* control by unpaired *t* test. Numbers of cells are shown in parentheses. **c**, Cells stably co-expressing TRPC4β and μOR were transiently cotransfected with EGFP and human G_qQL, trypsinized at 20 hrs post-transfection and plated on poly-L-ornithine coated coverslips. For calcium imaging, cells were loaded with Fura-2 dye for 40 minutes and then imaged. Solutions were applied with a gravity driven perfusion system. The 0 Ca^{2+} solution contained 0.2 mM EGTA to chelate all residual Ca^{2+} in the buffer. This Ca^{2+} free solution was allowed to wash over the cells for a few minutes before application of 1 μM CCh. Controls were cells transfected with only EGFP. Data are means ± SEM for 19 cells for each condition.

6.2 Ca^{2+}, H^+ and PLC

I tested whether the constitutively active PLCδ1 could overcome the necessity for Ca^{2+} to achieve maximal activation or the necessity for intracellular acidification to achieve the rapid kinetics of channel activation. Overexpression of constitutively active PLCδ1 was unable to support TRPC4 activation in the presence of 10 mM BAPTA (**Fig 47a**), suggesting that for its action on TRPC4, $[Ca^{2+}]_i$ rises are still needed.

Also the kinetics of channel activation at alkaline intracellular pH (8.5) was slower than that at pH 7.2 (**Fig 47b**) suggesting that protonation of intracellular targets still facilitated TRPC4 activation despite the constitutive activation of PLCδ1. It should be noted that the increased kinetics seen with overexpression of PLCδ1 or inhibition of RhoA are still slower than the fast kinetics seen with coincident $G_{i/o}$ and G_q stimulation or coincident intracellular acidification and $[Ca^{2+}]_i$ rise. Therefore, although PLCδ1 activation is a necessary part of the Ca^{2+} dependent facilitation of TRPC4 activation, it might not fulfill the same role as intracellular acidification. Clearly, the Ca^{2+} dependent facilitation mechanism and the proton dependent facilitation mechanism are distinct, although they are not mutually exclusive in the physiological scenario since the proton dependent facilitation also has a $[Ca^{2+}]_i$ dependence.

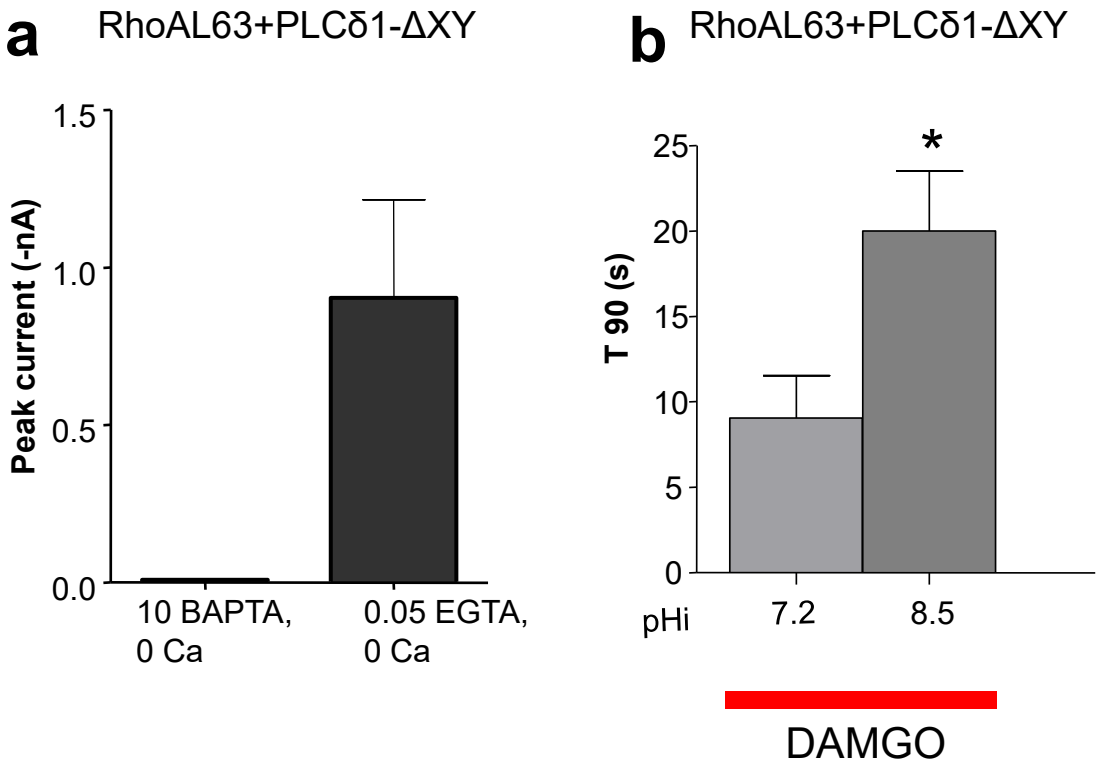

Figure 47. PLCδ1-ΔXY does not reverse Ca^{2+} and H^+ dependence

a, Whole-cell currents evoked by simultaneous application of DAMGO (1 μM) and IM (1 μM) in cells that stably co-expressed TRPC4β and μOR and transiently transfected with cDNAs for RhoAL63 (to inactivate endogenous PLCδ1) and PLCδ1-XY. Cells were tested in two conditions, one with 10 mM BAPTA in the patch pipette and the second with 0.05 mM EGTA and no added Ca^{2+}. **b**, The same set of cells as in **a.** were tested under two different conditions, one with pH_i clamped inside the cell at 7.2 and the other at 8.5 using 50 mM HEPES. Summary data (means ± SEM) for DAMGO + IM evoked peak currents at -60 mV are shown. * $p < 0.05$ *vs* control (pH_i 7.2) by unpaired *t* test.

Ca^{2+} and H^+ act cooperatively from the cytoplasmic side to facilitate $G_{i/o}$-mediated TRPC4 activation. The protonation reactions caused by the acidic pH_i are therefore merely facilitatory and not necessary for channel activation as tested within the experimental bounds described in **Ch 5**. Within the range of pH modulations performed here, inhibition of local pH fluctuations by using high concentrations of HEPES prevented the facilitation. Interestingly, both Ca^{2+} and H^+ only work within rather narrow concentration ranges, revealing an extremely tight regulation by

these factors on TRPC4 function. The micromolar $[Ca^{2+}]_i$ dependence and its bidirectional effect suggest a highly dynamic nature of cytosolic Ca^{2+} on TRPC4 activation, consistent with the observed high sensitivity to the slow Ca^{2+} chelator, EGTA. Even with as low as 0.5 mM intracellular EGTA, μOR-mediated TRPC4 activation was inhibited, implicating that Ca^{2+} has to travel a small distance from its source of generation to the target(s). The primary source of Ca^{2+} in PLC signaling is ER Ca^{2+} release mediated by IP_3Rs. This activity also causes store-operated Ca^{2+} influx. Either of these may provide the initial Ca^{2+} trigger for TRPC4 activation, but the more robust TRPC4 currents may arise from the positive-feedback mechanism owing to the Ca^{2+} permeability of opened TRPC4 channels that result in a cascade of activation of neighboring (TRPC4) channels. Thus, the initial cause of $[Ca^{2+}]_i$ rise may be immaterial for the facilitation. In neurons, native TRPC4 activity is strongly facilitated by the opening of voltage-gated Ca^{2+} channels (Tian, Thakur et al. 2013) but in HEK293 cells, IP_3R-mediated ER Ca^{2+} release seems to be critical even though it can be substituted by other mechanisms, e.g. IM-mediated $[Ca^{2+}]_i$ rise or clamping the $[Ca^{2+}]_i$ to micromolar levels.

The separation of Ca^{2+} and proton dependent processes is complicated by the fact that Ca^{2+} chelating agents and sensors are also pH dependent. However, there are some clues from the elucidation of the proton dependence of *Drosophila* TRP channels which could be put to use in this case. The protonation dependent redox reaction associated with INAD PDZ domains (Liu, Wen et al. 2011) could serve as s a template to examine a similar modulation of cysteine residues in the intracellular domains of TRPC4 and its associated proteins.

The effect of protons on TRPC4 may be indirect. Although intracellular acidification facilitated TRPC4 activation, this observation was made by manipulating the pH_i globally (across the entire cytosol). In the whole-cell configuration, a majority of cellular factors may be affected.

In the outside-out patch configuration, although the pH in proximity to the channel is better controlled than in whole-cells – several intracellular components may get extracted along with the patch and regulated by pH. Therefore, the effect of protons on TRPC4 may still be indirect. As such, the matching of the fast kinetics (in whole-cell patch clamp) seen in the two conditions: 1) with coincidental $G_{i/o}$ + G_q activation and 2) with coincidental $G_{i/o}$ activation, $[Ca^{2+}]_i$ and $[H^+]_i$ rise – may be a correlation. Although the G_q dependent facilitation of TRPC4 was slowed by clamping the intracellular pH to an alkaline value (8.5) - suggesting that the H^+ dependent facilitation may indeed be downstream of G_q in HEK293 cells, the manipulation of intracellular pH to 8.5 was also global - making the effect on TRPC4 currents probably a result of non-specific actions.

To examine whether protons directly modulate TRPC4, two types of experiments could be performed: a reconstitution of purified TRPC4 subunits in artificial lipid bilayers, or the testing of TRPC4 mutants in which appropriate protonatable residues are substituted with non-protonatable ones. There are several conserved amino acid residues in the cytoplasmic as well as pore regions of TRPC4 and TRPC5 that are candidates for pH regulation in the range optimal for TRPC4 and TRPC5 activation. The most likely candidate is histidine (H) which has a side chain pKa of 6.04 and is conserved frequently between TRPC4 and TRPC5 in the N termini, the inter-helical cytoplasmic domains, the pore loops and the C termini (**Fig. 48**). The next closest candidate is glutamic acid (E) with a side chain pKa of 4.25. It has been shown previously that extracellular glutamate residues at position 543 in TRPC5 are responsible for the sensitivity to the cations Gd^{3+}, La^{3+} and extracellular acidification. Although the pKa of glutamate side chain in the free amino acid is rather low, the pKa values of solvated glutamates within the TRPC4 structure are unknown. It is possible that the pKa values of the residues in the solvated structure fall within

the range tested in Chapter 3 and that E542, E543 or other residues may underlie the pH_i dependent regulation of TRPC4.

Figure 48. Candidate protonatable residues in cytoplasmic and pore loop domains of TRPC4 and C5

Sequence alignment of mouse TRPC4α, TRPC4β and TRPC5, A performed using Multalin (multalin.toulouse.inra.fr/multalin/) and exported via Bioedit (mbio.ncsu.edu) to MS Powerpoint for editing. Only regions exposed to the cytoplasm are shown. Transmembrane regions and extracellular loops between transmembrane-helices have been omitted (indicated by grey bars). Histidine (H) residues are in red and glutamate (E) residues are in blue. E542 and E543 that were previously mutated in TRPC4β (**Ch. 5**) are indicated by asterisks.

Any reconstitution experiment would have to account for the fact that TRPC4 activation requires $G_{i/o}$ (possibly through direct interactions), elevated $[Ca^{2+}]_i$ and PLCδ1. Therefore, in order to test the effects of pH on TRPC4 activity, purified G protein subunits, 10 μM or so free Ca^{2+} and either purified PLCδ1 would have to be added at the intracellular side or a membrane bound myristolyated PLCδ1 mutant could be used.

It is likely that the effects of Ca^{2+} and H^+ converge on CaM. It is known that proton exchange occurs when CaM associates with Ca^{2+} (Sellers, Laynez et al. 1991). The protons released by CaM upon Ca^{2+} binding may account for a part of the H^+ dependent facilitation of the TRPC4 current. The facilitatory effect of low pH may also be through a H^+ dependent facilitation of CaM. It has been reported that low pH can substitute the need for high $[Ca^{2+}]$ to associate with CaM and cause it to change its configuration from a collapsed state to an extended shape (Pandey, Dhoke et al. 2014). Therefore although a biphasic nature of pH regulation of CaM or Ca^{2+}-CaM has not been described in the pH range tested here, it is possible that protonation of CaM residues might modulate its activity in either or both of the two phases seen in Chapter 3 **(Fig. 39c)**. Additionally the point of convergence of Ca^{2+} and H^+ may also be at PLCδ1 which has a pH sensitivity that is biphasic (Ryu, Suh et al. 1987, Homma, Imaki et al. 1988). The peak activity (in purified proteins) is seen between pH 5.0 and 7.0, with strong inhibition seen at both acidic and alkaline pH values that are beyond this range.

In summary, the optimal $[Ca^{2+}]$ and pH_i ranges observed for TRPC4 activation coincide with optimal $[Ca^{2+}]$ and pH ranges for CaM and PLCδ1. As a result of this coincidence, the maximal TRPC4 activity may be an emergent property from the maximal activation of both CaM and PLCδ1.

6.4 The role of RhoA

In my study, RhoA was largely used as an experimental tool to inhibit PLCδ1, following previous work which had shown RhoA dependent inhibition of an SKF-96365 -sensitive Ca^{2+} entry pathway downstream of $G_{i/o}$ and PLCδ1 signaling (SKF-96365 is a broad spectrum inhibitor of store operated channels) (Murthy, Zhou et al. 2004). However, this raises interesting possibilities for the regulation of PLCδ1 via the $G_{12/13}$-Rho-GEF-RhoA pathway. p115-RhoGEF, PDZ-RhoGEF and LARG (leukemia-associated rhoGEF) are endogenously expressed in HEK293 cells (Wang, Liu et al. 2004). Both G_{12} and G_{13} show high mRNA levels as well in HEK293 cells (Atwood, Lopez et al. 2011). In addition to $G_{12/13}$, both receptor activation of G_q and overexpression of the constitutively active mutant G_qQL can activate RhoA independent of a G_{13}-RhoA pathway (Chikumi, Vázquez-Prado et al. 2002). Indeed, this may constitute another mechanism, in addition to PIP_2 depletion, that underlies the strong inhibition of TRPC4 by overexpression of G_qQL (**Fig. 46**). The activation of $G_{q/12/13}$ proteins would, in theory, inhibit PLCδ1 and TRPC4 rather than facilitate the activation of both proteins as shown here. Why this does not occur in the assays described above is intriguing. Interestingly, the G_qQL dependent inhibition of TRPC4 was reversed by the constitutively active PLCδ1-ΔXY mutant (**Fig. 46**). Whether the PLCδ1-ΔXY mutant escapes a RhoA dependent inhibition is not known, but this might be testable by co-immunoprecipitation assays. Additionally, ARHGAP6 – a RhoA activating protein, known to inhibit PLCδ1 (Ochocka, Grden et al. 2008) would be expected to inhibit TRPC4.

6.4 The roles of G protein subunits

Inhibiting PLC using U73122 and RhoA revealed that there is a PLC component, downstream of or in parallel with the $G_{i/o}$ pathway that is needed for TRPC4 activation. Though

PLCβ1/3 are known to be stimulated weakly by Gβγ subunits, it is unlikely that $G_{i/o}$ proteins induce TRPC4 activation via Gβγ-mediated stimulation of PLCβ (PLCβ2 is not expressed in HEK293 cells). In HEK293 cells, μOR stimulated $G_{i/o}$ activation rarely elicited $[Ca^{2+}]_i$ rise, indicating a poor production of IP_3. In addition, if PLCβ was the sole reason for $G_{i/o}$-coupled receptors to trigger TRPC4 activation, then $G_{q/11}$-coupled receptors would be more effective at opening TRPC4 channels than the $G_{i/o}$-coupled ones. Additionally, the overexpression of exogenous PLCβ2 which is strongly activated by Gβγ, did not result in larger peak currents or faster kinetics. Neither did it overcome a RhoA nor a G_qQL induced inhibition. Therefore, a Gβγ–PLCβ pathway is unlikely to underlie the activation mechanism of TRPC4 channels. The strong synergy between $G_{q/11}$ and $G_{i/o}$ stimulation for TRPC4 activation would also be difficult to explain without assigning a distinguished role to $G_{i/o}$. The previous study demonstrating the specific involvement of $G_{i/o}$α, especially G_{i2}α, rather than Gβγ, in TRPC4 activation (Jeon, Hong et al., 2012) also excludes Gβγ-PLCβ coupling as the mechanism of $G_{i/o}$ action. However, in previous microtiter plate-based fluorescence membrane potential assays (performed by Dr. M.X. Zhu, not shown) and in patch clamp assays shown below (**Fig. 49a**), the suppression of Gβγ activity by overexpression of the C-terminus of β adrenergic receptor kinase (βARK-Ct) did inhibit TRPC4 activation, suggesting that Gβγ is involved in the mechanism in some manner. Since the lack of functional Gβγ also prevents G protein cycles and hence the GTP/GDP exchanges of $G_{i/o}$α, these Gβγ-sequestering experiments do not necessarily suggest a specific involvement of either $G_{i/o}$α or Gβγ. Furthermore, in GST pulldown assays purified $Gβ_1γ_2$ subunits showed association with both full length TRPC4α C-terminus (615 – 974) and with the TRPC4α-765-974 fragment (**Fig. 49b**). Previously, the CIRB site had been identified as the site of interaction with G_{i2}α (Jeon, Hong et al. 2012). The presence of a $Gβ_1γ_2$ binding site downstream of the G_{i2}α binding site suggests a

novel role for $G\beta_1\gamma_2$ subunits to directly interact with the channel. Whether the direct interaction is necessary for TRPC4 function is not known.

Yet, PLC activity is required for $G_{i/o}$-mediated TRPC4 activation as shown by the inhibitory effect of U73122 and the increased probability and rate of TRPC4 activation with the costimulation of $G_{q/11}$-PLCβ and EGFR-PLCγ. The sensitivity to U73122, Ca^{2+}, RhoA and the dnPLCδ1 mutant suggests that PLCδ1 is a necessary component in the $G_{i/o}$ -TRPC4 pathway. Whether there is cross-talk between PLCδ1 and $G_{i/o}$ is not known. It is likely that PLCδ1 and $G_{i/o}$ are independently activated, but simultaneously necessary for TRPC4 activation. The PLCδ1, $G_{i/o}$ -TRPC4 mechanism may explain both phases in the biphasic activation of a whole cell TRPC4 current. In the initial phase, with small currents, it is possible that an activation of a small set of TRPC4 channels on the plasma membrane directly by $G_{i/o}$ and a few molecules of PLCδ1 in the vicinity, locally activated for whatever reason, can slowly elevate $[Ca^{2+}]_i$ sufficiently to levels which are needed to activate PLCδ1 (1 – 10 μM, Allen 1997) in the entire cell, which subsequently leads to the optimum conditions for activating a maximal number of TRPC4 channels in the cell. The global activation of PLCδ1 may underlie the fast rising phase, at the peak of which, the maximal whole-cell TRPC4 currents are achieved. The fact that $G_{q/11}$ activation or $[Ca^{2+}]_i$ elevation by other means categorically does not allow for TRPC4 activation in this manner reinforces the necessity for $G_{i/o}$ stimulation and points towards a way in which PLCδ1 may play a very specific role in TRPC4 activation either through specific localization or through a downstream component that is absent in $G_{q/11}$-PLCβ. Therefore, both a direct action of $G_{i/o}$ subunits with TRPC4 and activation of the PLC pathway can be critical for TRPC4 activation.

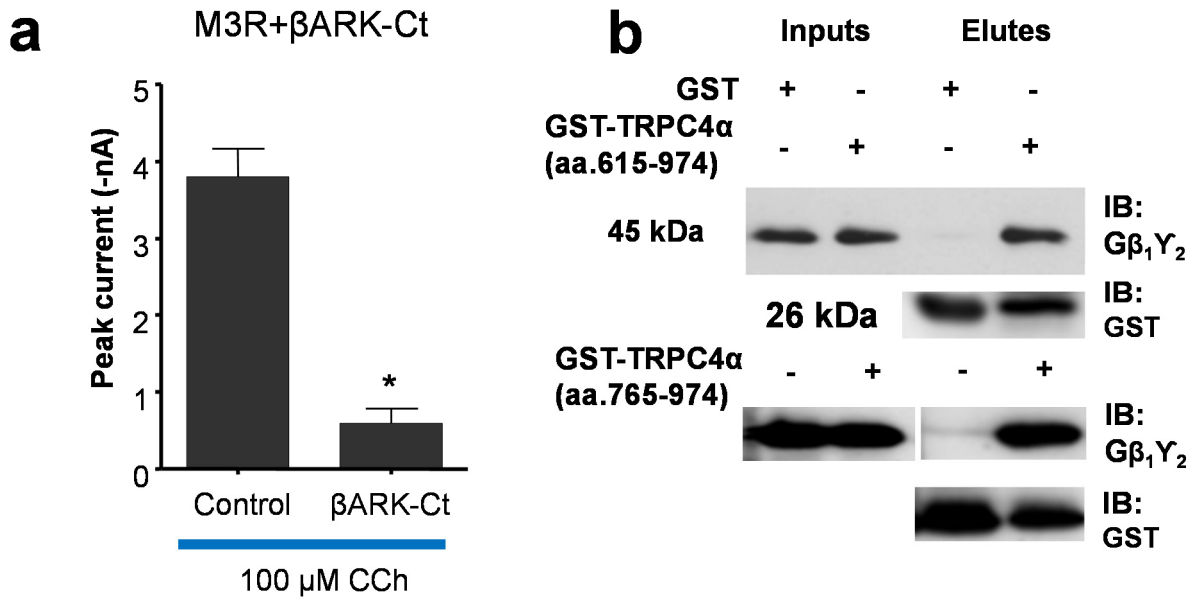

Figure 49. The role of Gβγ in TRPC4 activation

a. Similar to **figure 8**, in HEK 293 cells stably expressing μOR and TRPC4β, M3R and βARK-Ct were cotransfected. Cells were patched in the whole-cell configuration. Whereas overexpression of M3R led to robust activation of TRPC4 currents in response to CCh (100 μM), similar to that shown in **figure 8**, coexpression of βARK-Ct suppressed the current strongly. Summary data (means ± SEM) for CCh-evoked peak currents at -60 mV are shown. * $p < 0.05$ *vs* control by unpaired *t* test. **b.** Purified $G\beta_1\gamma_2$ subunits and GST (kindly provided by Dr. C. Dessauer, UT) were tested along with GST fused TRPC4α C-terminus fragments. $G\beta_1\gamma_2$ subunits showed association with full length C terminus of TRPC4α (615 – 974) and with the TRPC4α-765-974 fragment, suggesting that $G\beta_1\gamma_2$ interacts in a region downstream of the CIRB domain identified to be the site of $G_{i2}\alpha$ interaction (Jeon, Hong et al. 2012).

6.5 The role of scaffolding proteins

The proton dependent regulation of the *Drosophila* TRP is regulated by the scaffolding protein INAD consisting of 5 PDZ domains. The scaffolding protein endogenous to HEK293 cells that is known to be associated with TRPC4 is NHERF which consists of two PDZ domains. Moreover, NHERF has been shown to underlie the biphasic activation kinetics of TRPC5, where deletion of the PDZ binding domain at the C terminus of TRPC5 eliminated the biphasic mode of activation (Obukhov and Nowycky 2004). If the proton regulation of TRPC4 is similar to that of

the *Drosophila* TRP, I hypothesized that disruption of TRPC4-NHERF association would alter the kinetics of TRPC4 activation as well and such a change in the association may underlie the mechanism of proton dependent facilitation.

However, a TRPC4β mutant with the PDZ binding site deleted had similar kinetics of current development as the wild type channel. Stimulation by DAMGO or DAMGO + IM or stimulation by DAMGO following a pre-application of IM still resulted in biphasic kinetics of current development (**Fig. 50**). These preliminary results have two implications: 1) TRPC4 activation mechanism by $G_{i/o}$ differs from the $G_{q/11}$-dependent TRPC5 activation mechanism described previously and 2) the critical site of proton facilitation for TRPC4 is not at the C-terminal end where the channel associates with a PDZ domain-containing scaffolding protein.

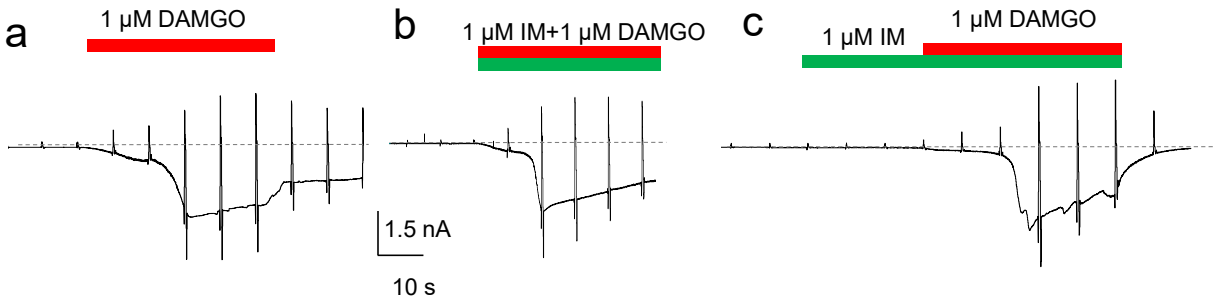

Figure 50. The C-terminal PDZ-binding domain does not regulate TRPC4 activation kinetics

A TRPC4β mutant with the PDZ-binding domain at the C-terminal end deleted was subcloned, in pIRESneo vector and transiently transfected into HEK293 cells stably expressing μOR. Cells were studies by whole-cell recording after 16-24 hours as shown in **Fig. 23**, with DAMGO and IM applied as indicated. Concentration of EGTA in all patch pipette solutions was 0.05 mM with no added Ca^{2+}.

6.6 Remaining questions and suggested future experiments

In summary, though I have made advances in identifying the elements underlying the $[Ca^{2+}]_i$ dependent facilitation of TRPC4 activation, several old and new questions need to be addressed. First, what is the mechanism of $G_{i/o}$'s action on TRPC4? If indeed the action of $G\alpha_{i/o}$ subunits is by covalent interactions with the TRPC4 CIRB domain, would, for example, the interchange of TRPC4 and TRPC6 CIRB domains render TRPC4 insensitive and TRPC6 sensitive to $G_{i/o}$ stimulation?

Second, what is the role of Gβγ subunits? Do they behave interchangeably with $G\alpha_{i/o}$ subunits or serve as scaffolding proteins supplementing $G\alpha_{i/o}$ in direct interaction with the TRPC4 CIRB domain? This could be tested by running competitive binding assays between $G\alpha_{i/o}$, Gβγ and GST-tagged-TRPC4 CIRB domain fragments.

Also, it has not been determined whether or not $G\alpha_{i/o}$ or Gβγ facilitates the activation of PLCδ1 directly or indirectly. Previous in vitro assays that examined the interactions of Gβγ

subunits with purified PLCδ1 showed a 2 fold facilitation of PLCδ1 activity by $G\beta_1\gamma_2$ subunits (Park, Jhon et al. 1993). These assays were performed in the presence of 200 nM free Ca^{2+}. It is likely that PLCδ1 might need a higher concentration of Ca^{2+} as a cofactor in its interactions with Gβγ. These assays could be reproduced with different buffer conditions to address this question. It is possible that this Gβγ dependent PLCδ1 activity also underlies the inhibition seen in **Fig. 46.**

Other G proteins such as $G\alpha_h$ (transglutaminase II) which increases the affinity of PLCδ1 to Ca^{2+} (Feng, Rhee et al. 1996) would be expected to facilitate TRPC4. It would be interesting to see whether overexpression of $G\alpha_h$ would lead to such facilitation.

Third, are the mechanisms of CaM dependent facilitation and PLCδ1 dependent facilitation independent? Would the IRB mutant, which showed a facilitation during sub-maximal activation, be as strongly inhibited as the wild-type channel is - in the presence of dn-PLCδ1?

What is the nature of PIP_2's interaction with TRPC4? The data above suggests that PIP_2 might behave only as a chaperone for PLCδ1. In this case, would a modified membrane localized PLCδ1 mutant be able to reverse the G_qQL dependent inhibition in a manner similar to PLCδ1-ΔXY?

Finally, what is the nature of PLCδ1's interaction with TRPC4? Is it a covalent interaction with TRPC4, or is it the creation of a PIP_2 hydrolysis product in close proximity to the channel that is critical for TRPC4 gating?

Addressing these questions would help to more completely elucidate the signal integration pathway associated with TRPC4 and identify its physiological significance.

Bibliography

Abramowitz, J. and L. Birnbaumer (2009). "Physiology and pathophysiology of canonical transient receptor potential channels." FASEB Journal **23**(2): 297-328.

Ahmmed, G. and A. Malik (2005). "Functional role of TRPC channels in the regulation of endothelial permeability." Pflügers Archiv - European Journal of Physiology **451**(1): 131-142.

Akbulut, Y., H. J. Gaunt, K. Muraki, M. J. Ludlow, M. S. Amer, A. Bruns, N. S. Vasudev, L. Radtke, M. Willot, S. Hahn, T. Seitz, S. Ziegler, M. Christmann, D. J. Beech and H. Waldmann (2015). "(-)-Englerin A is a potent and selective activator of TRPC4 and TRPC5 calcium channels." Angewandte Chemie International Edition **54**(12): 3787-3791.

Albert, A. P., S. N. Saleh and W. A. Large (2008). "Inhibition of native TRPC6 channel activity by phosphatidylinositol 4,5-bisphosphate in mesenteric artery myocytes." The Journal of Physiology **586**(13): 3087-3095.

Al-Shawaf, E., J. Naylor, H. Taylor, K. Riches, C. J. Milligan, D. O'Regan, K. E. Porter, J. Li and D. J. Beech (2010). "Short-term stimulation of calcium-permeable transient receptor potential canonical 5-containing channels by oxidized phospholipids." Arteriosclerosis, Thrombosis, And Vascular Biology **30**(7): 1453-1459.

Al-Shawaf, E., S. Tumova, J. Naylor, Y. Majeed, J. Li and D. J. Beech (2011). "GVI phospholipase A2 role in the stimulatory effect of sphingosine-1-phosphate on TRPC5 cationic channels." Cell Calcium **50**(4): 343-350.

Alzoubi, A., P. Almalouf, M. Toba, K. O'Neill, X. Qian, M. Francis, M. S. Taylor, M. Alexeyev, I. F. McMurtry, M. Oka and T. Stevens (2013). "TRPC4 inactivation confers a survival benefit in severe pulmonary arterial hypertension." The American Journal of Pathology **183**(6): 1779-1788.

Amaral, M. D. and L. Pozzo-Miller (2007). "BDNF induces calcium elevations associated with I(BDNF), a nonselective cationic current mediated by TRPC channels." Journal of Neurophysiology **98**(4): 2476-2482.

Antigny, F., C. Norez, L. Dannhoffer, J. Bertrand, D. Raveau, P. Corbi, C. Jayle, F. Becq and C. Vandebrouck (2011). "Transient receptor potential canonical channel 6 links Ca^{2+} mishandling to cystic fibrosis transmembrane conductance regulator channel dysfunction in cystic fibrosis." American Journal of Respiratory Cell and Molecular Biology 44(1): 83-90.

Atwood, B. K., J. Lopez, J. Wager-Miller, K. Mackie and A. Straiker (2011). "Expression of G protein-coupled receptors and related proteins in HEK293, AtT20, BV2, and N18 cell lines as revealed by microarray analysis." BMC Genomics 12:14.

Bahnasi, Y. M., H. M. Wright, C. J. Milligan, A. M. Dedman, F. Zeng, P. M. Hopkins, A. N. Bateson and D. J. Beech (2008). "Modulation of TRPC5 cation channels by halothane, chloroform and propofol." British Journal of Pharmacology 153(7): 1505-1512.

Bandell, M., G. M. Story, S. W. Hwang, V. Viswanath, S. R. Eid, M. J. Petrus, T. J. Earley and A. Patapoutian (2004). "Noxious cold ion channel TRPA1 is activated by pungent compounds and bradykinin." Neuron 41(6): 849-857.

Banner, K. H., F. Igney and C. Poll (2011). "TRP channels: emerging targets for respiratory disease." Pharmacology & Therapeutics **130**(3): 371-384.

Basora, N., G. Boulay, L. Bilodeau, E. Rousseau and M. D. Payet (2003). "20-hydroxyeicosatetraenoic acid (20-HETE) activates mouse TRPC6 channels expressed in HEK293 cells." The Journal of Biological Chemistry **278**(34): 31709-31716.

Becker, E. B., P. L. Oliver, M. D. Glitsch, G. T. Banks, F. Achilli, A. Hardy, P. M. Nolan, E. M. C. Fisher and K. E. Davies (2009). "A point mutation in TRPC3 causes abnormal Purkinje cell development and cerebellar ataxia in moonwalker mice." Proceedings of the National Academy of Sciences of the United States of America **106**(16): 6706-6711.

Berridge, M. J., P. Lipp and M. D. Bootman (2000). "The calcium entry pas de deux." Science **287**(5458): 1604-1605.

Blair, N. T., J. S. Kaczmarek and D. E. Clapham (2009). "Intracellular calcium strongly potentiates agonist-activated TRPC5 channels." The Journal of General Physiology **133**(5): 525-546.

Bollimuntha, S., S. Selvaraj and B. B. Singh (2011). "Emerging Roles of Canonical TRP Channels in Neuronal Function." Advances in Experimental Medicine and Biology **704**: 573-593.

Brownlow, S. L. and S. O. Sage (2005). "Transient receptor potential protein subunit assembly and membrane distribution in human platelets." Thrombosis and Haemostasis **94**(10): 839-845.

Camps, M., A. Carozzi, P. Schnabel, A. Scheer, P. J. Parker and P. Gierschik (1992). "Isozyme-selective stimulation of phospholipase C-β2 by G protein βγ-subunits." Nature **360**(6405): 684-686.

Cao, E., M. Liao, Y. Cheng and D. Julius (2013). "TRPV1 structures in distinct conformations reveal activation mechanisms." Nature **504**(7478): 113-118.

Caterina, M. J., M. A. Schumacher, M. Tominaga, T. A. Rosen, J. D. Levine and D. Julius (1997). "The capsaicin receptor: a heat-activated ion channel in the pain pathway." Nature **389**(6653): 816-824.

Chae, H. G., S. J. Ahn, Y. H. Hong, W. S. Chang, J. Kim and S. J. Kim (2012). "Transient Receptor Potential Canonical channels regulate the induction of cerebellar long-term depression." The Journal of Neuroscience **32**(37): 12909-12914.

Chatzigeorgiou, M., S. Yoo, J. D. Watson, W. H. Lee, W. C. Spencer, K. S. Kindt, S. W. Hwang, D. M. Miller, 3rd, M. Treinin, M. Driscoll and W. R. Schafer (2010). "Specific roles for

DEG/ENaC and TRP channels in touch and thermosensation in C. elegans nociceptors." Nature Neuroscience **13**(7): 861-868.

Chaudhuri, P., S. M. Colles, M. Bhat, D. R. Van Wagoner, L. Birnbaumer and L. M. Graham (2008). "Elucidation of a TRPC6-TRPC5 channel cascade that restricts endothelial cell movement." Molecular Biology of the Cell **19**(8): 3203-3211

Chikumi, H., J. Vázquez-Prado, J. M. Servitja, H. Miyazaki and J. S. Gutkind (2002). "Potent activation of RhoA by $G\alpha_q$ and G_q-coupled receptors." The Journal of Biological Chemistry **277**(30): 27130-27134.

Chu, W., L. Wan, D. Zhao, X. Qu, F. Cai, R. Huo, N. Wang, J. Zhu, C. Zhang, F. Zheng, R. Cai, D. Dong, Y. Lu and B. Yang (2012). "Mild hypoxia-induced cardiomyocyte hypertrophy via up-regulation of HIF-1alpha-mediated TRPC signalling." Journal of Cellular and Molecular Medicine **16**(9): 2022-2034.

Chyb, S., P. Raghu and R. C. Hardie (1999). "Polyunsaturated fatty acids activate the Drosophila light-sensitive channels TRP and TRPL." Nature **397**(6716): 255-259.

Cifuentes, M. E., L. Honkanen and M. J. Rebecchi (1993). "Proteolytic fragments of phosphoinositide-specific phospholipase C-delta 1. Catalytic and membrane binding properties." The Journal of Biological Chemistry **268**(16): 11586-11593.

Cioffi, D., C. Barry and T. Stevens (2010). “Store-operated calcium entry channels in pulmonary endothelium: the emerging story of TRPCs and Orai1.” Membrane Receptors, Channels and Transporters in Pulmonary Circulation. J. X. J. Yuan and J. P. T. Ward, Humana Press. **661:** 137-154.

Cioffi, D. L., K. Lowe, D. F. Alvarez, C. Barry and T. Stevens (2009). "TRPing on the Lung Endothelium: Calcium Channels That Regulate Barrier Function." Antioxidants & Redox Signaling **11**(4): 765-776.

Cosens, D. J. and A. Manning (1969). "Abnormal electroretinogram from a drosophila mutant." Nature **224**(5216): 285-287.

Davis, J., A. R. Burr, G. F. Davis, L. Birnbaumer and J. D. Molkentin (2012). "A TRPC6-dependent pathway for myofibroblast transdifferentiation and wound healing in vivo." Developmental Cell **23**(4): 705-715.

De Petrocellis, L. and V. Di Marzo (2009). "Role of endocannabinoids and endovanilloids in Ca^{2+} signalling." Cell Calcium **45**(6): 611-624.

Díaz Añel, Alberto M. (2007). "Phospholipase C-β3 is a key component in the Gβγ/PKCη/PKD-mediated regulation of trans-Golgi network to plasma membrane transport." The Biochemical Journal **406**(Pt 1): 157-165.

Dietrich, A., V. Chubanov and T. Gudermann (2010). "Renal TRPathies." Journal of the American Society of Nephrology **21**(5): 736-744.

Eder, P. and J. D. Molkentin (2011). "TRPC channels as effectors of cardiac hypertrophy." Circulation Research **108**(2): 265-272.

Eder, P., M. Poteser, C. Romanin and K. Groschner (2005). "Na^+ entry and modulation of Na^+/Ca^{2+} exchange as a key mechanism of TRPC signaling." Pflügers Archiv - European Journal of Physiology **451**(1): 99-104.

Eder, P., D. Probst, C. Rosker, M. Poteser, H. Wolinski, S. D. Kohlwein, C. Romanin and K. Groschner (2007). "Phospholipase C-dependent control of cardiac calcium homeostasis involves a TRPC3-NCX1 signaling complex." Cardiovascular Research **73**(1):111-119

Essen, L.O., O. Perisic, R. Cheung, M. Katan and R. L. Williams (1996). "Crystal structure of a mammalian phosphoinositide-specific phospholipase Cδ." Nature **380**(6575): 595-602.

Fauconnier, J., J. T. Lanner, A. Sultan, S. J. Zhang, A. Katz, J. D. Bruton and H. Westerblad (2007). "Insulin potentiates TRPC3-mediated cation currents in normal but not in insulin-resistant mouse cardiomyocytes." Cardiovascular Research **73**(2): 376-385.

Feng, J.F., S. G. Rhee and M. J. Im (1996). "Evidence That Phospholipase δ1 is the effector in the Gh (Transglutaminase II)-mediated signaling." The Journal of Biological Chemistry **271**(28): 16451-16454.

Feng, X., Y. Huang, Y. Lu, J. Xiong, C. O. Wong, P. Yang, J. Xia, D. Chen, G. Du, K. Venkatachalam, X. Xia and M. X. Zhu (2014). "Drosophila TRPML forms PI(3,5)P2-activated cation channels in both endolysosomes and plasma membrane." The Journal of Biological Chemistry **289**(7): 4262-4272.

Flemming, P. K., A. M. Dedman, S.Z. Xu, J. Li, F. Zeng, J. Naylor, C. D. Benham, A. N. Bateson, K. Muraki and D. J. Beech (2006). "Sensing of Lysophospholipids by TRPC5 Calcium Channel." The Journal of Biological Chemistry **281**(8): 4977-4982.

Fortin, D. A., T. Srivastava, D. Dwarakanath, P. Pierre, S. Nygaard, V. A. Derkach and T. R. Soderling (2012). "BDNF activation of CaM-kinase kinase via TRPC channels induces the translation and synaptic incorporation of GluA1 containing calcium-permeable AMPARs." The Journal of Neuroscience **32**(24): 8127-8137.

Foskett, J. K., C. White, K. H. Cheung and D. O. Mak (2007). "Inositol trisphosphate receptor Ca^{2+} release channels." Physiological Reviews **87**(2): 593-658.

Fowler, M. A., K. Sidiropoulou, E. D. Ozkan, C. W. Phillips and D. C. Cooper (2007). "Corticolimbic expression of trpc4 and trpc5 channels in the rodent brain." PLoS ONE **2**(6): e573.

Freichel M, Suh S H, Pfeifer A, Schweig U, Trost C, Weissgerber P, Biel M, Philipp S, Freise D, Droogmans G, Hofmann F, Flockerzi V, Nilius B. (2001) “Lack of an endothelial store-

operated Ca^{2+} current impairs agonist-dependent vasorelaxation in TRP4-/- mice." Nature Cell Biology **3**:121–127

Freichel, M., R. Vennekens, J. Olausson, M. Hoffmann, C. Muller, S. Stolz, J. Scheunemann, P. Weissgerber and V. Flockerzi (2004). "Functional role of TRPC proteins in vivo: lessons from TRPC-deficient mouse models." Biochemical and Biophysical Research Communications **322**(4): 1352-1358.

Fuchs, B., A. Dietrich, T. Gudermann, H. Kalwa, F. Grimminger and N. Weissmann (2010). "The role of classical transient receptor potential channels in the regulation of hypoxic pulmonary vasoconstriction." Advances in Experimental Medicine and Biology **661**: 187-200.

Fuchs, B., M. Rupp, H. A. Ghofrani, R. T. Schermuly, W. Seeger, F. Grimminger, T. Gudermann, A. Dietrich and N. Weissmann (2011). "Diacylglycerol regulates acute hypoxic pulmonary vasoconstriction via TRPC6." Respiratory Research **12**: 20.

Gaudet, R. (2008). "A primer on ankyrin repeat function in TRP channels and beyond." Molecular bioSystems **4**(5): 372-379.

Gees, M., B. Colsoul and B. Nilius (2010). "The role of transient receptor potential cation channels in Ca^{2+} signaling." Cold Spring Harbor Perspectives in Biology **2**(10): a003962.

Glitsch, M. D. (2010). "Activation of native TRPC3 cation channels by phospholipase D." FASEB Journal **24**(1): 318-325.

Goel, M. and W. P. Schilling (2010). "Role of TRPC3 channels in ATP-induced Ca^{2+} signaling in principal cells of the inner medullary collecting duct." American Journal of Physiology - Renal Physiology **299**(1): F225-F233.

Gracheva, E. O., N. T. Ingolia, Y. M. Kelly, J. F. Cordero-Morales, G. Hollopeter, A. T. Chesler, E. E. Sanchez, J. C. Perez, J. S. Weissman and D. Julius (2010). "Molecular basis of infrared detection by snakes." Nature **464**(7291): 1006-1011.

Graham, S., Y. Gorin, H. E. Abboud, M. Ding, D. Y. Lee, H. Shi, Y. Ding and R. Ma (2011). "Abundance of TRPC6 protein in glomerular mesangial cells is decreased by ROS and PKC in diabetes." American Journal of Physiology - Cell Physiology **301**(2): C304-C315.

Graziani, A., M. Poteser, W. M. Heupel, H. Schleifer, M. Krenn, D. Drenckhahn, C. Romanin, W. Baumgartner and K. Groschner (2010). "Cell-cell contact formation governs Ca^{2+} signaling by TRPC4 in the vascular endothelium: evidence for a regulatory TRPC4-beta-catenin interaction." The Journal of Biological Chemistry **285**(6): 4213-4223.

Gross, S. A., G. A. Guzman, U. Wissenbach, S. E. Philipp, M. X. Zhu, D. Bruns and A. Cavalie (2009). "TRPC5 is a Ca^{2+}-activated channel functionally coupled to Ca^{2+}-selective ion channels." The Journal of Biological Chemistry **284**(49): 34423-34432.

Guibert, C., T. Ducret and J. P. Savineau (2008). "Voltage-independent calcium influx in smooth muscle." Progress in Biophysics and Molecular Biology **98**(1): 10-23.

Hamada, F. N., M. Rosenzweig, K. Kang, S. R. Pulver, A. Ghezzi, T. J. Jegla and P. A. Garrity (2008). "An internal thermal sensor controlling temperature preference in Drosophila." Nature **454**(7201): 217-220.

Hamid, R. and J. H. Newman (2009). "Evidence for Inflammatory Signaling in Idiopathic Pulmonary Artery Hypertension: TRPC6 and Nuclear Factor-κB." Circulation **119**(17): 2297-2298.

Harada, M., X. Luo, X. Y. Qi, A. Tadevosyan, A. Maguy, B. Ordog, J. Ledoux, T. Kato, P. Naud, N. Voigt, Y. Shi, K. Kamiya, T. Murohara, I. Kodama, J. C. Tardif, U. Schotten, D. R. Van Wagoner, D. Dobrev and S. Nattel (2012). "Transient receptor potential canonical-3 channel-dependent fibroblast regulation in atrial fibrillation." Circulation **126**(17): 2051-2064.

Hardie, R. C. and B. Minke (1991). "The trp gene is essential for a light-activated Ca^{2+} channel in Drosophila photoreceptors." Neuron **8**(4): 643-651.

Hartmann, J., E. Dragicevic, H. Adelsberger, H. A. Henning, M. Sumser, J. Abramowitz, R. Blum, A. Dietrich, M. Freichel, V. Flockerzi, L. Birnbaumer and A. Konnerth (2008). "TRPC3 channels are required for synaptic transmission and motor coordination." Neuron **59**(3): 392-398.

He, Z., C. Jia, S. Feng, K. Zhou, Y. Tai, X. Bai and Y. Wang (2012). "TRPC5 channel is the mediator of neurotrophin-3 in regulating dendritic growth via CAMKIIα in rat hippocampal neurons." The Journal of Neuroscience **32**(27): 9383-9395.

Hicks, S. N., M. R. Jezyk, S. Gershburg, J. P. Seifert, T. K. Harden and J. Sondek (2008). "General and versatile autoinhibition of PLC isozymes." Molecular cell **31**(3): 383-394.

Hodson, E. A. M., C. C. Ashley, A. D. Hughes and J. S. Lymn (1998). "Regulation of phospholipase C-delta by GTP-binding proteins-rhoA as an inhibitory modulator." Biochimica et Biophysica Acta (BBA) - Molecular Cell Research **1403**(1): 97-101.

Hofmann, T., A. G. Obukhov, M. Schaefer, C. Harteneck, T. Gudermann and G. Schultz (1999). "Direct activation of human TRPC6 and TRPC3 channels by diacylglycerol." Nature **397**(6716): 259-263.

Homma, Y., J. Imaki, O. Nakanishi and T. Takenawa (1988). "Isolation and characterization of two different forms of inositol phospholipid-specific phospholipase C from rat brain." Journal of Biological Chemistry **263**(14): 6592-6598.

Huang, J., C. H. Liu, S. A. Hughes, M. Postma, C. J. Schwiening and R. C. Hardie (2010). "Activation of TRP channels by protons and phosphoinositide depletion in Drosophila photoreceptors." Current Biology **20**(3): 189-197.

Imai, Y., K. Itsuki, Y. Okamura, R. Inoue and M. X. Mori (2012). "A self-limiting regulation of vasoconstrictor-activated TRPC3/C6/C7 channels coupled to PI(4,5)P(2)-diacylglycerol signalling." The Journal of Physiology **590**(Pt 5): 1101-1119.

Itsuki, K., Y. Imai, H. Hase, Y. Okamura, R. Inoue and M. X. Mori (2014). "PLC-mediated PI(4,5)P(2) hydrolysis regulates activation and inactivation of TRPC6/7 channels." The Journal of General Physiology **143**(2): 183-201.

Itsuki, K., Y. Imai, Y. Okamura, K. Abe, R. Inoue and M. X. Mori (2012). "Voltage-sensing phosphatase reveals temporal regulation of TRPC3/C6/C7 channels by membrane phosphoinositides." Channels **6**(3): 206-209.

Jeon, J.P., K. P. Lee, E. J. Park, T. S. Sung, B. J. Kim, J.H. Jeon and I. So (2008). "The specific activation of TRPC4 by G_i protein subtype." Biochemical and Biophysical Research Communications **377**(2): 538-543.

Jeon, J. P., C. Hong, E. J. Park, J. H. Jeon, N. H. Cho, I. G. Kim, H. Choe, S. Muallem, H. J. Kim and I. So (2012). "Selective $G\alpha_i$ subunits as novel direct activators of transient receptor potential canonical (TRPC)4 and TRPC5 channels." The Journal of Biological Chemistry **287**(21): 17029-17039.

Jordt, S.E., D. M. Bautista, H.H. Chuang, D. D. McKemy, P. M. Zygmunt, E. D. Hogestatt, I. D. Meng and D. Julius (2004). "Mustard oils and cannabinoids excite sensory nerve fibres through the TRP channel ANKTM1." Nature **427**(6971): 260-265.

Ju, Y. K., Y. Chu, H. Chaulet, D. Lai, O. L. Gervasio, R. M. Graham, M. B. Cannell and D. G. Allen (2007). "Store-operated Ca^{2+} influx and expression of TRPC genes in mouse sinoatrial node." Circulation Research **100**(11): 1605-1614.

Jung, S., A. Muhle, M. Schaefer, R. Strotmann, G. Schultz and T. D. Plant (2003). "Lanthanides potentiate TRPC5 currents by an action at extracellular sites close to the pore mouth." The Journal of Biological Chemistry **278**(6): 3562-3571.

Jung, S., R. Strotmann, G. Schultz and T. D. Plant (2002). "TRPC6 is a candidate channel involved in receptor-stimulated cation currents in A7r5 smooth muscle cells." American Journal of Physiology. Cell Physiology **282**(2): C347-359.

Karashima, Y., K. Talavera, W. Everaerts, A. Janssens, K. Y. Kwan, R. Vennekens, B. Nilius and T. Voets (2009). "TRPA1 acts as a cold sensor in vitro and in vivo." Proceedings of the National Academy of Sciences of the United States of America **106**(4): 1273-1278.

Katz, A., D. Wu and M. I. Simon (1992). "Subunits [beta][gamma] of heterotrimeric G protein activate [beta]2 isoform of phospholipase C." Nature **360**(6405): 686-689.

Kettenmann, H. and W. R. Schlue (1988). "Intracellular pH regulation in cultured mouse oligodendrocytes." The Journal of Physiology **406**(1): 147-162.

Kim, E. Y., M. Anderson and S. E. Dryer (2012). "Sustained activation of n-methyl-d-aspartate receptors in podoctyes leads to oxidative stress, mobilization of Transient Receptor Potential Canonical 6 channels, nuclear factor of activated T cells activation, and apoptotic cell death." Molecular Pharmacology **82**(4): 728-737.

Kim, B. J., M. T. Kim, J.H. Jeon, S. J. Kim and I. So (2008). "Involvement of phosphatidylinositol 4,5-bisphosphate in the desensitization of Canonical Transient Receptor Potential 5." Biological and Pharmaceutical Bulletin **31**(9): 1733-1738.

Kim, H., J. P. Jeon, C. Hong, J. Kim, J. Myeong, J. H. Jeon and I. So (2013). "An essential role of PI(4,5)P(2) for maintaining the activity of the transient receptor potential canonical (TRPC)4beta." Pflügers Archiv - European Journal of Physiology **465**(7): 1011-1021.

Kim, J., M. Kwak, J.P. Jeon, J. Myeong, J. Wie, C. Hong, S.Y. Kim, J.H. Jeon, H. Kim and I. So (2014). "Isoform- and receptor-specific channel property of canonical transient receptor potential (TRPC)1/4 channels." Pflügers Archiv - European Journal of Physiology **466**(3): 491-504.

Kim, S., L. Ma, K. L. Jensen, M. M. Kim, C. T. Bond, J. P. Adelman and C. R. Yu (2012). "Paradoxical contribution of SK3 and GIRK channels to the activation of mouse vomeronasal organ." Nature Neuroscience **15**(9): 1236-1244.

Kim, Y., A. C. Y. Wong, J. M. Power, S. F. Tadros, M. Klugmann, A. J. Moorhouse, P. P. Bertrand and G. D. Housley (2012). "Alternative splicing of the TRPC3 ion channel calmodulin/IP3 receptor-binding domain in the hindbrain enhances cation flux." The Journal of Neuroscience **32**(33): 11414-11423.

Kini, V., A. Chavez and D. Mehta (2010). "A new role for PTEN in regulating Transient Receptor Potential Canonical Channel 6-mediated Ca^{2+} entry, endothelial permeability, and angiogenesis." The Journal of Biological Chemistry **285**(43): 33082-33091.

Kinoshita-Kawada, M., J. Tang, R. Xiao, S. Kaneko, J. K. Foskett and M. Zhu (2005). "Inhibition of TRPC5 channels by Ca^{2+}-binding protein 1 in Xenopus oocytes." Pflügers Archiv - European Journal of Physiology **450**(5): 345-354.

Kiselyov, K., J. Y. Kim, W. Zeng and S. Muallem (2005). "Protein-protein interaction and functionTRPC channels." Pflügers Archiv - European Journal of Physiology **451**(1): 116-124.

Komatsu, T., I. Kukelyansky, J. M. McCaffery, T. Ueno, L. C. Varela and T. Inoue (2010). "Organelle-specific, rapid induction of molecular activities and membrane tethering." Nature methods **7**(3): 206-208.

Kuwahara, K., Y. Wang, J. McAnally, J. A. Richardson, R. Bassel-Duby, J. A. Hill and E. N. Olson (2006). "TRPC6 fulfills a calcineurin signaling circuit during pathologic cardiac remodeling." Journal of Clinical Investigation **116**(12): 3114-3126.

Kwiatek, A. M., R. D. Minshall, D. R. Cool, R. A. Skidgel, A. B. Malik and C. Tiruppathi (2006). "Caveolin-1 Regulates store-operated Ca^{2+} influx by binding of its scaffolding domain to transient receptor potential channel-1 in endothelial cells." Molecular Pharmacology **70**(4): 1174-1183.

Kwan, H. Y., B. Shen, X. Ma, Y. C. Kwok, Y. Huang, Y. B. Man, S. Yu and X. Yao (2009). "TRPC1 associates with BK(Ca) channel to form a signal complex in vascular smooth muscle cells." Circulation Research **104**(5): 670-678.

Ladilov, Y., C. Schäfer, A. Held, M. Schäfer, T. Noll and H. M. Piper (2000). "Mechanism of Ca^{2+} overload in endothelial cells exposed to simulated ischemia." Cardiovascular Research **47**(2): 394-403.

Lee, K. P., J. Y. Jun, I. Y. Chang, S. H. Suh, I. So, K. W. Kim (2005). "TRPC4 is an essential component of the nonselective cation channel activated by muscarinic stimulation in mouse visceral smooth muscle cells." Molecules and Cells **20**(3): 435-441.

Lemonnier, L., M. Trebak and J. W. Putney, Jr. (2008). "Complex regulation of the TRPC3, 6 and 7 channel subfamily by diacylglycerol and phosphatidylinositol-4,5-bisphosphate." Cell Calcium **43**(5): 506-514.

Lepage, P. K., M. P. Lussier, H. Barajas-Martinez, S. M. Bousquet, A. P. Blanchard, N. Francoeur, R. Dumaine and G. Boulay (2006). "Identification of two domains involved in the assembly of transient receptor potential canonical channels." The Journal of Biological Chemistry **281**(41): 30356-30364.

Levitan, I., Y. Fang, A. Rosenhouse-Dantsker and V. Romanenko (2010). "Cholesterol and ion channels." Sub-cellular Biochemistry **51**: 509-549.

Leypold, B. G., C. R. Yu, T. Leinders-Zufall, M. M. Kim, F. Zufall and R. Axel (2002). "Altered sexual and social behaviors in trp2 mutant mice." Proceedings of the National Academy of Sciences **99**(9): 6376-6381.

Li, J., P. Sukumar, C. J. Milligan, B. Kumar, Z. Y. Ma, C. M. Munsch, L. H. Jiang, K. E. Porter and D. J. Beech (2008). "Interactions, functions, and independence of plasma membrane STIM1 and TRPC1 in vascular smooth muscle cells." Circulation Research **103**(8): e97-104.

Li, H.S., X.Z. Xu and C. Montell (1999). "Activation of a TRPC3-dependent cation current through the neurotrophin BDNF." Neuron **24**(1): 261-273

Liao, M., E. Cao, D. Julius and Y. Cheng (2013). "Structure of the TRPV1 ion channel determined by electron cryo-microscopy." Nature **504**(7478): 107-112.

Linse, S., A. Helmersson and S. Forsén (1991). "Calcium binding to calmodulin and its globular domains." The Journal of Biological Chemistry **266**(13): 8050-8054.

Lipton, P. (1999). "Ischemic cell death in brain neurons." Physiological Reviews **79**(4): 1431-1568.

Liu, Y., R. Wang, J. Li, J. Rao, W. Li, J. R. Falck, V. L. Manthati, M. Medhora, E. R. Jacobs and D. Zhu (2011). "Stable EET urea agonist and soluble epoxide hydrolase inhibitor regulate rat pulmonary arteries through TRPCs." Hypertension Research **34**(5): 630-639.

Liu, W., W. Wen, Z. Wei, J. Yu, F. Ye, C.H. Liu, R.C. Hardie and M. Zhang (2011). "The INAD scaffold is a dynamic, redox-regulated modulator of signaling in the drosophila eye." Cell **145**(7): 1088-1101.

Liu, X. R., M. F. Zhang, N. Yang, Q. Liu, R. X. Wang, Y. N. Cao, X. R. Yang, J. S. Sham and M. J. Lin (2012). "Enhanced store-operated Ca^{2+} entry and TRPC channel expression in pulmonary arteries of monocrotaline-induced pulmonary hypertensive rats." American journal of physiology. Cell physiology. **302**(1): C77-87.

Löf, C., T. Viitanen, P. Sukumaran and K. Törnquist (2011). "TRPC2: Of Mice But Not Men." Transient Receptor Potential Channels, Advances in Experimental Medicine and Biology **704**: 125-134.

Maier, T., M. Follmann, G. Hessler, H. W. Kleemann, S. Hachtel, B. Fuchs, N. Weissmann, W. Linz, T. Schmidt, M. Löhn, K. Schroeter, L. Wang, H. Rütten and C. Strübing (2015). "Discovery and pharmacological characterization of a novel potent inhibitor of diacylglycerol-sensitive TRPC cation channels." British Journal of Pharmacology **172**(14): 3650-3660.

Malarkey, E. B., Y. Ni and V. Parpura (2008). "Ca^{2+} entry through TRPC1 channels contributes to intracellular Ca^{2+} dynamics and consequent glutamate release from rat astrocytes." Glia **56**(8): 821-835.

McKemy, D. D., W. M. Neuhausser and D. Julius (2002). "Identification of a cold receptor reveals a general role for TRP channels in thermosensation." Nature **416**(6876): 52-58.

Mehta, D., G. U. Ahmmed, B. C. Paria, M. Holinstat, T. Voyno-Yasenetskaya, C. Tiruppathi, R. D. Minshall and A. B. Malik (2003). "RhoA interaction with inositol 1,4,5-trisphosphate receptor and transient receptor potential channel-1 regulates Ca^{2+} entry. Role in signaling increased endothelial permeability." The Journal of Biological Chemistry **278**(35): 33492-33500.

Meissner M., V. Obmann., M. Hoschke, S. Link, M. Jung, G. Held G, S. E. Philipp, R. Zimmermann, and V. Flockerzi (2011). "Lessons of studying trp channels with antibodies." TRP Channels, Zhu MX, editor, Boca Raton (FL): CRC Press.

Mery, L., F. Magnino, K. Schmidt, K. H. Krause and J. F. Dufour (2001). "Alternative splice variants of hTrp4 differentially interact with the C-terminal portion of the inositol 1,4,5-trisphosphate receptors." FEBS Letters **487**(3): 377-383.

Miehe, S., A. Bieberstein, I. Arnould, O. Ihdene, H. Rutten and C. Strubing (2010). "The phospholipid-binding protein SESTD1 is a novel regulator of the transient receptor potential channels TRPC4 and TRPC5." The Journal of Biological Chemistry **285**(16): 12426-12434.

Miller, M., J. Shi, Y. Zhu, M. Kustov, J. B. Tian, A. Stevens, M. Wu, J. Xu, S. Long, P. Yang, A. V. Zholos, J. M. Salovich, C. D. Weaver, C. R. Hopkins, C. W. Lindsley, O. McManus, M. Li and M. X. Zhu (2011). "Identification of ML204, a novel potent antagonist that selectively modulates native TRPC4/C5 ion channels." The Journal of Biological Chemistry **286**(38): 33436-33446.

Minke, B., C. F. Wu and W. L. Pak (1975). "Induction of photoreceptor voltage noise in the dark in Drosophila mutant." Nature **258**(5530): 84-87.

Miyagi, K., S. Kiyonaka, K. Yamada, T. Miki, E. Mori, K. Kato, T. Numata, Y. Sawaguchi, T. Numaga, T. Kimura, Y. Kanai, M. Kawano, M. Wakamori, H. Nomura, I. Koni, M. Yamagishi and Y. Mori (2009). "A pathogenic C terminus-truncated polycystin-2 mutant enhances receptor-activated Ca^{2+}entry via association with TRPC3 and TRPC7." The Journal of Biological Chemistry **284**(49): 34400-34412.

Montell, C. (2011). "The history of TRP channels, a commentary and reflection." Pflügers Archiv - European Journal of Physiology **461**(5): 499-506.

Montell, C., L. Birnbaumer, V. Flockerzi, R. J. Bindels, E. A. Bruford, M. J. Caterina, D. E. Clapham, C. Harteneck, S. Heller, D. Julius, I. Kojima, Y. Mori, R. Penner, D. Prawitt, A. M. Scharenberg, G. Schultz, N. Shimizu and M. X. Zhu (2002). "A unified nomenclature for the superfamily of trp cation channels." Molecular Cell **9**(2): 229-231.

Montell, C. and G. M. Rubin (1989). "Molecular characterization of the drosophila trp locus: A putative integral membrane protein required for phototransduction." Neuron **2**(4): 1313-1323.

Munsch, T., M. Freichel, V. Flockerzi and H. C. Pape (2003). "Contribution of transient receptor potential channels to the control of GABA release from dendrites." Proceedings of the National Academy of Sciences **100**(26): 16065-16070.

Murthy, K. S., H. Zhou, J. Huang and S. N. Pentyala (2004). "Activation of PLC-δ1 by $G_{i/o}$-coupled receptor agonists." American Journal of Physiology - Cell Physiology **287**(6): C1679-C1687.

Nagarajan, A., Y. Ning, K. Reisner, Z. Buraei, J. P. Larsen, O. Hobert and M. Doitsidou (2014). "Progressive degeneration of dopaminergic neurons through TRP channel-induced cell death." The Journal of Neuroscience **34**(17): 5738-5746.

Nelson, C. and M. D. Glitsch (2012). "Lack of Kinase Regulation of Canonical Transient Receptor Potential 3 (TRPC3) Channel-dependent Currents in Cerebellar Purkinje Cells." The Journal of Biological Chemistry **287**(9): 6326-6335.

Niemeyer, M. I., L. P. Cid, G. Peña-Münzenmayer and F. V. Sepúlveda (2010). "Separate gating mechanisms mediate the regulation of K2P potassium channel TASK-2 by intra- and extracellular pH." The Journal of Biological Chemistry **285**(22): 16467-16475.

Nijenhuis, T., A. J. Sloan, J. G. J. Hoenderop, J. Flesche, H. van Goor, A. D. Kistler, M. Bakker, R. J. M. Bindels, R. A. de Boer, C. C. Möller, I. Hamming, G. Navis, J. F. M. Wetzels, J. H. M. Berden, J. Reiser, C. Faul and J. van der Vlag (2011). "Angiotensin II contributes to podocyte injury by increasing TRPC6 expression via an NFAT-mediated positive feedback signaling pathway." The American Journal of Pathology 179(4): 1719-1732.

Ng, L. C., J. A. Airey and J. R. Hume (2010). "The contribution of TRPC1 and STIM1 to capacitative Ca^{2+} entry in pulmonary artery." Advances in Experimental Medicine and Biology 661: 123-135.

Ng, L. C., M. D. McCormack, J. A. Airey, C. A. Singer, P. S. Keller, X. M. Shen and J. R. Hume (2009). "TRPC1 and STIM1 mediate capacitative Ca^{2+} entry in mouse pulmonary arterial smooth muscle cells." The Journal of Physiology 587(Pt 11): 2429-2442.

Obukhov, A. G. and M. C. Nowycky (2004). "TRPC5 activation kinetics are modulated by the scaffolding protein ezrin/radixin/moesin-binding phosphoprotein-50 (EBP50)." Journal of Cellular Physiology 201(2): 227-235.

Obukhov, A. G. and M. C. Nowycky (2008). "TRPC5 channels undergo changes in gating properties during the activation-deactivation cycle." Journal of Cellular Physiology **216**(1): 162-171.

Ochocka, A. M., M. Grden, M. Sakowicz-Burkiewicz, A. Szutowicz and T. Pawelczyk (2008). "Regulation of phospholipase C-δ1 by ARGHAP6, a GTPase-activating protein for RhoA: Possible role for enhanced activity of phospholipase C in hypertension." The International Journal of Biochemistry & Cell Biology **40**(10): 2264-2273.

Okada, T., R. Inoue, K. Yamazaki, A. Maeda, T. Kurosaki, T. Yamakuni, I. Tanaka, S. Shimizu, K. Ikenaka, K. Imoto and Y. Mori (1999). "Molecular and Functional Characterization of a Novel Mouse Transient Receptor Potential Protein Homologue TRP7: Ca^{2+}-permeable cation

channel that is constitutively activated and enhanced by stimulation of G protein-coupled receptor." The Journal of Biological Chemistry **274**(39): 27359-27370.

Okada, T., S. Shimizu, M. Wakamori, A. Maeda, T. Kurosaki, N. Takada, K. Imoto and Y. Mori (1998). "Molecular cloning and functional characterization of a novel receptor-activated TRP ca^{2+} channel from mouse brain." The Journal of Biological Chemistry **273**(17): 10279-10287.

Okumura, K., H. Matsui, K. Murase, A. Shimauchi, K. Shimizu, Y. Toki, T. Ito and T. Hayakawa (1996). "Insulin increases distinct species of 1,2-diacylglycerol in isolated perfused rat heart." Metabolism **45**(6): 774-781.

Ong, H. L. and I. S. Ambudkar (2011). "The dynamic complexity of the TRPC1 channelosome." Channels (Austin) **5**(5): 424-431.

Ordaz, B., J. Tang, R. Xiao, A. Salgado, A. Sampieri, M. X. Zhu and L. Vaca (2005). "Calmodulin and calcium interplay in the modulation of TRPC5 channel activity. Identification of a novel C-terminal domain for calcium/calmodulin-mediated facilitation." The Journal of Biological Chemistry **280**(35): 30788-30796.

Otsuguro, K., J. Tang, Y. Tang, R. Xiao, M. Freichel, V. Tsvilovskyy, S. Ito, V. Flockerzi, M. X. Zhu and A. V. Zholos (2008). "Isoform-specific inhibition of TRPC4 channel by phosphatidylinositol 4,5-bisphosphate." The Journal of Biological Chemistry **283**(15): 10026-10036.

Pandey, K., R. R. Dhoke, Y. S. Rathore, S. K. Nath, N. Verma, S. Bawa and Ashish (2014). "Low pH overrides the need of calcium ions for the shape–function relationship of calmodulin: resolving prevailing debates." The Journal of Physical Chemistry B **118**(19): 5059-5074.

Park, D., D. Y. Jhon, C. W. Lee, K. H. Lee and S. G. Rhee (1993). "Activation of phospholipase C isozymes by G protein beta gamma subunits." The Journal of Biological Chemistry **268**(7): 4573-4576.

Parrau, D., G. Ebensperger, E. A. Herrera, F. Moraga, R. A. Riquelme, C. E. Ulloa, R. T. Rojas, P. Silva, I. Hernandez, J. Ferrada, M. Diaz, J. T. Parer, G. Cabello, A. J. Llanos and R. V. Reyes (2013). "Store-operated channels in the pulmonary circulation of high- and low-altitude neonatal lambs." American Journal of Physiology: Lung Cellular and Molecular Physiology **304**(8): L540-548.

Paulsen, C. E., J. P. Armache, Y. Gao, Y. Cheng and D. Julius (2015). "Structure of the TRPA1 ion channel suggests regulatory mechanisms." Nature **520**(7548): 511-517.

Pavlov, I. and M. C. Walker (2013). "Tonic GABA(A) receptor-mediated signalling in temporal lobe epilepsy." Neuropharmacology **69**: 55-61.

Peier, A. M., A. Moqrich, A. C. Hergarden, A. J. Reeve, D. A. Andersson, G. M. Story, T. J. Earley, I. Dragoni, P. McIntyre, S. Bevan and A. Patapoutian (2002). "A TRP channel that senses cold stimuli and menthol." Cell **108**(5): 705-715.

Phelan, K. D., M. M. Mock, O. Kretz, U. T. Shwe, M. Kozhemyakin, L. J. Greenfield, A. Dietrich, L. Birnbaumer, M. Freichel, V. Flockerzi and F. Zheng (2012). "Heteromeric canonical transient receptor potential 1 and 4 channels play a critical role in epileptiform burst firing and seizure-induced neurodegeneration." Molecular Pharmacology **81**(3): 384-392.

Phelan, K. D., U. T. Shwe, J. Abramowitz, H. Wu, S. W. Rhee, M. D. Howell, P. E. Gottschall, M. Freichel, V. Flockerzi, L. Birnbaumer and F. Zheng (2013). "Canonical transient receptor channel 5 (TRPC5) and TRPC1/4 contribute to seizure and excitotoxicity by distinct cellular mechanisms." Molecular Pharmacology **83**(2): 429-438.

Philipp, S., A. Cavalié, M. Freichel, U. Wissenbach, S. Zimmer, C. Trost, A. Marquart, M. Murakami and V. Flockerzi (1996). "A mammalian capacitative calcium entry channel homologous to Drosophila TRP and TRPL." The EMBO Journal **15**(22): 6166-6171.

Philipp, S., J. Hambrecht, L. Braslavski, G. Schroth, M. Freichel, M. Murakami, A. Cavalié and V. Flockerzi (1998). "A novel capacitative calcium entry channel expressed in excitable cells." The EMBO Journal **17**(15): 4274-4282.

Plant, T. D. and M. Schaefer (2003). "TRPC4 and TRPC5: receptor-operated Ca^{2+}-permeable nonselective cation channels." Cell Calcium **33**(5-6): 441-450.

Plant, T. D. and M. Schaefer (2005). "Receptor-operated cation channels formed by TRPC4 and TRPC5." Naunyn Schmiedebergs Arch Pharmacol **371**(4): 266-276.

Poteser, M., A. Graziani, C. Rosker, P. Eder, I. Derler, H. Kahr, M. X. Zhu, C. Romanin and K. Groschner (2006). "TRPC3 and TRPC4 associate to form a redox-sensitive cation channel. Evidence for expression of native TRPC3-TRPC4 heteromeric channels in endothelial cells." The Journal of Biological Chemistry **281**(19): 13588-13595.

Poteser, M., H. Schleifer, M. Lichtenegger, M. Schernthaner, T. Stockner, C. O. Kappe, T. N. Glasnov, C. Romanin and K. Groschner (2011). "PKC-dependent coupling of calcium permeation through transient receptor potential canonical 3 (TRPC3) to calcineurin signaling in HL-1 myocytes." Proceedings of the National Academy of Sciences of the United States of America **108**(26): 10556-10561.

Rosenzweig, M., K. M. Brennan, T. D. Tayler, P. O. Phelps, A. Patapoutian and P. A. Garrity (2005). "The Drosophila ortholog of vertebrate TRPA1 regulates thermotaxis." Genes & Development **19**(4): 419-424.

Rowell, J., N. Koitabashi and D. A. Kass (2010). "TRP-ing up heart and vessels: canonical transient receptor potential channels and cardiovascular disease." Journal of Cardiovascular Translational Research **3**(5): 516-524.

Ryu, S. H., P. G. Suh, K. S. Cho, K. Y. Lee and S. G. Rhee (1987). "Bovine brain cytosol contains three immunologically distinct forms of inositolphospholipid-specific phospholipase C." Proceedings of the National Academy of Sciences of the United States of America **84**(19): 6649-6653.

Saito, H., Y. Minamiya, H. Watanabe, N. Takahashi, M. Ito, H. Toda, H. Konno, M. Mitsui, S. Motoyama and J. Ogawa (2011). "Expression of the Transient Receptor Potential channel C3 correlates with a favorable prognosis in patients with adenocarcinoma of the lung." Annals of Surgical Oncology **18**(12): 3377-3383.

Sawada, Y., H. Hosokawa, A. Hori, K. Matsumura and S. Kobayashi (2007). "Cold sensitivity of recombinant TRPA1 channels." Brain Research **1160**(0): 39-46.

Samapati, R., Y. Yang, J. Yin, C. Stoerger, C. Arenz, A. Dietrich, T. Gudermann, D. Adam, S. Wu, M. Freichel, V. Flockerzi, S. Uhlig and W. M. Kuebler (2012). "Lung endothelial Ca^{2+} and permeability response to platelet-activating factor is mediated by acid sphingomyelinase and Transient Receptor Potential Classical 6." American Journal of Respiratory and Critical Care Medicine **185**(2): 160-170.

Schaefer, M. (2005). "Homo- and heteromeric assembly of TRP channel subunits." ." Pflügers Archiv - European Journal of Physiology **451**(1): 35-42.

Schaefer, M., T. D. Plant, N. Stresow, N. Albrecht and G. Schultz (2002). "Functional Differences between TRPC4 Splice Variants." The Journal of Biological Chemistry **277**(5): 3752-3759.

Schleifer, H., B. Doleschal, M. Lichtenegger, R. Oppenrieder, I. Derler, I. Frischauf, T. N. Glasnov, C. O. Kappe, C. Romanin and K. Groschner (2012). "Novel pyrazole compounds for pharmacological discrimination between receptor-operated and store-operated Ca^{2+} entry pathways." British Journal of Pharmacology **167**(8): 1712-1722.

Sel, S., B. R. Rost, A. O. Yildirim, B. Sel, H. Kalwa, H. Fehrenbach, H. Renz, T. Gudermann and A. Dietrich (2008). "Loss of classical transient receptor potential 6 channel reduces allergic airway response." Clinical and Experimental Allergy **38**(9): 1548-1558.

Sellers, P., J. Laynez, E. Thulin and S. Forsén (1991). "Thermodynamics of Ca^{2+} binding to calmodulin and its tryptic fragments." Biophysical Chemistry **39**(2): 199-204.

Semtner, M., M. Schaefer, O. Pinkenburg and T. D. Plant (2007). "Potentiation of TRPC5 by Protons." The Journal of Biological Chemistry **282**(46): 33868-33878.

Sharif-Naeini, R., J. H. Folgering, D. Bichet, F. Duprat, P. Delmas, A. Patel and E. Honore (2010). "Sensing pressure in the cardiovascular system: G_q-coupled mechanoreceptors and TRP channels." Journal of Molecular and Cellular Cardiology **48**(1): 83-89.

Shi, J., M. Ju, J. Abramowitz, W. A. Large, L. Birnbaumer and A. P. Albert (2012a). "TRPC1 proteins confer PKC and phosphoinositol activation on native heteromeric TRPC1/C5 channels in vascular smooth muscle: comparative study of wild-type and TRPC1-/- mice." FASEB Journal **26**(1): 409-419.

Shi, J., M. Ju, W. A. Large and A. P. Albert (2012b). "Pharmacological profile of phosphatidylinositol 3-kinases and related phosphatidylinositols mediating endothelin(A) receptor-operated native TRPC channels in rabbit coronary artery myocytes." British Journal of Pharmacology **166**(7): 2161-2175.

Shi, J., M. Ju, S. N. Saleh, A. P. Albert and W. A. Large (2010). "TRPC6 channels stimulated by angiotensin II are inhibited by TRPC1/C5 channel activity through a Ca^{2+}- and PKC-dependent mechanism in native vascular myocytes." The Journal of Physiology **588**(19): 3671-3682.

Shim, S., E. L. Goh, S. Ge, K. Sailor, J. P. Yuan, H. L. Roderick, M. D. Bootman, P. F. Worley, H. Song and G. L. Ming (2005). "TRPC1-dependent chemotropic guidance of neuronal growth cones." Nature Neuroscience 8(6): 730-735.

Spassova, M. A., T. Hewavitharana, W. Xu, J. Soboloff and D. L. Gill (2006). "A common mechanism underlies stretch activation and receptor activation of TRPC6 channels." Proceedings of the National Academy of Sciences **103**(44): 16586-16591.

Story, G. M., A. M. Peier, A. J. Reeve, S. R. Eid, J. Mosbacher, T. R. Hricik, T. J. Earley, A. C. Hergarden, D. A. Andersson, S. W. Hwang, P. McIntyre, T. Jegla, S. Bevan and A. Patapoutian (2003). "ANKTM1, a TRP-like channel expressed in nociceptive neurons, is activated by cold temperatures." Cell **112**(6): 819-829.

Stowers, L., T. E. Holy, M. Meister, C. Dulac and G. Koentges (2002). "Loss of sex discrimination and male-male aggression in mice deficient for TRP2." Science **295**(5559): 1493-1500.

Strübing, C., G. Krapivinsky, L. Krapivinsky and D. E. Clapham (2001)"TRPC1 and TRPC5 form a novel cation channel in mammalian brain." Neuron **29**(3): 645-655.

Strubing, C., G. Krapivinsky, L. Krapivinsky and D. E. Clapham (2003). "Formation of novel TRPC channels by complex subunit interactions in embryonic brain." The Journal of Biological Chemistry **278**(40): 39014-39019

Suh, P.G., J.I. Park, L. Manzoli, L. Cocco, J. C. Peak, M. Katan, K. Fukami, T. Kataoka, S. Yun and S. H. Ryu (2008). "Multiple roles of phosphoinositide-specific phospholipase C isozymes." BMB reports **41**(6):415-34.

Sundivakkam, P. C., M. Freichel, V. Singh, J. P. Yuan, S. M. Vogel, V. Flockerzi, A. B. Malik and C. Tiruppathi (2012). "The Ca^{2+}sensor stromal interaction molecule 1 (STIM1) is necessary and sufficient for the store-operated Ca^{2+}entry function of transient receptor potential canonical (TRPC) 1 and 4 channels in endothelial cells." Molecular Pharmacology **81**(4): 510-526.

Sundivakkam, P. C., A. M. Kwiatek, T. T. Sharma, R. D. Minshall, A. B. Malik and C. Tiruppathi (2009). "Caveolin-1 scaffold domain interacts with TRPC1 and IP(3)R3 to regulate Ca^{2+} store release-induced Ca^{2+} entry in endothelial cells." American Journal of Physiology - Cell Physiology **296**(3): C403-C413.

Tai, Y., S. Feng, R. Ge, W. Du, X. Zhang, Z. He and Y. Wang (2008). "TRPC6 channels promote dendritic growth via the CaMKIV-CREB pathway." Journal of Cell Science **121**(14): 2301-2307.

Takahashi, N. and Y. Mori (2011). "TRP channels as sensors and signal integrators of redox status changes." Frontiers in Pharmacology **2**:58.

Tang, J., Y. Lin, Z. Zhang, S. Tikunova, L. Birnbaumer and M. X. Zhu (2001). "Identification of common binding sites for calmodulin and inositol 1,4,5-trisphosphate receptors on the carboxyl termini of TRP channels." The Journal of Biological Chemistry **276**(24): 21303-21310.

Tang, Y., J. Tang, Z. Chen, C. Trost, V. Flockerzi, M. Li, V. Ramesh and M. X. Zhu (2000). "Association of mammalian TRP4 and phospholipase C isozymes with a PDZ domain-containing protein, NHERF." Journal of Biological Chemistry 275(48): 37559-37564.

Tewson, P., M. Westenberg, Y. Zhao, R. E. Campbell, A. M. Quinn and T. E. Hughes (2012). "Simultaneous detection of Ca^{2+} and diacylglycerol signaling in living cells." PLoS ONE 7(8): e42791.

Thilo, F., C. Loddenkemper, E. Berg, W. Zidek and M. Tepel (2009). "Increased TRPC3 expression in vascular endothelium of patients with malignant hypertension." Modern Pathology **22**(3): 426-430.

Thompson, J. L. and T. J. Shuttleworth (2011). "Orai channel-dependent activation of phospholipase C-δ: a novel mechanism for the effects of calcium entry on calcium oscillations." The Journal of Physiology **589**(Pt 21): 5057-5069.

Tian, D., S. M. Jacobo, D. Billing, A. Rozkalne, S. D. Gage, T. Anagnostou, H. Pavenstädt, H. H. Hsu, J. Schlondorff, A. Ramos and A. Greka (2010). “Antagonistic Regulation of Actin Dynamics and Cell Motility by TRPC5 and TRPC6 Channels.” Science Signaling **3**(145): ra77-ra77.

Tian, J., D. P. Thakur, Y. Lu, Y. Zhu, M. Freichel, V. Flockerzi and M. X. Zhu (2014). "Dual depolarization responses generated within the same lateral septal neurons by TRPC4-containing channels." Pflügers Archiv - European Journal of Physiology **466**(7):1301-1316

Tiruppathi, C., R. D. Minshall, B. C. Paria, S. M. Vogel and A. B. Malik (2002). "Role of Ca^{2+} signaling in the regulation of endothelial permeability." Vascular Pharmacology **39**(4-5): 173-185.

Tiruppathi, C., M. Freichel, S. M. Vogel, B. C. Paria, D. Mehta, V. Flockerzi and A. B. Malik (2002). "Impairment of store-operated Ca^{2+} entry in TRPC4−/− mice interferes with increase in lung microvascular permeability." Circulation Research **91**(1): 70-76.

Trebak, M., L. Lemonnier, W. DeHaven, B. Wedel, G. Bird and J. Putney, Jr. (2009). "Complex functions of phosphatidylinositol 4,5-bisphosphate in regulation of TRPC5 cation channels." Pflügers Archiv - European Journal of Physiology **457**(4): 757-769.

Tsvilovskyy, V. V., A. V. Zholos, T. Aberle, S. E. Philipp, A. Dietrich, M. X. Zhu, L. Birnbaumer, M. Freichel and V. Flockerzi (2009). "Deletion of TRPC4 and TRPC6 in mice impairs smooth muscle contraction and intestinal motility in vivo." Gastroenterology **137**(4): 1415-1424.

Vaca, L. and A. Sampieri (2002). "Calmodulin modulates the delay period between release of calcium from internal stores and activation of calcium influx via endogenous trp1 channels." Journal of Biological Chemistry **277**(44): 42178-42187.

Venkatachalam, K. and C. Montell (2007). "TRP channels." Annual review of biochemistry **76**: 387-417.

Wang, M., R. Bianchi, S.C. Chuang, W. Zhao and R. K. S. Wong (2007). "Group I metabotropic glutamate receptor-dependent TRPC channel trafficking in hippocampal neurons." Journal of Neurochemistry **101**(2): 411-421.

Wang, Y., G. Jarad, P. Tripathi, M. Pan, J. Cunningham, D. R. Martin, H. Liapis, J. H. Miner and F. Chen (2010). "Activation of NFAT signaling in podocytes causes glomerulosclerosis." Journal of the American Society of Nephrology **21**(10): 1657-1666.

Wang, Q., M. Liu, T. Kozasa, J. D. Rothstein, P. C. Sternweis and R. R. Neubig (2004). "Thrombin and lysophosphatidic acid receptors utilize distinct rhoGEFs in prostate cancer cells." Journal of Biological Chemistry **279**(28): 28831-28834.

Wang, G. X. and M. M. Poo (2005). "Requirement of TRPC channels in netrin-1-induced chemotropic turning of nerve growth cones." Nature **434**(7035): 898-904.

Wang, X., J. L. Pluznick, P. Wei, B. J. Padanilam and S. C. Sansom (2004). "TRPC4 forms store-operated Ca^{2+} channels in mouse mesangial cells." American Journal of Physiology - Cell Physiology **287**(2): C357-C364.

Weick, J. P., M. Austin Johnson and S.C. Zhang (2009). "Developmental regulation of human embryonic stem cell-derived neurons by calcium entry via transient receptor potential channels." Stem Cells **27**(12): 2906-2916.

Weissmann, N., A. Sydykov, H. Kalwa, U. Storch, B. Fuchs, M. M. y. Schnitzler, R. P. Brandes, F. Grimminger, M. Meissner, M. Freichel, S. Offermanns, F. Veit, O. Pak, K. H. Krause, R. T. Schermuly, A. C. Brewer, H. H. H. W. Schmidt, W. Seeger, A. M. Shah, T. Gudermann, H. A. Ghofrani and A. Dietrich (2012). "Activation of TRPC6 channels is essential for lung ischaemia–reperfusion induced oedema in mice." Nature Communications **3**: 649.

Wes, P. D., J. Chevesich, A. Jeromin, C. Rosenberg, G. Stetten and C. Montell (1995). "TRPC1, a human homolog of a Drosophila store-operated channel." Proceedings of the National Academy of Sciences of the United States of America **92**(21): 9652-9656.

Wu, X., P. Eder, B. Chang and J. D. Molkentin (2010). "TRPC channels are necessary mediators of pathologic cardiac hypertrophy." Proceedings of the National Academy of Sciences of the United States of America **107**(15): 7000-7005.

Xiao, J.H., Y.M. Zheng, B. Liao and Y.X. Wang (2010). "Functional role of Canonical Transient Receptor Potential 1 and Canonical Transient Receptor Potential 3 in normal and asthmatic airway smooth muscle cells." American Journal of Respiratory Cell and Molecular Biology **43**(1): 17-25.

Xu, S. Z., P. Sukumar, F. Zeng, J. Li, A. Jairaman, A. English, J. Naylor, C. Ciurtin, Y. Majeed, C. J. Milligan, Y. M. Bahnasi, E. Al-Shawaf, K. E. Porter, L. H. Jiang, P. Emery, A. Sivaprasadarao and D. J. Beech (2008). "TRPC channel activation by extracellular thioredoxin." Nature **451**(7174): 69-72.

Xu, S. Z., B. Zeng, N. Daskoulidou, G. L. Chen, S. L. Atkin and B. Lukhele (2012). "Activation of TRPC cationic channels by mercurial compounds confers the cytotoxicity of mercury exposure." Toxicological Sciences **125**(1): 56-68.

Yildirim, E., M. A. Carey, J. W. Card, A. Dietrich, G. P. Flake, Y. Zhang, J. A. Bradbury, Y. Rebolloso, D. R. Germolec, D. L. Morgan, D. C. Zeldin and L. Birnbaumer (2012). "Severely blunted allergen-induced pulmonary Th2 cell response and lung hyperresponsiveness in type 1 transient receptor potential channel-deficient mice." American Journal of Physiology - Lung Cellular and Molecular Physiology **303**(6): L539-L549.

Yoshida, T., R. Inoue, T. Morii, N. Takahashi, S. Yamamoto, Y. Hara, M. Tominaga, S. Shimizu, Y. Sato and Y. Mori (2006). "Nitric oxide activates TRP channels by cysteine S-nitrosylation." Nature Chemical Biology **2**(11): 596-607.

Yu, Y., S. H. Keller, C. V. Remillard, O. Safrina, A. Nicholson, S. L. Zhang, W. Jiang, N. Vangala, J. W. Landsberg, J. Y. Wang, P. A. Thistlethwaite, R. N. Channick, I. M. Robbins, J. E. Loyd, H. A. Ghofrani, F. Grimminger, R. T. Schermuly, M. D. Cahalan, L. J. Rubin and J. X. Yuan (2009). "A functional single-nucleotide polymorphism in the TRPC6 gene promoter associated with idiopathic pulmonary arterial hypertension." Circulation **119**(17): 2313-2322.

Yuan, Y., M. Shimura and B. A. Hughes (2003). "Regulation of inwardly rectifying K^+ channels in retinal pigment epithelial cells by intracellular pH." The Journal of Physiology **549**(Pt 2): 429-438.

Zhang, S., C. V. Remillard, I. Fantozzi and J. X. J. Yuan (2004). "ATP-induced mitogenesis is mediated by cyclic AMP response element-binding protein-enhanced TRPC4 expression and activity in human pulmonary artery smooth muscle cells." American Journal of Physiology - Cell Physiology **287**(5): C1192-C1201.

Zhang, J. and D. M. Webb (2003). "Evolutionary deterioration of the vomeronasal pheromone transduction pathway in catarrhine primates." Proceedings of the National Academy of Sciences of the United States of America **100**(14): 8337-8341.

Zhang, Z., J. Tang, S. Tikunova, J. D. Johnson, Z. Chen, N. Qin, A. Dietrich, E. Stefani, L. Birnbaumer and M. X. Zhu (2001). "Activation of Trp3 by inositol 1,4,5-trisphosphate receptors through displacement of inhibitory calmodulin from a common binding domain." Proceedings of the National Academy of Sciences of the United States of America **98**(6): 3168-3173.

Zholos, A. V., A. A. Zholos and T. B. Bolton (2004). "G-protein–gated trp-like cationic channel activated by muscarinic receptors: effect of potential on single-channel gating." The Journal of General Physiology **123**(5): 581-598.

Zhou, J., W. Du, K. Zhou, Y. Tai, H. Yao, Y. Jia, Y. Ding and Y. Wang (2008). "Critical role of TRPC6 channels in the formation of excitatory synapses." Nature Neuroscience **11**(7): 741-743.

Zhu, M. X. (2005). "Multiple roles of calmodulin and other Ca^{2+}-binding proteins in the functional regulation of TRP channels." Pflügers Archiv - European Journal of Physiology **451**(1): 105-115.

Zhu, X., P. B. Chu, M. Peyton and L. Birnbaumer (1995). "Molecular cloning of a widely expressed human homologue for the Drosophila trp gene." FEBS Letters **373**(3): 193-198.

Zhu, X., M. Jiang, M. Peyton, G. Boulay, R. Hurst, E. Stefani and L. Birnbaumer (1996). "trp, a Novel Mammalian Gene Family Essential for Agonist-Activated Capacitative Ca^{2+} Entry." Cell **85**(5): 661-671.

Zimmermann, K., J. K. Lennerz, A. Hein, A. S. Link, J. S. Kaczmarek, M. Delling, S. Uysal, J. D. Pfeifer, A. Riccio and D. E. Clapham (2011). "Transient receptor potential cation channel, subfamily C, member 5 (TRPC5) is a cold-transducer in the peripheral nervous system." Proceedings of the National Academy of Sciences of the United States of America **108**(44): 18114-18119.

Vita

Dhananjay Thakur was born to Arundhati Thakur and Pramod Thakur in Thane, Maharashtra, India. After completing high school he entered a Bachelors of Science program in Fergusson College, University of Pune and graduated with a B.Sc. in Physics after which he completed a Masters degree in Physics from the University of Pune. After a two-year stint in industry - at the Electrical Engineering section of the Tata Motors Ltd, Engineering Research Center, he enrolled at The Ohio State University, Columbus, Ohio and graduated with an MS in Biophysics. In July 2010 he entered the Graduate School of Biomedical Sciences at the University of Texas Health Science Center in Houston, TX.